博士論文

Microfabricated device and technology to manipulate cells for regenerative medicine

(再生医療のための細胞制御を目指したマイクロデバイス)

金 成 昊

Department of Bioengineering

The University of Tokyo

Table of contents

Contents of figure

Abstract

Development of microfabrication technology lead to multiple microfluidics tools for chemical and biological fields and development of materials technology has involved various biocomposite materials for medical applications. In this study, the microfabrication-based technologies were employed for directing neuronal regeneration and cytoplasmic transfer associated with protein modification.

The first focused on development of a biocomposite material to replace the conventional cell culture system using serum. Photo-immobilization that can enable to effectively immobilize biomolecules such as a growth factor on a biological substrate was introduced. We found that nerve growth factor (NGF)-immobilized material can induce neurite formation of rat adrenal pheochromocytoma (PC12) cells as did soluble NGF.

We also found that the method with immobilization overcame current limitations of soluble growth factors such as poor stability. In particular, the neurite formation of neurons can be modulated by micropatterned surface through various micropatterns of a photomask. The 3D structure (height of the formed micropattern) regulated the behavior of neurite guidance. As a result, the orientation of neurites was regulated by the strip pattern width.

The second is investigation on cytoplasmic fusion by a newly designed microfluidic system as a novel method for induction of cellular resource or protein transduction by cytoplasm transfer. In terms of cytoplasmic fusion, the research was achieved by a microfluidic device which has a cell pairing structure (CPS) making cell pairs through microtunnels with several μm width. After trapping one kind of cell with hydrodynamic forces, another kind of cell was fused through the microtunnel by the Sendai virus

envelope (HVJ-E) method. Using this method, cytoplasmic fraction was transferred through the microtunnel without nuclear mixing. Although it was previously reported that the usual cell fusion between somatic cell and embryonic stem cell induced initiation of cellular reprogramming of somatic cell, the resulting cell was tetraploid which was not normal and could not be used for medical applications because of the nuclei fusion.

Our microfluidic platform-based cytoplasmic fusion may provide important keys and new insights for protein modification and pluripotency induction without requirement of genetic incorporation. In essence, several issues like pluripotency which would be occurred after cytoplasmic exchange are still subject to the attractive and undiscovered field for regenerative medicine.

In conclusion, the methods developed in this study offer new approaches useful for the required cell manipulation in regenerative medicine through the integrated and organized microenvironments.

Keywords: Microfabrication technology, Photo-immobilization, Micropatterning, Neurite formation, Microfluidic device, Cell fusion, regenerative medicine

Chapter 1. Introduction

1.1. General introduction

1.1.1. Microfabricated technology and device

A microfabrication technology has involved the process of fabrication of micro scale structures or much small scale. Miniaturization of various devices is required in many fields of science and engineering such as chemistry, materials science, design for equipment, and etc. as a multi-purpose tool.

In the 90's, application of micro electro mechanical systems (MEMS) was introduced and investigated in biology, chemistry, and biomedical fields [1]. The application needed to control the movement of liquids in micro channels and also has significantly contributed to the development of microfluidics [2]. Polydimethylsiloxane (PDMS) is one of the common materials used in the procedure of lithography such as soft lithography and to make flow delivery in microfluidic chips [3,4].

Up to this day, the applications of polymers such as PDMS for microfabrication have involved varying ranges from daily supplies to medical devices due to its flexible and easy fabrication.

In biomedical micro electro mechanical systems (bio-MEMS), the integrated tools using PDMS and microfabrication also have been utilized to design and improve the current device and technology in medical fields because of its non-toxic characteristic and flexibility [5].

1.1.2. Microdevice

Microdevices have changed our view of science associated with various categories in biology, biochemistry, microengineering, and so on [6]. Since the microdevices in the last decade of the 20th century have been introduced to varying spheres, the potential and feasibility of applications led to new inceptions from optics, semiconductors, and microelectronics industry to drug discovery, clinical diagnosis, bioanalytical systems and other areas of the biological field such as single cell manipulation. The micro devices have been fabricated by photolithography and micro-mold technology using MEMS [7].

In particular, cellular microdevices impact the field of tissue engineering in both regenerative medicine and organ assist devices such as organ on a chip. The application of microdevices based on microfluidics has been studied with a lot of approaches and methods from single cell level to expansion of the scale [8].

A. Photolithography

Photolithography, also termed UV lithography, is a process utilized in microfabrication for transferring patterns on a substrate [9,10]. Light source has been used to transfer geometric patterns from a photomask to a light sensitive chemical such a photoresist on substrates. Photolithography indicates some principles such as etching resist added in many areas of manufacturing to create a pattern. The procedure can be created by exposing it to light with or without a mask. Also, the process with etching can produce small patterns, shapes and sizes of the objects under clean operating environments.

During the procedures of photolithography, several steps are combined as shown in **Figure 1.1**. For example, cleaning, photoresist application, exposure to UV light, etching, and photoresist removal. Photolithography has become multiple application and has been explored in industry and science fields such as electron beam lithography, X-ray lithography, and extreme ultraviolet lithography [11,12]. Based on this technique, we can make various tools to produce the surface of substrate with micropatterns through photomask or to manipulate cells via microfluidics with microstructures.

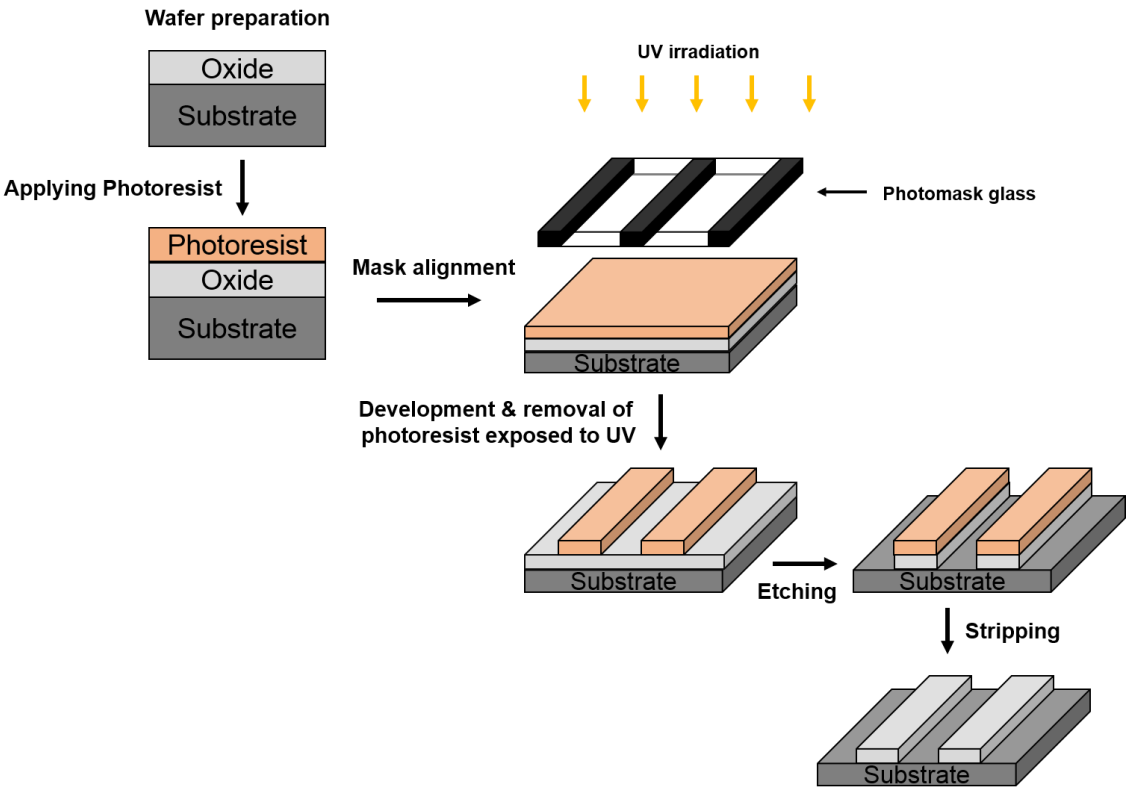

Figure 1.1. Illustrated description of photolithography.

B. Micromold-based microfluidic device

In the early 2000s, mold-based microfluidic devices have been applied from a glass microfluidic device to an advanced form based on molding microchannels in polymers such as PDMS. Such a PDMS device leads to a tremendous growth of microfluidics with the reduction of cost and production time [13,14].

The microfluidic technology is widely used to various fields such as biomedical, chemistry, cell biology research, and so on for multiple purposes. The technology also involves many applications in the following areas. Drug screening, micro fuel cells, glucose tests, and chemical microreactor are also one of applicable fields in microfluidics [15–17]. In the biomedical field, this technology allows the integration of various medical tests on a microchip [18–20].

In case of cell biology research, particularly, microfluidic chips allow easy manipulations of single cell with a reagent or drug changes because the movement of liquids containing such a reagent can be employed in the microchannels. The microchannels also have the similar characteristic size as a biological cell so that we may achieve better understanding toward biological mechanism [21–24]. Therefore, the microfluidic device increases its practical use through single cell manipulation in the regenerative medicine.

A laboratory on a chip (Lab on a chip) that enables the integration of the processes required for biological, biomedical, and chemical application has received many attentions in regenerative medicine [25–27]. Because this concept has been employed to develop and study disease modeling, transplantation of tissues and organs. This may include the possibility of growing tissues and organs in the laboratory and implanting them when the body cannot heal itself.

In particular, the concept of microfluidic device including lab on a chip has deeply associated with the mechanism of cellular individuality. In terms of single cell manipulation, the microfluidic device is considered as a crucial tool. Cellular microdevices impact the field of tissue engineering in both regenerative medicine and organ assist devices such as organ on a chip. The application of microdevices based on microfluidics has been studied with a lot of approaches and methods from single cell level to expansion of the scale [8].

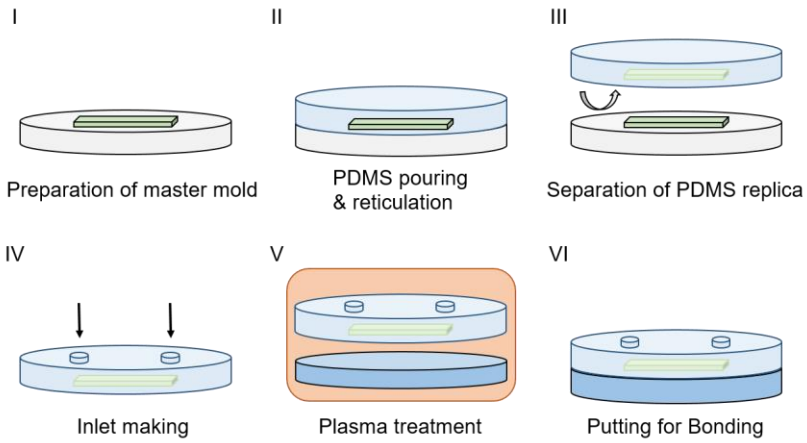

Figure 1.2. The molding of a microfluidic chip using PDMS.

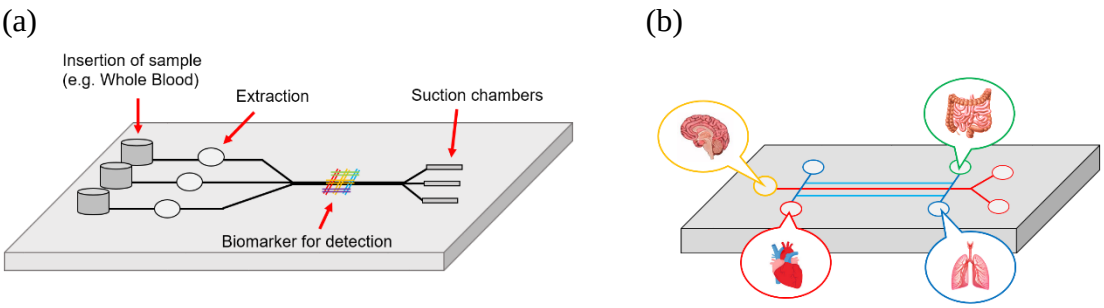

Figure 1.3. Microfluidic devices. (a) Microfluidic device for diagnosis and (b) Organ on a chip.

1.1.3. Cell manipulation by microfabricated devices

The microfabricated device-based technology such as microfluidic device or microfluidic chip enables the study of cellular activity and behavior from single cell level to multi cellular organelles level with precisely localized application [28].

The microfabricated device is fundamentally based on topological components such as patterning and a channel. With desired designed-master mold, the structures of device can be integrated with single- or multi-layer in PDMS devices.

The topological property in the device involves laminar flows, liquid flows (e.g. growth medium), resulting in complex functionalization.

In particular, it has provided promising tools for enhancing biological research at the single cell level to study the molecular biology and genetic analysis involving the cell biology field [29]. Because the microfluidic devices can create biological experiments with a high-throughput. For example, the micro-scale devices enable spatial control of liquid composition, change of medium, and single cell handling and analysis.

Therefore, the application of the device involves many parts of cell manipulation such as cell trapping and sorting, cell culture, and cell fusion according to various functional applications of microfluidic devices.

For precise control of cell microenvironments through the microfluidic device, moreover, monitoring of cellular behaviors such as cytoplasmic transfer will be discussed in this thesis.

1.1.4. Critical issues and approaches for regenerative medicine

In regenerative medicine, several important issues and approaches such as nerve regeneration and cellular resource have been arisen from many attentions and requirements in terms of therapy. As shown in **Figure 1.4**, a lot of strategies have been studied and suggested for those issues through aforementioned various techniques (e.g. cell fusion, micropatterned substrate, and microfluidic device) and materials (e.g. biomaterials and proteins).

For nerve regeneration, many researchers have developed various kinds of clinical treatments depending on the type of diseases and symptoms such as peripheral nerve injury, spinal cord injury, nerve cell regrowth, and so on. The limited capacity for nerve repair is still a big issue in a medical challenge. To create a suitable microenvironment for nerve regeneration and to effectively control the process of nerve injury and degeneration, new tools have been developed in regenerative medicine and neural engineering fields. In case of neural engineering applications, neurotrophic factors (e.g. nerve growth factor) and biochemical and topographical properties have been utilized to provide feasible platforms for neuronal regeneration. Various models such as a nanofiber [30,31], a conducting scaffold [32,33], a biological substrate [34], and a microfluidic tool [35] have showed its ability to elicit and control nerve regeneration. However, a solution to completely repair nerve injury has not been found and many barriers and limitations are still remaining to be solved.

In terms of cellular resource, diverse factors such as proteins, ribosomes, and other cellular components have been studied due to its importance in clinical application as well as basic biology. In particular, protein modification is considered as one of promising tools to create therapeutic conjugates and probe natural systems [36]. Although there are

several types of protein modification through post-translational modification and chemical synthesis, the capacity and property of protein after modification remains to be explored for its application.

In the meantime, other approaches also have been introduced to apply the protein to cells for regenerative medicine. For a medical application, many challenges have been performed based on different types of techniques and methods such as induced pluripotent stem (iPS) cell and cell fusion. Tada et al. [37] suggested cell fusion-based method using ES cell and somatic cell to induce ES-like cell. Yamanaka and Takahashi et al. [38,39] described the genetic transduction to induce iPS cell and that Zhou et al. [40] and Kim et al. [41] also presented protein-induced pluripotent cell by protein transduction.

Taken together, the modifications for cellular resource have been suggested ranging from genetic modification to protein modification. With short time, the direct protein transduction using live cells (e.g. ES cell) containing fresh cellular components (e.g. proteins) is also supposed to a promising approach. Because the protein can be easily denatured by additional treatment processes for long time.

The application of microfabricated tools-based cell fusion has been recently tried to properly mediate cells and protein modification and to treat damaged tissues and organs. Particularly, the microfluidic devices with various platforms (e.g. electrofusion and PDMS chip) [42–44] have been successfully used for cell fusion to produce the cellular resource. However, a promising tool is still required to improve the current cellular resource.

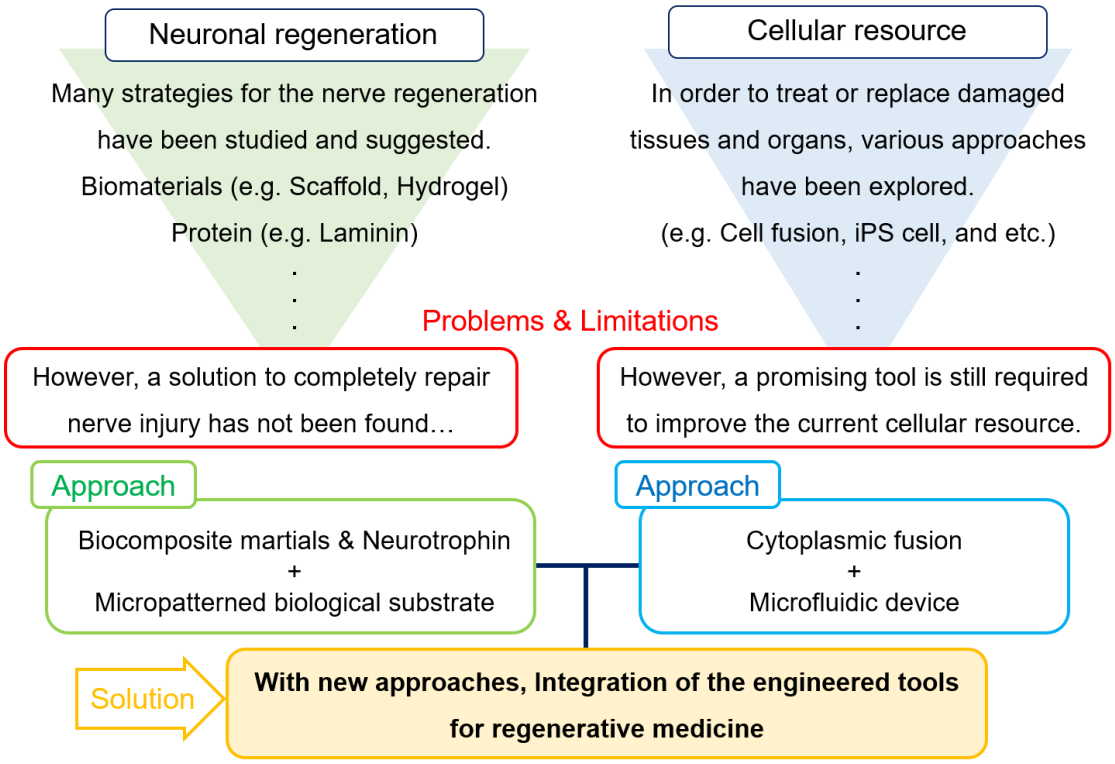

Figure 1.4. Critical issues and approaches for regenerative medicine.

1.2. Composition and objective of this thesis

This thesis focused on the development of microfabrication technology to effectively manipulate cells through a microfabricated technology and a device for regenerative medicine. For this objectives and applications, in this study, a micropattern-immobilized substrate using biocomposite materials and a microfluidics technology were respectively proposed for nerve regeneration and cellular manipulation. In essence, understanding the cellular behavior such as neurite formation is fundamental manner in neuronal network and regeneration. Also, understanding interconnection of neuronal cells mimicking neuronal architecture may provide the unknown mechanisms in neuronal diseases and new insights to efficiently generate neuronal differentiation.

In chapter 2, we therefore aimed that the controlling neuronal cell organization via micropatterned immobilization and the finding an effective way through biochemical and topographical cues of immobilized nerve growth factor. Since the immobilized protein or biomolecules show the effect on cellular behaviors (e.g. proliferation), we expected that the micropatterned substrates with biomolecules may modulate the cellular behaviors of neurons.

Meanwhile, the ultimate goal of regenerative medicine is to replace damaged cells or tissues and it can be potentially accomplished via the process of cellular modification. Although various approaches such as iPS cell method and cell fusion method have been suggested for regeneration medicine, some critical manners are still remaining such as slow and inefficient induction process, contamination of exogenous genes, and etc. In this regard, both improving the current system (In this case, cell fusion method) and producing

useful method with new approach are pursued for varying applications with compatible protocols.

In chapter 3, we therefore aimed to develop the cytoplasmic fusion system which enables the use of resulting cell without genetic modification and to reveal the feasibility of multi-purpose application through various cell combinations for regenerative medicine. The application of microfluidic device is described to effectively manipulate embryonic stem (ES) cell and somatic cell.

In chapter 4, the conclusion and future perspective of this thesis is shown. This chapter summarizes the results and discussion in previous chapters and the feasibility of the immobilization system, cell fusion method, and microfluidic systems underlying the microfabricated device and technology for regenerative medicine.

Overall, we aimed to develop microfabricated device and technology for neuronal regeneration and cellular resource based on protein modification as shown in **Figure 1.5**. For example, the micropatterned substrates with biochemical and topographical cues can be improved through a microfluidic system because the microfluidic device mimicking neural network can be designed to elicit nerve regeneration. In other aspect, the protein modification using live cells by a microfluidic chip can be supported by immobilized substrates with various biomolecules because cellular behavior such as migration and signal transduction is properly modulated depending on the type of micropatterns and biomolecules.

Therefore, the useful platforms through well organized-microfabricated technology (e.g. micropatterned biological substrate) and device (e.g. microfluidic chip) have been developed by us to solve current problems.

The integrated approaches and engineered tools for its application in regenerative medicine will be discussed in this thesis through creating the desirable environment for nerve regeneration and developing the promising method for protein modification.

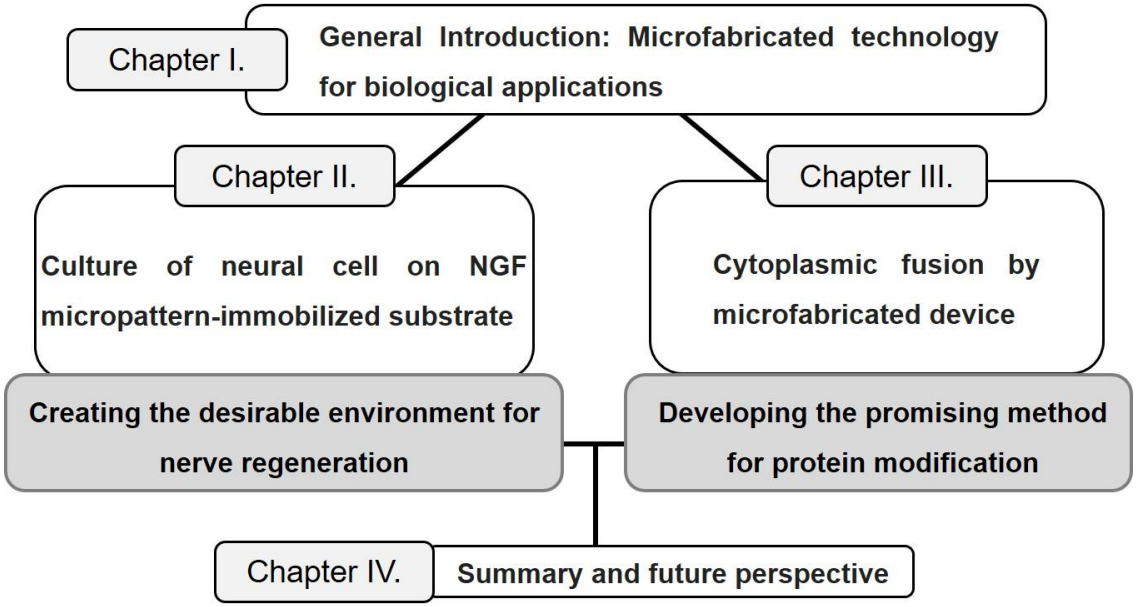

Figure 1.5. Schematic diagram of composition and objective of this thesis.

Chapter 2.

Micropatterned substrate immobilized with nerve growth factor for neurite formation of neuronal cells

2.1. Introduction

Nerve regeneration has been considered as a crucial issue in the medicine field for the treatment of neurodegenerative diseases and injured neurons [45]. Neural tissue engineering is rapidly becoming a growing field of for the discovery of new methods to regenerate the nervous system [46–48]. In order to elicit regeneration after peripheral nerve or spinal cord injuries, several neurotrophic factors such as nerve growth factor (NGF) can be applied to provide a way finding cues in neuronal network [49,50].

However, application of growth factors is usually difficult to be adapted at the injury sites because of their rapid diffusion and poor stability and also requires excessive doses [51–54]. To improve the efficacy and the current limitations, an effective and alternative approach is to immobilize it onto biological substrates that can enable to support nerve repair [55,56]. Immobilization of NGF has been considered useful for material development for the regeneration of neural systems because it is one of the neurotrophic factors that play important roles in neuron survival and neurite outgrowth.

The immobilization of NGF has been performed using various kinds of materials such as gelatin [57], poly(2-hydroxyethylmethacrylate) gel [58], photoreactive chitosan [59], and allylamine-grafted glass [60]. To enhance the activity of immobilized NGF, other approaches such as co-immobilization with an extracellular matrix protein (e.g. laminin) and electrical signal with some surface modifications using conductive polymer (e.g. polypyrrole) have been reported [33,61,62], since it is known that electrical cue is also one of the factors to enhance the activity [63]. In addition to these physical parameters, topographical factors have been recently taken into consideration [64–67].

In this study we prepared nanolayers of NGF-immobilized substrate that can induce neurite outgrowth, resulting in nerve regeneration for investigation of biochemical and topographical effects. As described above, the immobilization is an attractive method to exhibit the ability of growth factors that not only contribute to a high potency and also sustain the signaling pathways for a long time compared with soluble growth factors [58,68]. Here we employed photo-immobilization method using photoreactive gelatin (P-gel) which contains azido phenyl groups to effectively immobilize NGF on a substrate and a rat adrenal pheochromocytoma (PC12) cell. The PC12 cell is one of some cell lines which are widely used as neuronal cell models for neural differentiation. Although it is not originally a neuronal cell type, its neurite formation has been extensively investigated. The photo-immobilization method is simple and effective approach that can improve the stability and promote the performance of growth factors [69–71]. Since neurite outgrowth can be simultaneously correlated with diverse cues in developing neurons, we investigated cell behaviors on the immobilized surface at varying doses and utilized micropatterned substrate by photomask which can modulate the neurite formation and outgrowth [67,72,73]. The topographical (thickness) regulation was performed by the amount of cast P-gel. With regard to the effect of micropatterned immobilization, the immobilized surface with specific topographical property may effectively enhance neurite outgrowth and guidance [59,66,74]. Guiding and promoting neurite outgrowth are essential steps in nerve regeneration and nervous system development [67].

In this chapter 2, we demonstrated controlling neuronal cell organization via micropatterns-immobilized NGF and the biochemical and topographical cues of immobilized NGF as a practical way in understanding neurite formation and neuronal network.

2.2. Objective and approach

2.2.1. Manipulation of neurons

Recent research of neural tissue engineering has focused on the development of bioartificial nerve guidance conduits to guide neurons. A nerve functions correctly when it is able to move freely within its surrounding structures. The effective manipulation for neurons is achieved by the combination of many elements such as biomimetic materials and neurotrophic factors. Better technology for neuronal manipulation in dependent manners is ultimately pursed for modelling diseases of nervous systems and effectively controlling neuronal network via better biomaterials and/or tools [75].

With regards to the better conditions for neuronal manipulation, we aimed to precisely control neurite formation by understanding the relationship between neuronal cells and topology of the substrate with biochemical cues. By considering cell, matrix, and growth factor, ultimately, we approached proper manipulation of neurons to understand neuronal network for nerve regeneration.

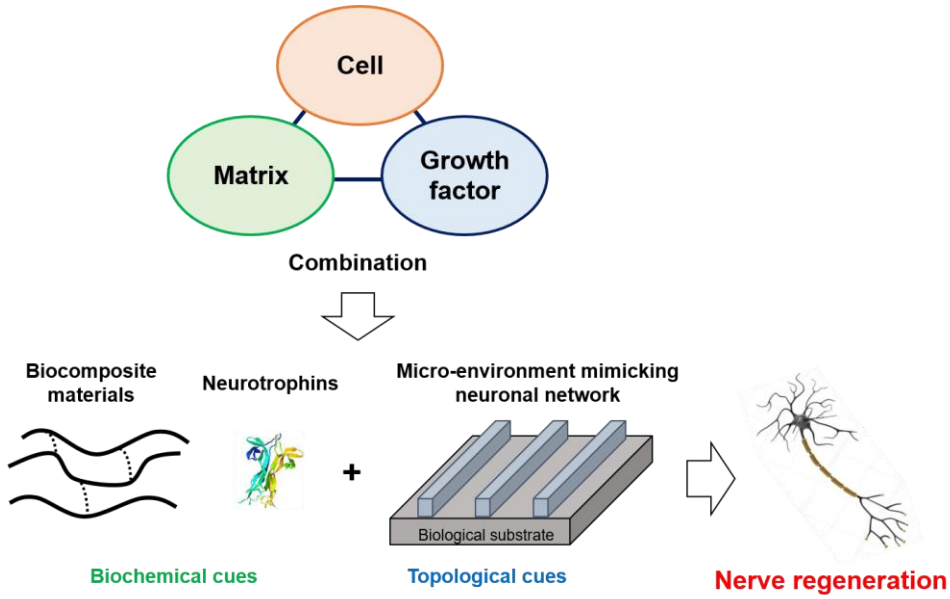

Figure 2.1. Approach for nerve regeneration.

2.2.2. Immobilization of biomolecules

Immobilization can refer to many concepts such as enzyme immobilization in organic chemistry, whole cell immobilization and biomolecule immobilization in biology and biochemistry methods [76–78]. The methods for immobilization have fundamentally involved physical, chemical, biochemical factors such as cross-linking and several types such as encapsulation. The methods have been classified relying on such a reversible (e.g. adsorption) or an irreversible state (e.g. covalent coupling, entrapment, crosslinking). In terms of binding to a support, physical adsorption, ionic binding, and covalent binding is accompanied to immobilized enzyme or biomolecules such as a growth factor.

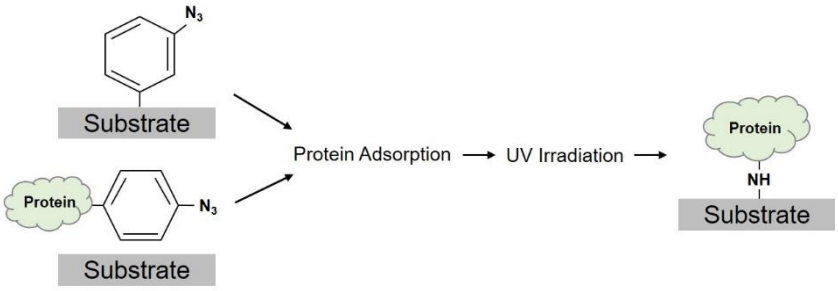

Figure 2.2. Immobilization of biomolecules on substrate.

To immobilize biomolecules on biological substrate, one of the useful methods is photo-immobilization based on photoreactive biomaterials such as azido-phenyl gelatin [79,80]. This involves functionalizing the growth factor with a photo reactive group and binding the modified growth factor to biomaterials and biocompatible substrates upon exposure to a long wave ultraviolet (UV). In this chapter, we presented this method to effectively introduce NGF for neurons manipulation and focused on how to regulate the neuronal cell behaviors on the immobilized substrate with different patterns and thicknesses through nano- and micro-level roughness. Therefore, we aimed to create the desirable environment for nerve regeneration with simultaneous effect of multiple cues.

2.3. Materials and Methods

2.3.1. Preparation of photoreactive gelatin

Photoreactive gelatin (P-gel) was synthesized according to the method as previously reported [81–83]. Briefly, gelatin powder (200 mg) was completely dissolved in Milli-Q water (100 mL). N-(4-Azidobenzoyloxy)succinimide prepared from the 4-azidobenzoic acid dissolved in 1,4-dioxane (4 mL) was added to the gelatin solution. The mixture was stirred at room temperature for 2 days. The resulting solution was dialyzed against Milli-Q water twice. The P-gel was recovered as powder by the freeze-dry process. The content of azidophenyl groups in the gelatin was determined from the absorbance of azidophenyl groups (λ: 270 nm) using a V-550 spectrophotometer.

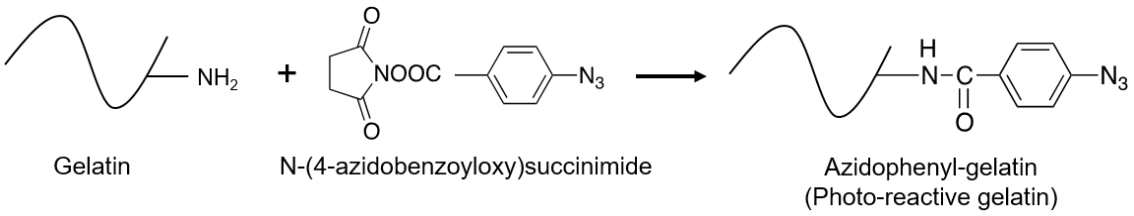

Figure 2.3. Synthesis of azidophenyl-gelatin (photoreactive gelatin).

2.3.2. Surface immobilization of nerve growth factor

The micropattern-immobilized substrate was prepared using P-gelatin as describe in **Figure 2.4**. Nerve growth factor (NGF, Rhβ-NGF, R&D System, USA) was immobilized on Thermanox Coverslip (15 mm in diameter, Thermo Fisher Scientific, USA). The aqueous solution (0.1%) of P-gel was poured (20 μL per plate) onto the coverslip. After

air-drying at room temperature, the plate was irradiated by a UV spot light lamp at 10 cm from light source (12 mW/cm^2) for 10 s and then the plate was washed with Milli-Q water. Subsequently, NGF solution containing P-gel at the varying concentration (From 0.35 to 3.5 pmol/per plate) was poured onto the P-gel-immobilized plate. After air-drying in the dark at room temperature, the plate was exposed to UV at the same condition as above with or without photomask (Toppan Printing, Tokyo, Japan).. The plate was then washed with Milli-Q water repeatedly and prepared for *in vitro* test.

According to specific objectives, photomasks with different width micropatterns were used when the second layer is immobilized by UV irradiation.

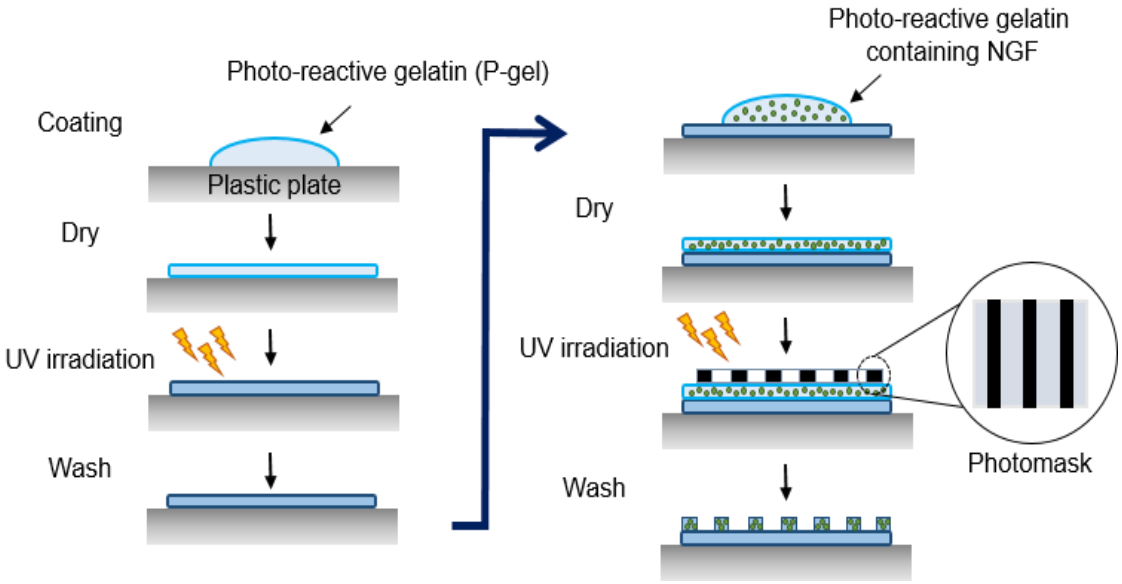

Figure 2.4. Schematic illustration of photo-immobilization.

2.3.3. Staining of NGF-immobilized surface

The NGF-immobilized substrate was blocked with 0.5% goat serum, and incubated with a primary antibody (Rabbit polyclonal to NGF) for 1h at room temperature. After thrice washing with Milli-Q water, the surface was incubated with a secondary antibody (Alexa Flour 488 goat anti-rabbit IgG) in the dark at room temperature for 1 h. The fluorescent signal was observed using a fluorescence microscope (IX71, Olympus, Tokyo, Japan).

2.3.4. Determination of NGF immobilization

To investigate completeness of immobilized NGF, concentration dependent-measurement was performed by changing feeding amount of gelatin. The NGF-immobilized substrate was prepared for *in vitro* quantitative measurement of NGF amount. The prepared sample was repeatedly washed with Milli–Q water until no NGF was confirmed and the released amount was calculated using a rat beta-NGF ELISA kit (Thermo Fisher Scientific, USA). The ELISA assay was performed according to the manufacture's protocol.

2.3.5. Morphological characteristic of materials

A reflective confocal laser microscope (RCLM, LEXT OLS4100, Olympus, Japan) was used to observe morphology of gelatin immobilized micropattern surface. The immobilized substrate was prepared by changing feed amount of gelatin. The sample was

then put on the stage of RCLM and the multiple mirrors of RCLM scanned the laser across the sample and descanned the images across a fixed pinhole and detector. The thickness on micropatterned substrate was measured simultaneously. All procedures of RCLM measurement was conducted in the clean room to avoid any contamination of surface.

2.3.6. Cell culture

PC12 cells were purchased from Japanese Collection of Research Bioresources (JCRB) Cell Bank (Tokyo, Japan) and were cultured in Roswell Park Memorial Institute medium-1640 (RPMI-1640) (Wako, Japan) supplemented with 10% fetal bovine serum (FBS; Cellect MP Biomedicals, Canada) and 5% horse serum originating in New Zealand (HS; Life technologies). The cells were cultured in an incubator at 37 °C with 5% CO_2. When the cells became approximately 70-80% confluent, the cells were harvested and maintained under experimental conditions. To investigate differentiation of PC12 cells in a soluble state of NGF, the culture medium was removed and replaced with differentiating medium containing 1.0% FBS and 0.5% HS with 0.35, 1.0, and 3.5 pmol/mL NGF, respectively. To investigate differentiation of PC12 cells on the NGF-immobilized surface, the cells were cultured in soluble NGF-free growth medium containing 1.0% FBS and 0.5% HS. After the cells were cultured for 2 days, they were then analyzed.

2.3.7. Estimation of neurite formation

Neurite formation of the PC12 cell body was analyzed using Image J and Neuron J programs as reported previously [84–87]. The calculation images are shown in Figure 2.4.

To determine neurite lengths, the neurites were segmented from the cell body and traced by automated tracing of the software. The length was then calculated by the "Analyze skeleton" plugin [86]. For each substrate, the length of neurites was calculated using at least 30 neurites in five independent fields of each image from three different images.

To determine the frequency of neurite-forming cells, the cells were categorized into neurite-forming and non-forming neurites [85,86]. If at least one neurite length in a cell was longer than the cell size, which was calculated by the longest width of the cell, the cell was defined as neurite-forming cell (Cell B). Otherwise, cells were defined as non-neurite-forming cell (Cell A). The frequency of neurite extension was estimated according to the above definition and the following equation [85]. The value was calculated using 30 cells (Cell A + Cell B) in five independent fields of each image from three different images for each substrate.

$$\text{The frequency of neurite extended cell (\%)} = \frac{Cell\ B}{Cell\ A + \text{Cell}\ B} \times 100$$

For analysis of neurite crossing the pattern step, formed neurites were randomly chosen for each substrate, and the ratio of crossing the step was calculated as shown in **Figure 2.5a**. The value was calculated using 30 neurites in five independent fields of each image from three different images for each substrate.

For analysis of neurite-guided cells, the neurite angle between a neurite and patterned direction was determined based on previous reports [88,89]. Neurite-formed cells were randomly chosen and the longest neurite of the cells was analyzed. When the angle of the longest neurite with the cell body was lower than 15°, as shown in **Figure 2.5b**, the neurite-formed cell was categorized as a neurite-aligned cells (Cell B). Otherwise, cells

were defined as non-neurite-aligned cells (Cell A). The value was calculated using 30 cells (Cell A + cell B) in five independent fields of each image from three different images for each substrate.

$$\text{Ratio of neurite-aligned cell (\%)} = \frac{\text{Cell B}}{\text{Cell A + Cell B}} \times 100$$

(a)

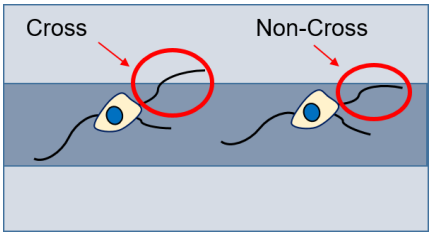

(b)

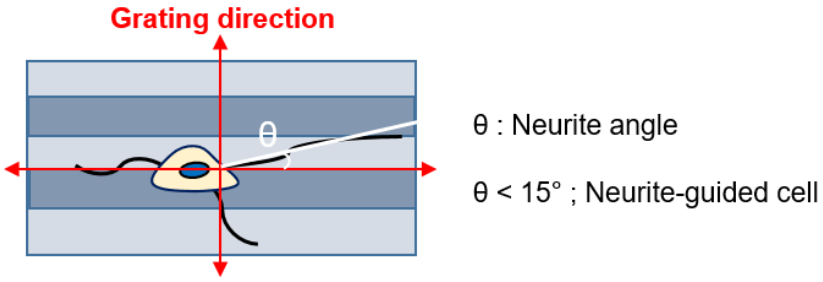

Figure 2.5. Schematic illustration for estimation of neurite formation. (a) Neurite formation on the patterned substrate. (b) Measurement of neurite guidance. The direction of neurites is determined on the micropatterned substrate by the linear pattern of photomask. Neurite angle with $\theta < 15°$ is considered as a neurite-guided cell.

2.3.8. Immunocytochemistry

The PC12 cell was seeded under soluble or immobilized NGF, and then investigated based on immunocytochemistry. For analysis of differentiation, the cells were stained

with antibody against beta-tubulin. In order to determine cell response towards different state of NGF, moreover, the cell signaling based on phosphorylation of NGF was tested using a phospho-TrkA (Tyr490, Neuromics, USA) antibody which detects activated site of Trk proteins when phosphorylated at the corresponding residues. By corresponding to residues surrounding Tyr490 of TrkA, the detected signal of TrkA to neuronal membrane indicates cell response to NGF.

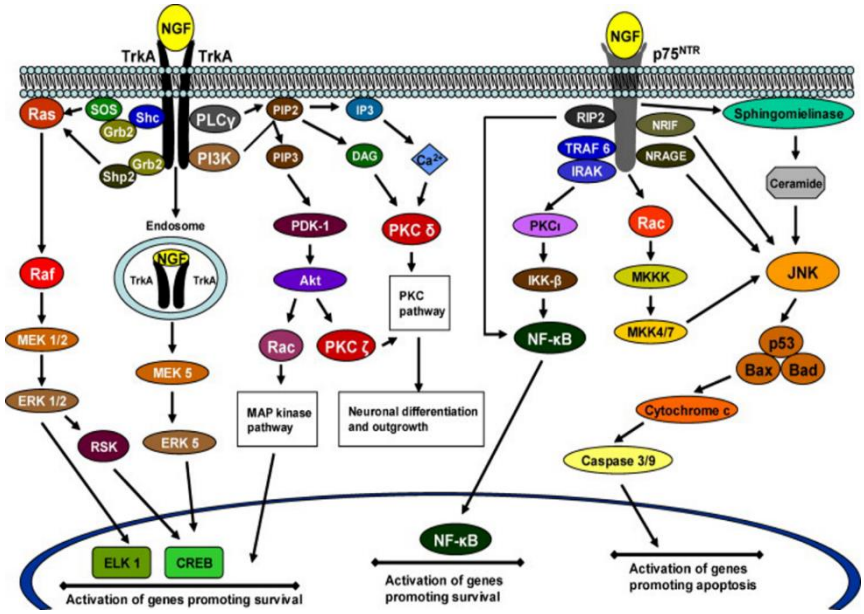

Figure 2.6. Signaling, pathway, and phosphorylation of NGF. © Sciencedirect.com.

2.3.9. Biological scanning electron microscope (SEM) analysis

After cell culture on substrate, samples were rinsed with PBS to remove growth medium components. PC12 cells on the substrates were fixed with 2.5% glutaraldehyde in 0.1 M sodium cacodylate solution pH 7.4 overnight. Samples were then rinsed with 0.1 M sodium cacodylate solution and proceeded to dehydration sequentially via an aqueous

replacement process by soaking in a series of 60%, 80%, and 100% alcohol. The samples were transferred to 100% hexamethyldisilazane (HDMS; HMS) for 10 min and dried overnight. The prepared samples were observed using scanning electron microscope (Thermo Fisher Quattro SEM, Thermo Fisher Scientific, USA).

2.3.10. Statistical analysis

The data were presented as the mean value ± standard deviation (S.D.). Statistical comparisons were performed by a Student's t test and a one-way ANOVA followed by the post–hoc Tukey test. $P < 0.01$ and $P < 0.05$ was considered as statistically significant**.**

2.4. Results

2.4.1. UV spectra measurement

To immobilize NGF on substrate, we first synthesized photoreactive gelatin as we did previously [71,90]. Azidophenyl group introduced gelatin, P-gel, was synthesized by the condensation of amino group on gelatin and *N*-(4-azidobenzoyloxy) succinimide. Before and after the modification of gelatin used for immobilization of NGF was measured using UV spectra (**Figure 2.7**). The resultant gelatin (P-gel) has specific UV absorbance at 270 nm ascribed to the azidophenyl group. Assuming that the molecular absorption was the same as that of azidoaniline, this was slightly red-shifted. Because it may be due to the electron delocalization of the azidophenyl group caused by amide bond formation as previously reported.

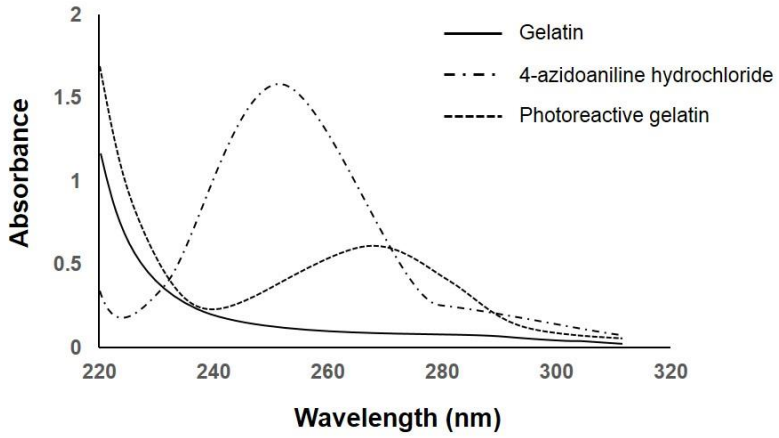

Figure 2.7. UV spectra of before and after modification. A 0.1 w/v% aqueous solution of gelatin (Black-solid), 4-azidoaniline hydrochloride (Black-dash dot), and photoreactive gelatin (Black-square dot) in a 1-cm light path quartz cell at room temperature.

2.4.2. Surface immobilization of NGF

NGF-immobilized sample was prepared according to the protocol as shown in **Figure 2.4**. Upon UV irradiation, the azidophenyl groups in P-gel decompose to form nitrene as a reactive radical to crosslink the NGF, P-gel, and substrate. As described in **Figure 2.8**, P-gel generates radicals and reacts randomly with itself, NGF, and the substrate surface to immobilize NGF by covalent binding or entrapment.

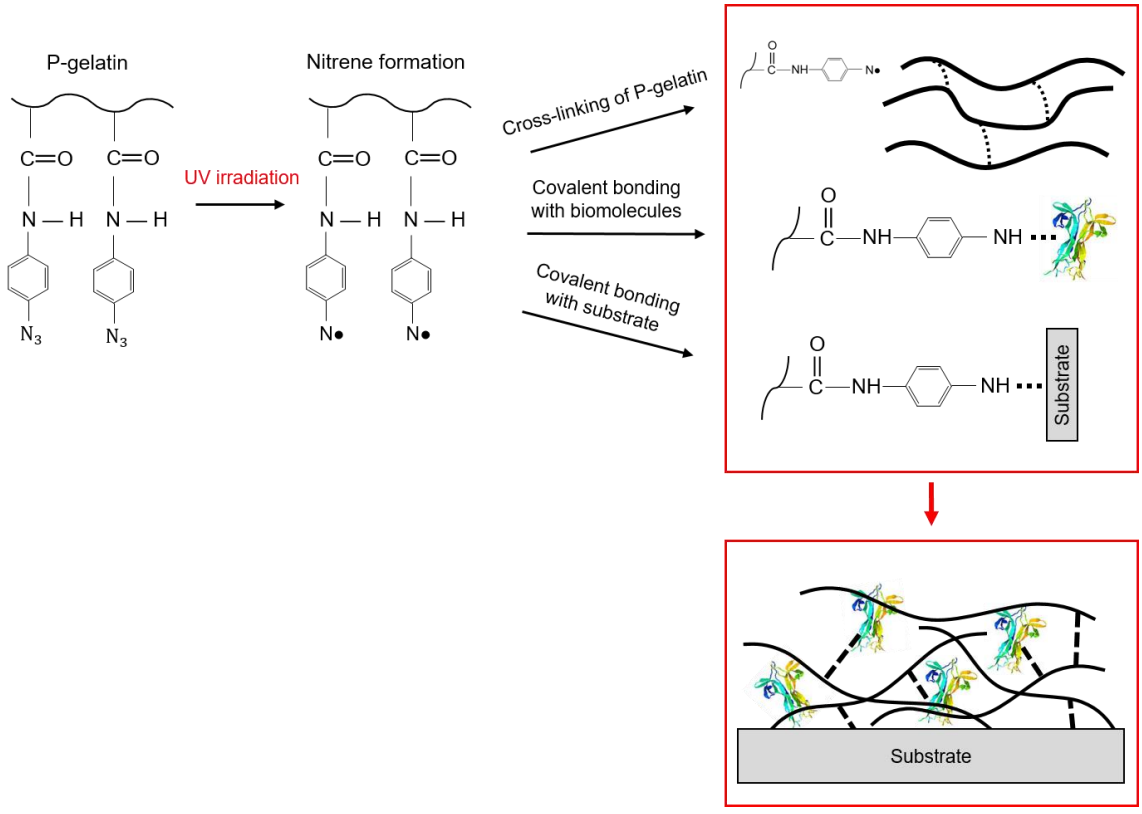

Figure 2.8. Schematic illustration of the mechanism of immobilized biomolecules.

NGF immobilization was confirmed by immunostaining method using stripe NGF patterned surface. As shown in **Figure 2.9**, green fluorescent derived from the Alexa 488 conjugated second antibody was confirmed on the NGF-immobilized area. By changing the shape of patterning photomask, the substrates with covalently immobilized NGF were successfully prepared with different width stripe patterns.

(a)

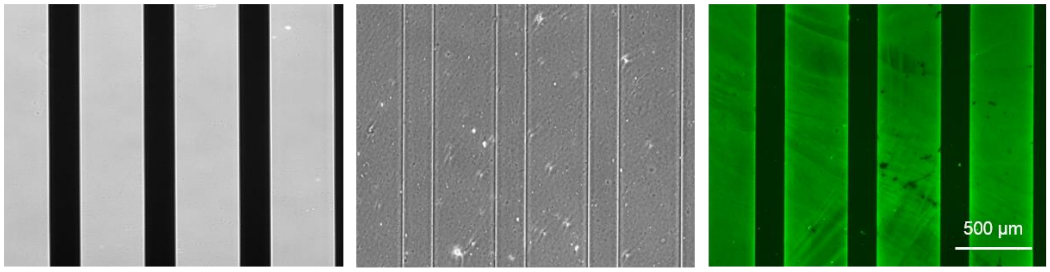

(b)

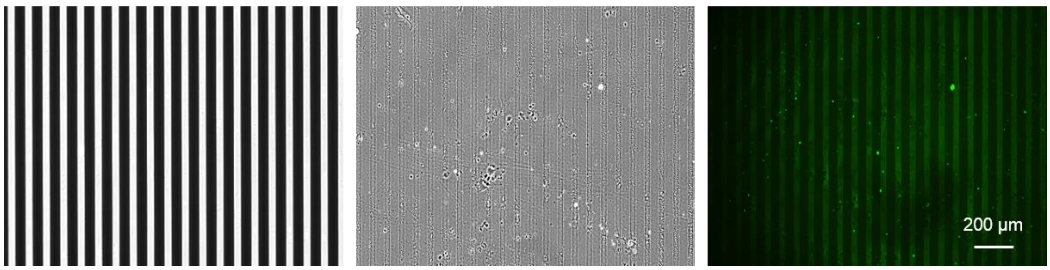

Figure 2.9. Visualization of micropatterned surface. Phase contrast images of the photomask (Left) and micropatterned surface by photoreactive gelatin with the photomask (Middle). Immunofluorescence staining of the immobilized NGF (Right). The wide (a) and narrow stripe pattern (b) were prepared with different width of photomask.

2.4.3. Determination of NGF amount using ELISA assay

To investigate completeness of immobilized NGF, concentration dependent-measurement was performed by changing feeding amount of gelatin. The NGF-immobilized substrate was prepared for *in vitro* quantitative measurement of NGF amount. In order to eliminate the loosely encapsulated NGF, the sample was repeatedly washed with Milli-Q water until no NGF was confirmed and the released amount was calculated using a rat beta-NGF ELISA kit. The ELISA assay was performed according to the manufacture's protocol. As shown in **Figure 2.10a**, the efficiency of NGF immobilization in the P-gel layer increased with increasing the feeding amount of P-gel and NGF. As summarized in **Figure 2.10b**, 100% immobilization of various amounts of NGF (1, 5, 20, and 50 ng) was completed by 0.1%, and 0.5% of P-gel.

Additionally, the NGF-immobilized substrate was tested whether NGF released after immobilization. The sample was prepared by using 20 ng NGF in 0.1% gelatin and the prepared sample was stored at medium in an incubator at 37 $^{\circ}$C. After stored up to 3 days, the medium sample was collected and tested by the ELISA method. No NGF released from the immobilized sample was found as shown in **Figure 2.10c**. Based on these conditions for NGF immobilization, the samples were prepared with the minimal required amount of P-gel (0.1%) to reduce the effect of P-gel in further *in vitro* experiments.

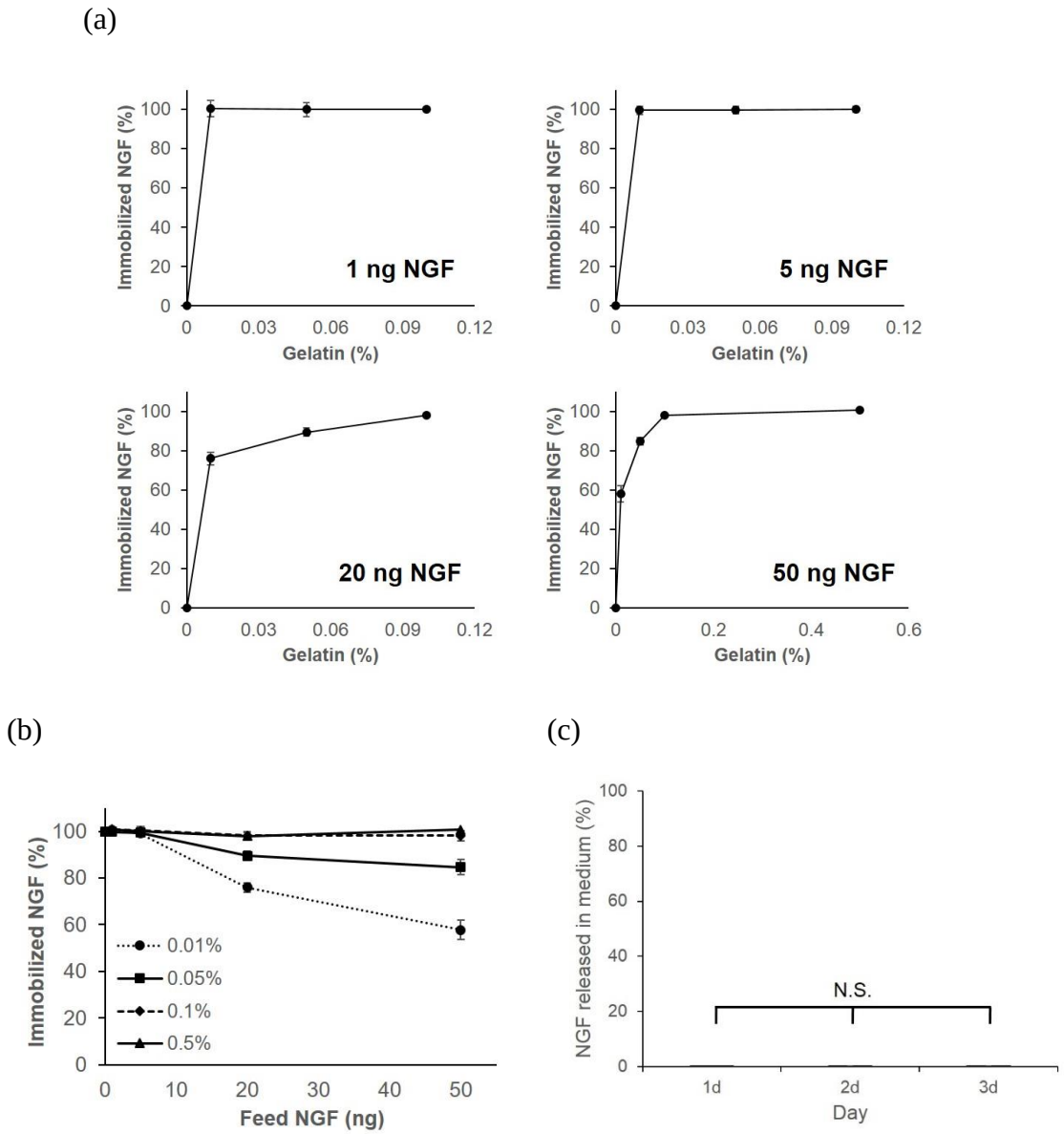

Figure 2.10. Measurement of immobilized NGF on the substrate by ELISA. (a) Immobilized 1 ng, 5 ng, 20 ng, and 50 ng NGF using various amounts of P-gel. (b) The percentage of Immobilized NGF (1, 5, 20, and 50 ng) in gelatin solution using different concentration of P-gel (0.01%, 0.05%, 0.1%, and 0.5%). (c) Released amount of immobilized NGF. The sample was prepared using 20 ng NGF in 0.1% gelatin. Data are presented as the means ± standard deviation from three 96-well plates.

2.4.4. Morphological characteristic of immobilized surface with a micropattern

A reflective confocal laser microscope (RCLM) was employed to observe morphological property of P-gel-immobilized surface such as thickness (**Figure 2.11**).

In case of 0.05% concentration of P-gel, the height change derived from immobilized gelatin was slightly confirmed as 0.02 ± 0.01 μm. In contrast, the surface on 0.1%, 0.5%, and 1.0% concentration of P-gel showed two clear linear distinct areas with increasing thickness. Those thickness at 0.1%, 0.5%, and 1.0% concentration of P-gel were 0.11 ± 0.04 μm, 0.23 ± 0.07 μm (0.5%), and 0.64 ± 0.09 μm (1.0%), respectively. The thickness was increased in accordance with the concentration of P-gel.

Moreover, the thickness at various concentrations was compared with theoretical thickness. The gelatin solution was poured on the plastic plate and the solution was then spread on the substrate (**Figure 2.11b)**. The theoretical thickness was calculated from the amount of cast gelatin on the substrate and compared with RCLM results (**Figure 2.11c**). Using the density of gelatin (1.27 g/cm^3), the volume was calculated and was finally divided by the surface area (15 mm diameter of the plastic disc) to calculate the height based on the relationship between the following two equations.

$$\text{Density (d)} = \frac{\text{Mass (m)}}{\text{Volume (v)}} \qquad \text{(Eq. 1)}$$

$$\text{Volume (v)} = \text{Surface area } (\pi r^2) \text{ x Height (h)} \qquad \text{(Eq. 2)}$$

(a)

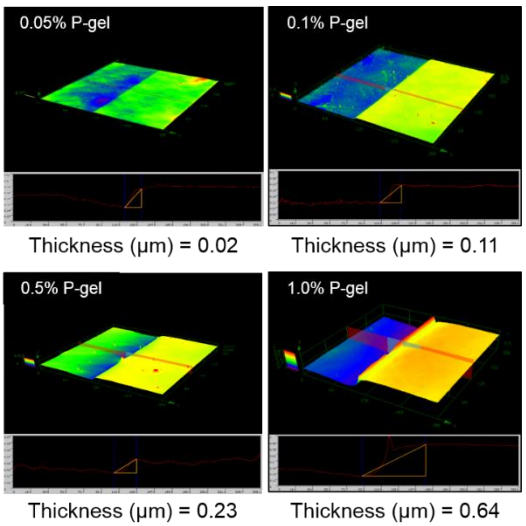

(b)

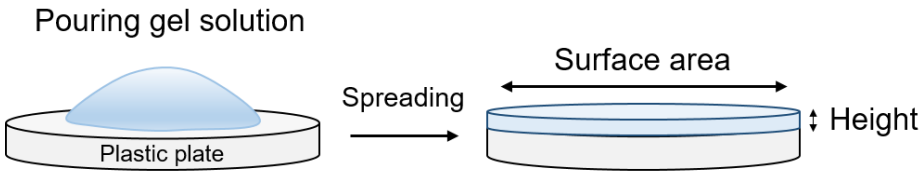

(c)

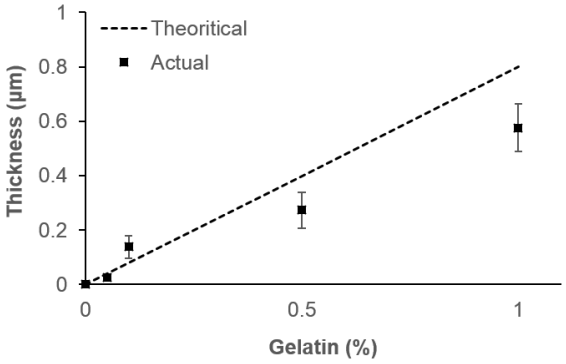

Figure 2.11. Morphology of immobilized surface at various concentrations of P-gel. (a) 3D measurement using RCLM. (b) Schematic illustration for the measurement of thickness by gelatin coating. (c) Comparison of thickness on those immobilized substrate. Average and standard error of measurement for at least three samples per condition are shown.

2.4.5. Cellular behavior on NGF-immobilized surface

We focused on the NGF-activated TrkA receptor in PC12 cell. To compare the TrkA activation by soluble NGF and immobilized NGF, the phosphorylation status of TrkA was investigated by immunohistochemistry using phospho-TrkA (Tyr490) antibody (**Figure 2.12**). As shown in **Figure 2.12a**, the phosphorylation of Tyr490 was found while in soluble and immobilized NGF. By corresponding to residues surrounding Tyr490 of TrkA, the detected signal of TrkA to neuronal membrane indicates cell response to NGF. Although it is suggested that the presence of TrkA leads to cell differentiation by phosphorylation, the direct evidence on signaling under soluble and immobilized NGF is still poor. We assumed that the NGF-TrkA activated sites under diffusible and immobilized state would be different. Therefore, we sought to find the NGF-activated position in the cell under soluble and immobilized NGF (**Figure 2.12b**). The fluorescence signal using Tyr490 antibody was observed by confocal laser microscope to understand the activated position in the cell.

Moreover, the activated signal was used to define the resolution relying on the position in Z-stack images (**Figure 2.12c**). The intensity distributions were compared under the varying positions (From 0 to 12 μm). In case of soluble NGF, the intensity at middle and/or top areas which indicate the activated signal was higher than that of bottom area. On the other hand, immobilized NGF showed the higher intensity at the bottom area compared with that middle and/or top areas. As shown in illustration (**Figure 2.12d**), the signal was detected around middle and/or top area of the cell, in which soluble NGF activates the phosphorylation. In contrast, the signal was existing around bottom area of the immobilized substrate in case of immobilized NGF.

(a)

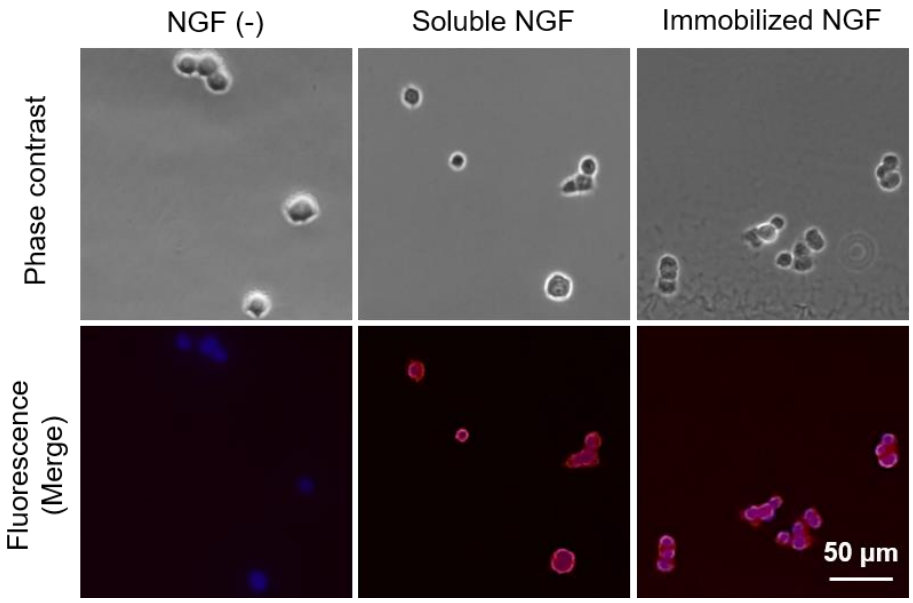
NGF (-)
Soluble NGF
Immobilized NGF
Phase contrast
Fluorescence (Merge)
50 μm

(b)

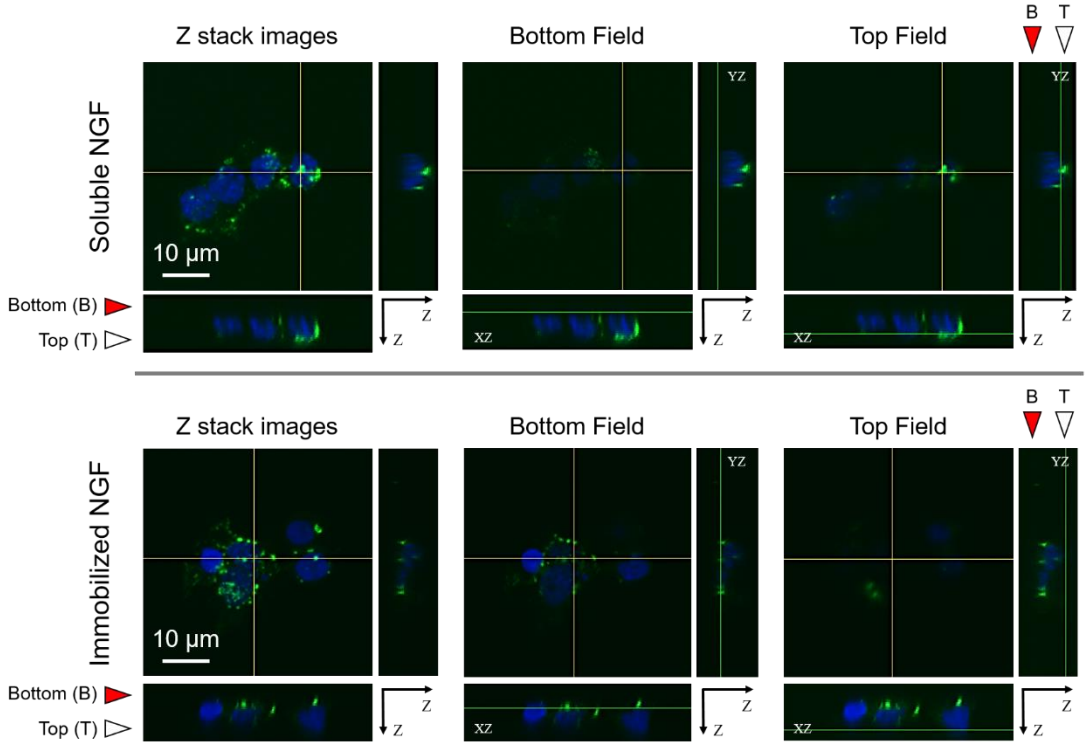
Z stack images
Bottom Field
Top Field
B
T
Soluble NGF
10 μm
Bottom (B)
Top (T)
YZ
XZ
Z
Immobilized NGF
10 μm

(c)

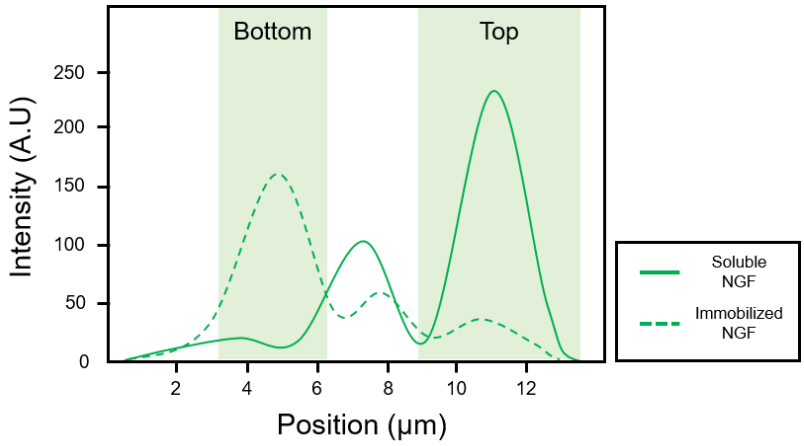

(d)

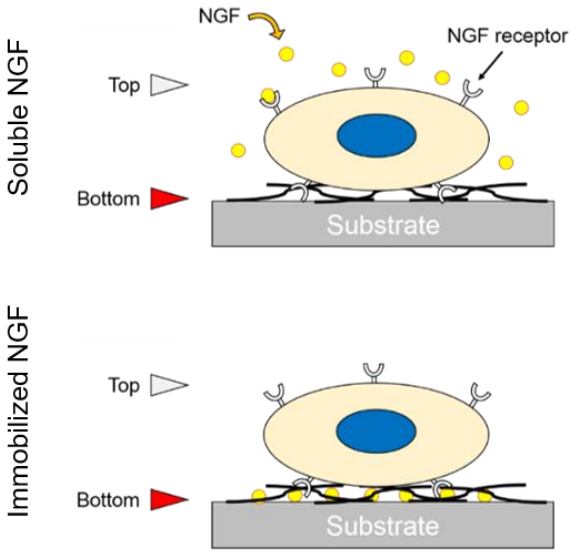

Figure 2.12. Comparison of cell signaling under different state of NGF. Using immunostaining method, the signaling under soluble NGF and immobilized-NGF was detected by (a) fluorescence microscope (2D) and (b) confocal laser microscope (3D). (c) Analysis of the fluorescence signals using Z-distribution of stack images by confocal laser microscope. (d) Based on the result, the NGF-activated signal in the cell is described with additional illustration.

Micropatterned substrate with NGF-immobilized region and non-immobilized region (In this case, only gelatin-immobilized region) was introduced using photomask with a linear micropattern to investigate the effect of NGF-immobilized surface on the cell behaviors (**Figure 2.13**). PC12 cells were homogeneously seeded on the micropatterned substrate. Although the cells were distributed both on non-immobilized (200 μm) and NGF-immobilized regions (400 μm) when they were seeded, the PC12 cells seemed to preferentially migrate towards NGF-immobilized region after 12-24 hours and significant neurite extension only occurred on NGF-immobilized region after 48 hours.

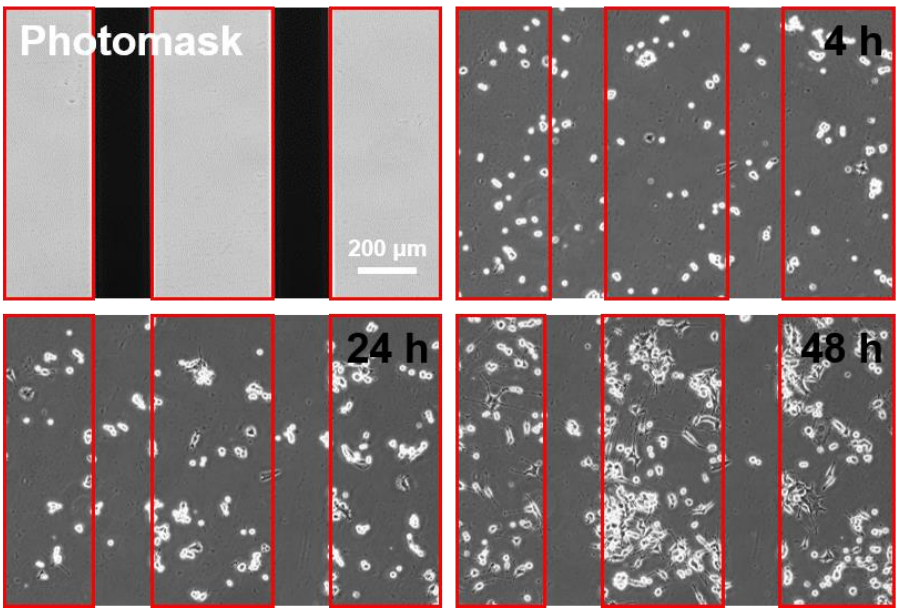

Figure 2.13. Cellular behavior on the micropattern-immobilized NGF substrate. Based on a linear pattern photomask, the non-immobilized region (shaded area of the photomask) and NGF-immobilized region (open area of the photomask; red line) were 200 μm and 400 μm, respectively. The phase contrast images show the cellular behavior on the micropattern-immobilized NGF substrate.

In order to test growth tendency, PC12cell was cultured on non-patterned substrate with soluble and immobilized NGF and without NGF (Negative control). As shown in **Figure 2.14**, The cells proliferated approximately 150% at 24 h and 220% at 48 h under all conditions, but the cell growth without NGF shows high confluent (approximately 300%) at 72 h compared with those of soluble and immobilized NGF (approximately 250%). While the cells underwent proliferation until 72 h when no NGF, the cell proliferation almost stopped under soluble and immobilized NGF and accordingly the cells initiated differentiation with neurite outgrowth similar to previous reports [91,92].

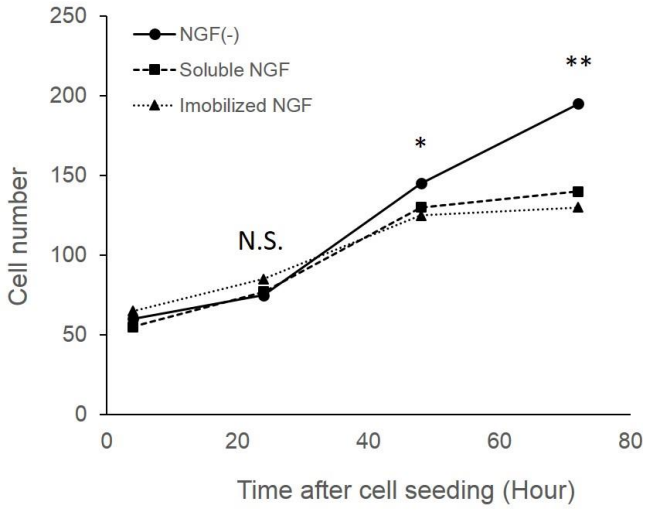

Figure 2.14. Proliferation assay of PC12 cell. The cells were cultured with soluble and immobilized NGF and without NGF and the proliferation was measured at 4, 24, 48, and 72 h. None treated group is used as a negative control; NGF (-). N.S., no significant difference, $P < 0.05$; *, significant difference, $P < 0.01$; **, significant difference. Average and standard error of measurement for at least three samples per condition are shown.

2.4.6. Quantitative comparison of soluble and immobilized NGF

Moreover, the neuronal behaviors such as neurite extension and formation are characterized under different state of NGF. As shown in **Figure 2.15a**, neuron cell body shape is divided in two morphological categories (I and II: round or elongated body shapes). Neurite branches are defined as two (III and IV: Neuron cell body and neurite branches) or more neurite branches (V and VI: Neuron cell body and neurite branches). The morphological characteristic was used to evaluate neurite length and frequency of neurite-extended cells based on the method section. PC12 cells were cultured under either soluble or immobilized NGF (**Figure 2.15b**). PC12 cells cultured without NGF had round cell bodies and almost no neurites as did the cell cultured on non-immobilized region. In contrast, the cells under soluble or immobilized NGF at varying dose increased the number of neurites per cell. Based on the results, the frequency of neurite extended cells and neurite length was furthermore estimated to determine NGF-dependent neurite formation (**Figure 2.15c**). By increasing the dose of NGF, both soluble and immobilized NGF increased the frequency of neurite-extended cells, although the dependence on immobilized NGF was lower than that on soluble NGF when the dose was at < 1 pmol/well. However, the immobilized NGF showed the similar level on neurite formation of PC12 cells as soluble NGF when the dose is at > 1 pmol/well. In case of neurite length, neurites do extend with increased NGF concentration. When a dose of NGF is higher than 1.0 pmol/well, it significantly enhanced greater neurite extension of PC12 cells. In particular, neurite length on the NGF-immobilized surface with relatively high concentration (3.5 pmol/well) did extend 87.33 ± 8.32 μm two times longer than that on the NGF-immobilized surface (0.35 pmol/well). These results indicate that NGF can be immobilized with varying dose to effectively elicit neurite outgrowth.

(a)

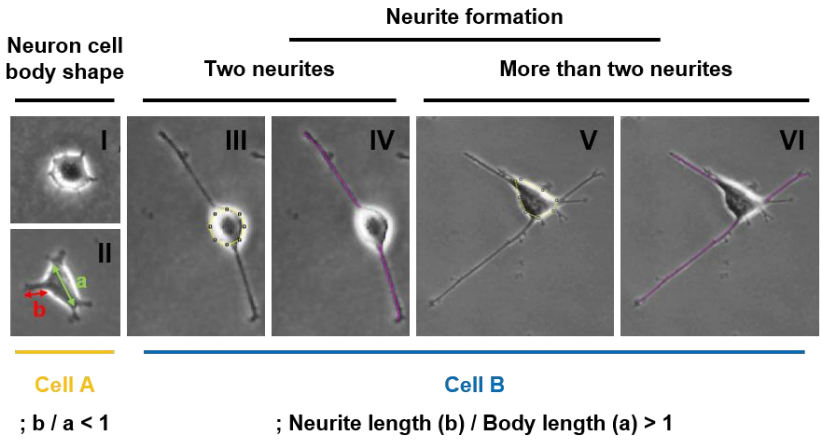

(b)

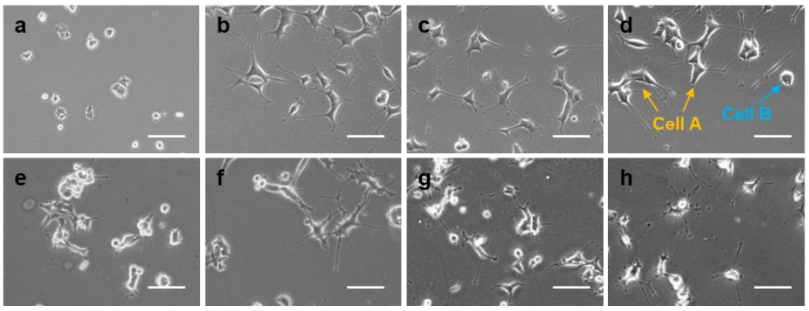

(c)

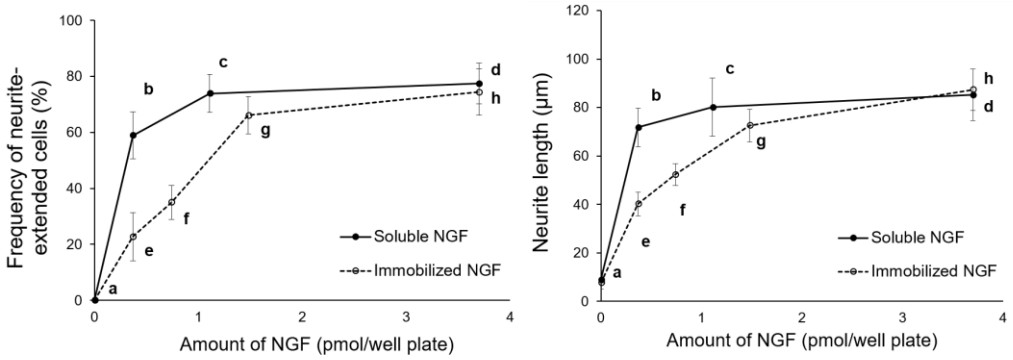

Figure 2.15. Characterization of neuronal behavior under soluble and immobilized NGF. (a) Definition of neuron cell shape and neurite formation. (b) Representative images of cellular morphology at various concentrations of soluble and immobilized NGF. No NGF; Negative control (a), Soluble NGF; 0.35, 1.0, and 3.5 pmol/well (b-d), Immobilized NGF; 0.35, 0.75, 1.5, and 3.5 pmol/well (e–h). Scale bar: 100 μm. (c) Frequency of neurite-extended cells and neurite length with soluble and immobilized NGF. Average and standard error of measurement for at least three samples per condition are shown.

2.4.7. PC12 cell differentiation under soluble and immobilized NGF

Since PC12 cells formed neurite outgrowth on non- or NGF-immobilized substrate, the nerites outgrowth indicating differentiation of PC12 cell was estimated by immunohistochemistry using monoclonal antibody against beta-tubulin. As shown in **Figure 2.16**, the visualized neurites showed significantly lengths of neurite extensions on NGF-immobilized substrate similar to those on soluble NGF. In contrast, no significant neurite extension was found in the cultured cells without NGF. This result indicates that the soluble and immobilized NGF effectively induce differentiation of PC12 cells.

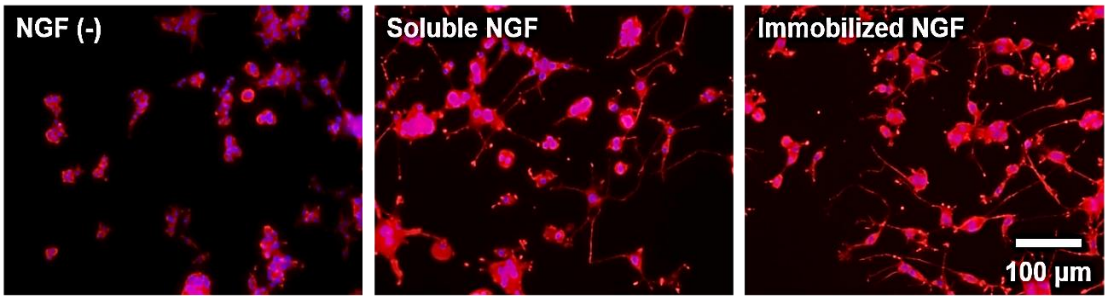

Figure 2.16. Morphology of PC12 cells cultured with or without NGF. To measure differentiation of PC12 cells based on neurite visualization, the cells were stained with antibody against beta-tubulin (red) and the nuclei were stained with DAPI (blue).

2.4.8. Thermal stability and reusability of immobilized NGF

To investigate the thermal stability of immobilized NGF, samples were incubated at 37, 42, and 60 °C for various durations. As shown in **Figure 2.17**, significant loss of NGF activity was observed in soluble case. On the other hand, the immobilized NGF showed a lesser decrease of activity at any temperature. Therefore, the immobilization maintained the biological activity.

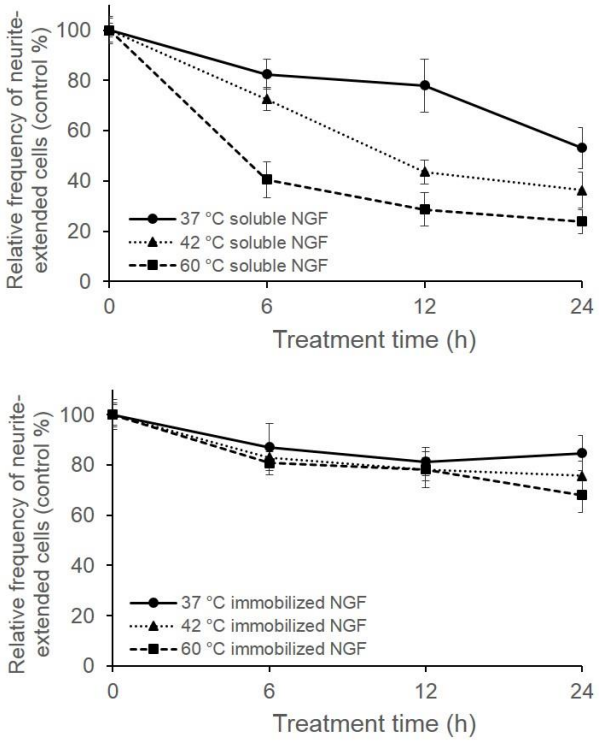

Figure 2.17. Frequency of neurite-extended cells cultured with soluble NGF and immobilized NGF pretreated at 37, 42, and 60 °C for 6, 12, and 24 h. Cells cultured with soluble and immobilized NGF without pretreatment were used as controls, and cells at 0 h were considered as 100%. Cells were cultured with either pretreated soluble NGF in growth medium or pretreated immobilized NGF. Data are presented as the mean ± SD, *n* = 3.

To confirm the stability of immobilized NGF, it was repeatedly used after cell culture as shown in **Figure 2.18**. The results showed no significant decrease in the biological activity of the reused plates with immobilized NGF in comparison with that of the fresh plates. It indicates at least two reuses without losing the biological activity that induced neurite outgrowth.

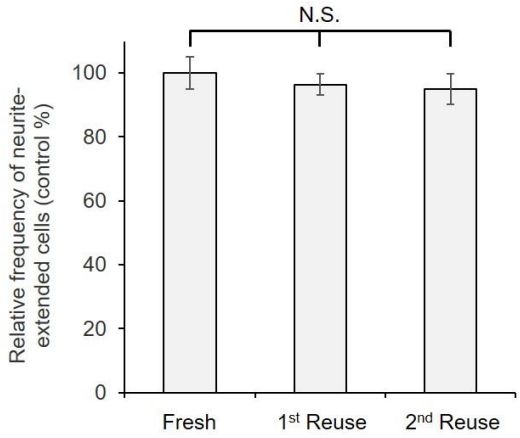

Figure 2.18. Frequency of neurite-extended cells cultured on immobilized NGF that was reused twice. Cells cultured on a freshly prepared surface with immobilized NGF were used as controls and considered as 100%. Data are presented as the mean ± SD, n = 3. N.S., no significant difference.

2.4.9. Height effect of micropatterned substrates on neurite direction

We designed the immobilized substrates with different height between first and second gelatin layers to evaluate the neurite direction on those substrate (**Figure 2.19**).

The contact guidance of formed neurites was investigated on the different thicknesses of micropatterned layers in the presence of 100 ng/mL soluble NGF. In case of a low height (26 nm), the neurites had sporadically formed and outgrew regardless of the patterned surface. The uncontrolled direction of neurite outgrowth was observed between first and second layers by growing over the second layer. In case of high height (>130 nm), on the other hand, the neurites had extended and aligned on the borderline of the two layers. Neurite direction seemed to be decision depending on the relationship between neurite diameter (30–40 nm) and height (< 26 nm or > 130 nm) of the immobilized substrate.

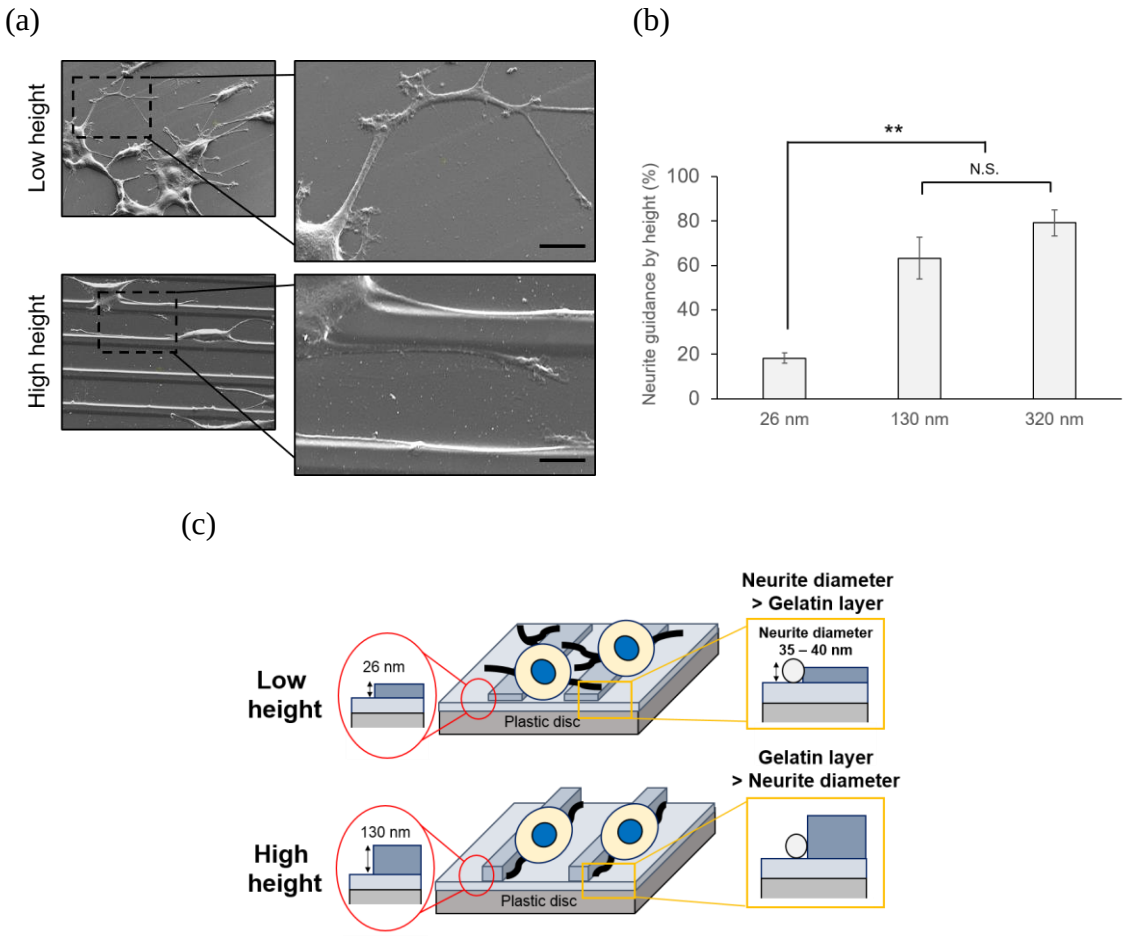

Figure 2.19. Control of neurite direction by immobilized height. (a) Observation of the cellular response towards different height using SEM analysis. The micropatterned surface was prepared by a narrow linear pattern using a photomask (10 μm: 15 μm). Scale bar: 10 μm. NGF at 3.5 pmol was added in each well. (b) Comparison of neurite guidance by height. The neurite direction was estimated on the NGF-immobilized substrates with different height. The height between first and second gelatin layers was adjusted by the different concentration of gelatin. NGF at 3.5 pmol was added in each well. (c) Schematic illustration for neurite formation by the relationship between neurite diameter and immobilized height. Data are presented as the mean ± SD, n = 3. N.S., no significant difference, $P < 0.01$; **, significant difference.

2.4.10. Effect of micropatterned surface on neurite formation

Since the neurite has been shown in response to topographical cues of substrates such as height as shown in **Figure 2.19** and others [35,93], the micropatterned surfaces by various linear widths were prepared to identify the further cues of immobilized NGF on neurite orientation which is correlated with neural network. The size of NGF-immobilized region and non-immobilized region was designed with different widths by photomask and the micropatterned surface was uniformly achieved according to each width. In case of only gelatin-immobilized substrate, the soluble NGF was added to growth medium to trigger neurite outgrowth. As shown in **Figure 2.20a**, widths of a linear pattern photomask with shaded and open areas are 10 μm: 15 μm, 25 μm: 40 μm, 50 μm: 25 μm, and 400 μm: 200 μm, respectively. Prior to cell culture, all substrates were immobilized by gelatin through photomask with various ratios of the linear between UV-transparent and non-transparent regions. In case of soluble NGF, NGF was added to growth medium to assist in neurite outgrowth when the cells were cultured. PC12 cells were homogeneously seeded on those substrates and the neurite formation was then estimated.

The extension of neurites showed similar tendency to the results as shown in **Figure 2.15**. The neurites of PC12 cell cultured on the narrow micropatterned surfaces (10 μm: 15 μm) with NGF immobilization showed elongation by aligning with the immobilized direction (**Figure 2.20b**). The ratio of neurite oriented cells on the substrate is about 81%. Most cells on the patterns extended two or more neurites bi-directionally and the extended neurites are much larger than cell body. In cells cultured on NGF-micropatterned surface with 25 μm: 40 μm, the direction of neurites seemed to be extend similar to that on NGF-micropatterned surface with 10 μm though the ratio of neurite oriented cell was decreased

to 51%. On the contrary, the cells seemed not to be oriented, in which NGF-micropatterned surface over 50 μm: 25 μm and accordingly the total ratio of neurite oriented cells was decreased to approximately 35%. In case of much wide pattern (400 μm: 200 μm), the neurites were sporadically and asymmetrically extended and they were not oriented by the patterned surface. All gelatin-micropatterned substrate with soluble NGF tested showed varying ratio of neurite orientation as did all NGF-micropatterned substrate. Importantly, NGF-immobilized substrate with narrow pattern (< 25 μm) moreover showed orienting and promoting neurite outgrowth which may enable to modulate neural network. By utilizing the surface with micropatterned-NGF immobilization, we could achieve distinct components such as promoting outgrowth of neurites and steady neurite orientation at once, resulting in the development of nervous system [67,82].

Overall, elongated cells on narrow-patterned substrate apparently produced oriented neurite directions, in contrast with neurite formation showing arbitrary directions on wide patterned substrate. More importantly, we found that the biochemical and topographical cues of NGF-immobilized substrate are correlated with neurite formation.

(a)

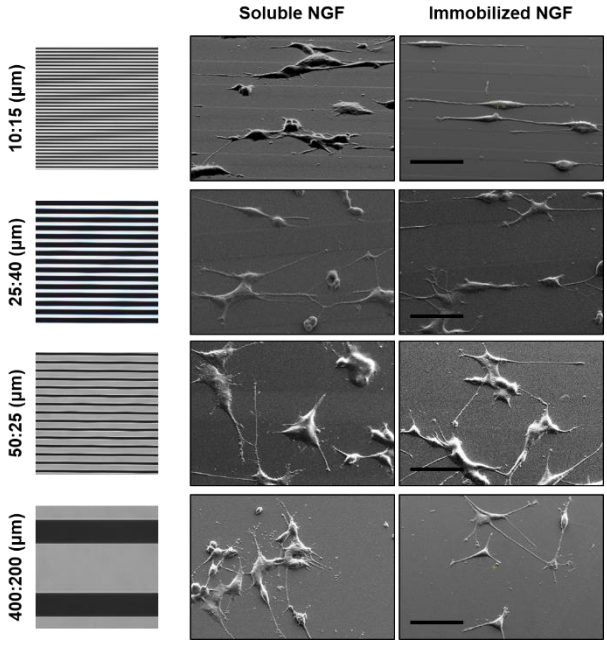

(b)

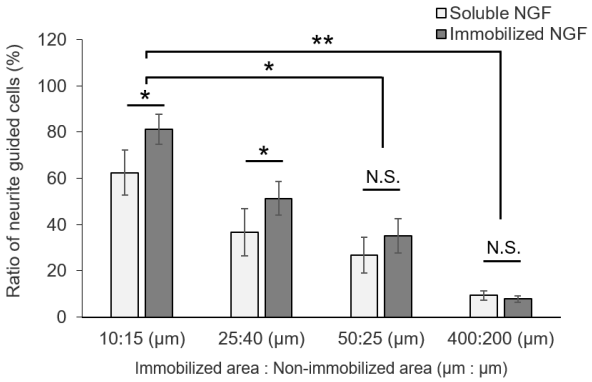

Figure 2.20. Orientation of neurite direction by micropatterned substrate. (a) Photomask with different linear patterns and SEM images of the outgrowing neurite of PC12 cells on micropatterned substrates. Scale bar: 50 μm. (b) Estimation of the neurite orientation. Data are presented as the mean ± SD, $n = 3$. N.S., no significant difference, $P < 0.05$; *, significant difference, $P < 0.01$; **, significant difference.

2.5. Discussion

Characterization of immobilized surface

NGF was covalently immobilized by P-gel on substrate and the substrate was successfully prepared with different width stripe patterns. Using high concentration of P-gel (0.1% and 1.0%), the distinction indicating height difference between first and second layers on immobilized surface was significantly different. Based on the coffee-ring effect in the drying process [94,95], we assumed that the thickness would be slightly different relying on the measured region on the immobilized substrates. When compared the thickness of immobilized surface with the theoretical thickness based on the reported density of gelatin [96], the thickness on the immobilized layers was very close to the theoretical thickness. More importantly, the result indicates that the surface thickness can be easily controlled by changing the concentration of gelatin. Therefore, we can perform *in* vitro cell tests for understanding neuronal behaviors under the different topographical surfaces.

Cellular behavior on NGF-immobilized surface

To investigate the effect of NGF immobilization on PC12 cell behavior, we suggested the micropatterned-substrate immobilized with NGF because the micropatterning enables us to observe the effect of immobilized growth factors at a glance [97,98]. They were randomly distributed both on non-immobilized and NGF-immobilized regions when cells were seeded. However, the cell density increased on the NGF-immobilized regions during the culture. The tendency on the NGF-immobilized region was considered to be due to the migration of cells and their gradual trapping by immobilized NGF. The cells on the NGF-immobilized region consequently resulted in significant neurite outgrowth. The

micropatterned-substrate immobilized with NGF simultaneously showed both of the trapping of cells and neurite outgrowth. Also, the immobilized NGF showed the superiority in the maintenance of its biological activity and the reusability compared with the soluble NGF. The immobilization maintained the activity of NGF through reduction of the conformational flexibility of NGF by fixation as observed in enzymes [Ref]. Taken into consideration with other previous reports [Ref], we concluded that the reusability of biomolecules, such as growth factors, enzymes, and antibodies, may be facilitated by immobilization.

Quantitative comparison of soluble and immobilized NGF

With regard to appropriate environment for cellular experiment, we considered that the substrate with different topology also affects various cellular behaviors such as neurite formation. Neurite is a unique feature of neurons allowing formation and maintenance of the nervous system. Neurite formation of PC12 cells such as neurite extension was accordingly assessed by software programs as well as immunocytochemistry using beta-tubulin antibody associated with differentiation of PC12 cell. Extension and frequency of neurites of PC12 cell was investigated on the NGF-immobilized substrate at varying dose and compared with the soluble NGF state. The neurite extension and frequency of neurite outgrowth from PC12 cells cultured with NGF was increased when compared to that of no NGF group. The cells cultured on the NGF-immobilized substrate had neurite-per-cell counts and frequency of neurite-forming cells similar to those of cells cultured with soluble NGF. Interestingly, the neurite extension seems to respond dependently to the varying dose of NGF and the effect was saturated at > 1 pmol/well plate, although the soluble NGF showed higher activity at a low concentration compared with immobilized NGF. Previously, Yu et al. [59] described almost the same effect on neuron survival (70%)

after 3 days of culture using 30 ng/cm^2 chitosan-immobilized NGF and 50 ng/mL soluble NGF, and Lee et al. [33] demonstrated almost the same level of PC12 neurite formation (30%, 14 μm length) was achieved by both of immobilized NGF and 50 ng/mL soluble NGF. The immobilized NGF 30 ng/cm^2 reported by Yu et al. [59] corresponds to 1.5 pmol/well plate in the present study and the soluble NGF 50 ng/mL reported by Lee et al. [33] corresponds to 1.7 pmol/well plate in the present study. Therefore, the present results indicate that the same level effect was obtained by the same amounts of NGF as reported previously.

Signaling of the cell toward soluble and immobilized NGF

In terms of the effect of immobilized biomolecules on cellular behaviors, we have demonstrated the good performance with the sustained efficacy for various cellular behaviors [79,99,100]. Moreover, understanding the signaling under different state (soluble or immobilized state) of biomolecules (In this case, NGF) is one of the new approach to demonstrate the signal transduction towards the neurotrophic biomolecule. NGF as neurotrophin family is critical for cell survival and differentiation in both the central and peripheral nervous system [101,102]. The intimate receptor which binds NGF is Tropomyosin receptor kinase A (TrkA). Phosphorylation at Tyr490 is required for association to trigger the Ras-MAP kinase signaling cascade and transcription factors. The resulting changes in gene expression induce differentiation and neurite outgrowth. We found that the NGF-activated position in the cell seemed different under soluble and immobilized NGF. The results based on the activated position in the cell suggest that NGF-immobilized substrate plays a role in internalizing the NGF-TrkA complex from the NGF-immobilized region to cell body. More importantly, immobilized NGF directly

elicits the phosphorylation of TrkA from the immobilized surface and NGF allowed the cells to achieve the signal of activating neuronal differentiation through immobilization. It has been known that the immobilized growth factors such as insulin, epidermal growth factor (EGF), fibroblast growth factor enhance cell growth more than soluble growth factors, because of inhibition of down regulation of signal transduction caused by cellular internalization of growth factors [55,70,103]. It is also been reported that immobilized EGF promotes neurite formation of PC12 cells, although soluble EGF enhances the growth of PC12 cells [104]. In case of NGF immobilization, neither promotion of neurite formation nor switching of gene expression occurred. The signal transduction mechanism of growth is different from that of differentiation in PC12 cells [105]. It is also well known that the differentiation depends on sustained signaling [106]. On the other hand, it is also been reported that nerve growth cone exhibits adaptation through desensitization and resensitization by wide ranges of concentrations of guidance factors and the down-regulation depends on the endocytosis of receptors [107,108]. Considering these studies, cone guidance is up-/down-regulated but neurite formation requires sustained and monotonous signaling. Therefore, it was considered that no down-regulation process which occurred in the growth regulation occurred in the differentiation process. As a result, a specific difference between soluble and immobilized NGF was found in neurite formation.

Evaluation of the topographical effect of micropatterned substrates

Although the effect of NGF-immobilized substrate on extended neurites was explored, there exists less information on the topographical influence of micropatterns-immobilized NGF on the cellular behaviors. Hereby, we explored how immobilized surface with micropattern influences neurite network. In terms of topographical effect, different

heights between first and second gelatin layers were introduced to evaluate the neurite direction on those substrate. The contact guidance of formed neurites was investigated on the different thickness of micropatterned layers in the presence of 100 ng/mL soluble NGF. In the case of a low height (26 nm) of the step, the neurites had sporadically formed and outgrew regardless of the patterned surface. However, in the case of a high height (>130 nm), the neurites had extended and aligned on the borderline of the two layers. Considering the largest diameter of a neurite was about 30–40 nm, a 100 nm of layer thickness was sufficient for contact guidance of neurite. Previously, Chua et al. [88] and Beduer et al. [89] and reported the neurite guidance by microfabricated polydimethylsiloxane (PDMS). According to Chua et al., the height ranged from 350 nm to 4,000 nm, and the neurite alignment of hippocampal murine neural progenitor cells monotonously increased with the increase in height. Considering that the present material was based on gelatin, the greater adhesiveness than PDMS to neurites may reduce the threshold height that a cell can recognize. Taken together, neurite direction seemed to be decision depending on the relationship between neurite diameter and height of immobilized substrate. These results imply that the height of immobilized substrate by gelatin plays an important role in controlling neurite formation, resulting in neuronal network. Understanding the topographical cues on neurite outgrowth is critical to interpret neural network in strategies for neuroregeneration [109–111].

Effect of micropatterned surface on neurite formation

Since we found that the neurite formation respond to topographical cues of immobilized substrates, the further cues of immobilized NGF was estimated using the micropatterned substrates by various linear widths of photomask. In order to guide neurites, we chose micropatterned substrate with narrow stripe because it may enable to

elucidate the guidance of neurite formation as well as prevent the sporadic formation of neurite. NGF-immobilized substrate with narrow pattern showed guiding and promoting neurite outgrowth which may enable to modulate neural network. In such a certain environment, the ratio of neurite-guided cells became increased. When the micropattern width was enlarged, the neurite orientations became more random. This result indicates that the neurite alignment of cells can be finely modulated when the number of gelatin-based step increased. Ferrari et al. [112] performed nanotopographic control of PC12 cell on nanoprinted cyclic olefin copolymer films and they found that a 500 nm width was the most effective for the formation of a bipolar shape, and that on a width lager than 1,500 nm, cells had the tendency to form a multipolar shape. However, Beduer et al. [89] reported a 60 μm groove width contributed more to alignment than au unpattern surface. The present study showed that neurites can be modulated by a sufficient height for neurite guidance and a sufficient narrow groove, and indicates the NGF immobilization increased the alignment of neurites. Considering that NGF concentration-dependent neurite formation [72,73] as well as chick dorsal-root axons turn toward high concentrations of NGF [113], the enhanced alignment was due to the direct interaction between neurites and immobilized NGF. By utilizing surfaces with micropatterned NGF immobilization, we could simultaneously achieve distinct components such as neurite extension, promoting outgrowth of neurites, and steady neurite guidance, resulting in the development of nervous system. Elongated cells on the narrow patterned substrate produced longer neurites and guided neurite directions, in contrast with neurite formation showing arbitrary directions on the wide patterned substrate. Overall, we demonstrated that the biochemical and topographical cues of NGF-immobilized substrate are correlated with neurite formation.

2.6. Conclusion

We prepared NGF-immobilized substrates by the photo-crosslinking to study neurite formation. We found that the immobilized NGF induced neurite outgrowth similar to soluble NGF. The micropatterns-immobilized substrates with the different topographical surfaces effectively led to the specific cellular behaviors such as neurite orientation.

Through the micropatterned substrate involving different height, we revealed neurite morphogenesis and its relationship with topographical cues. The micropatterned immobilization of NGF simultaneously showed biochemical and topographical effects on neurite formation. Therefore, organizing neuronal cells in narrow cell-adhesive patterns mimicking neural network may result in effective applications for neuronal regeneration.

In neural engineering applications, various models such as nanofiber [30,31], conducting materials [32,33], biological substrates [34], and microfluidic systems [35] have been studied and suggested for nerve regeneration. Although the methods have also shown its efficiency, the development of desirable environment and the useful platform are still required for nerve regeneration. Understanding the previous models and NGF immobilization system, the microfabricated tool by combining aforementioned parameters will provide important cues to generate neuronal networks.

Thus, we expect that the combined-NGF immobilization system will provide important cues to generate neuronal networks through synergetic effect of topographical and biochemical property.

Chapter 3.

Cytoplasmic fusion by a microfluidic device

3.1. Introduction

Cell fusion is an important part of normal growth and development of organisms including human. It has been involved in a technology and a natural process. In terms of cellular development, cell fusion is an important process during differentiation of muscle and bone cells, embryogenesis, immune response, and tissue formation [114–116]. Despite the importance of these processes in organisms, there is not fully understanding in the mechanism of cell fusion and the factors which can regulate the process [117,118].

A number of researchers have studied cellular fusion and various factors about the fusion involving human cell types (e.g. stem cell) owing to its importance and therapeutic significance [119]. Considering the applicable characteristic of various somatic cells, the cellular reprogramming into pluripotent stem cell has attracted huge attention in the medicine field. Various approaches such as nuclear transfer into enucleated oocytes [120], co-culture with stem cell [121], and genetic factor transduction [38] enable us to obtain great knowledge and prospect in regenerative medicine. To enhance the approach, induced pluripotent stem (iPS) cells and cell fusion have been demonstrated to be a potent way of clinical application due to its high efficiency and celerity [39,122].

In regenerative medicine, particularly, the cell fusion technology opens new possibilities of genetic repair with a notable role in stem cell plasticity, and it has been shown to be implicated in tissue regeneration [123,124]. Although cell fusion has been considered as a traditional technology in methodology, the technology still possesses a lot of potential for various purposes and making new discoveries as a promising research field. The better understanding regarding the mechanism and application has been required for future research such as human therapy [125]. In other words, the feasible and

promising cellular resource has been pursued for the multi-purpose application in regenerative medicine.

Fusion using either same or different types of cells can be obtained by several ways such as chemical (e.g. polyethylene glycol; PEG) [126,127], physical (electric pulse) [128,129], or biological (e.g. viruses or receptors) [130–132] methods. The fusion by above methods is basically relying on random cell-cell contacting and pairing, resulting in low fusion efficiencies, and that the traditional fusion methods such as electrofusion are still inefficient. The selection step to isolate the desired resulting cells is also required by antibiotic selection or lengthy subculture.

Recently, microfluidic chip-based method has shown its prominent feasibility and potential to improve the current limitations such as low efficiency and to precisely manipulate cells, ranging from single cell to hybrid cell [133]. The cell fusion research has been performed by diverse kinds of microfludic platforms such as droplet-based device [42], microfludic perfusion [134], electrofusion chip [135], and PDMS chip [44,136]. Remarkably, PDMS-based microfludic devices with various designs have led to precise manipulation of cells. Both improving the process of cell fusion and controlling the cell contacting and pairing are fundamentally crucial parts in this technology and cell fusion.

In this study, we have presented that a microfluidic device-based the cell fusion method to investigate the feasibility of cytoplasmic transfer between two different cells that is probably associated with cellular reprogramming and to improve the unsolved problem (e.g. abnormal karyotypes) caused by nuclei mixing, thus inapplicable to regenerative medicine. Therefore, various attempts have gradually focused on the potential from

genetic modification involving transcriptional factors to protein modification involving cytoplasmic factors.

The cell fusion in the present study was performed using a novel microfluidic device which can enable two different cells to be cytoplasmic fusion without nuclear mixing. This approach has involved protein modification rather than genetic modification so that we may understand the potential of cytoplasm regarding reprogramming. Using the newly designed-microfluidic device by us [137,138], we can consider application of the resulting cells after cytoplasmic fusion for regenerative medicine as well as the approach revealing the unknown mechanism for cellular reprogramming.

Another important issue is feasibility and application of stem cell (e.g. embryonic stem (ES) cell) to the microfluidic chip for cellular protein modification [139,140]. The use of ES cell with our novel method was also considered as a potent cellular resource due to its great potential in regenerative medicine. ES cell normally exists in small shape and size (~ 10 μm) compared with normal somatic cell (10–20 μm). Accordingly it is difficult to apply the ES cell to current PDMS chip which has cell pairing structure. It also implies that the cell contains small amount of cytoplasm which might not enough to induce cellular reprogramming, resulting in slow and inefficient induction process like conventional limitations. In terms of protein modification using cytoplasmic elements, therefore, the sufficient amount of protein in the cytoplasm and enlarged cell size is ultimately required for high acquisition efficiency. Especially for ES cell application, demecolcine (DC), one of colchicine derivatives, was used for establishment of polyploid mammalian frequently cell lines [141,142].

Consequently, we can obtain enlarged ES cell containing increased cytoplasm amount, solve the above limitations, and perform the cytoplasmic experiment with high efficiency.

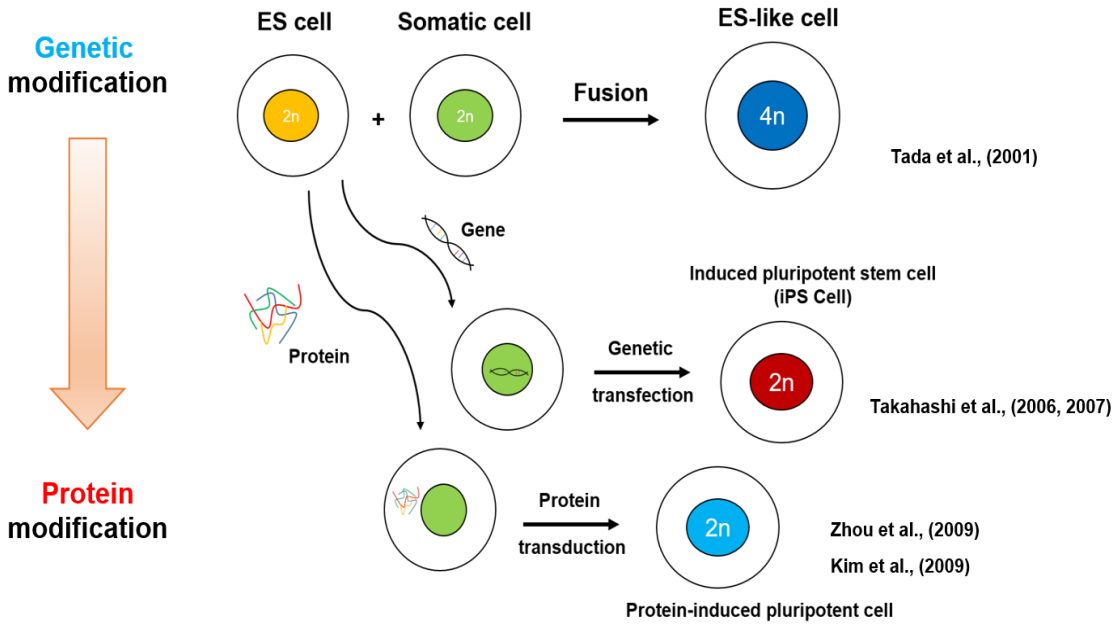

Figure 3.1. Schematic diagram from genetic modification to protein modification.

3.2. Objective and approach

3.2.1. Application of microfluidic device and ES cell

In terms of cellular resources, various methods such as induced pluripotent stem (iPS) cells and cell fusion have been introduced for regenerative medicine and cell therapy [37,38,143]. However, there are still some critical issues remaining such as slow and inefficient induction process, some risk of tumorigenesis and insertional mutagenesis and that the conventional method still contains some limitations such as nuclear mixing resulting in abnormal karyotypes, thus being inapplicable to regenerative medicine.

Therefore, other approaches to produce cellular resources have been explored by us and others [136,144]. One promising method to avoid such abnormal karyotypes is to make cell fusion without nuclei mixing through microstructured. Herein, we introduced the novel cell fusion methods based on microfabricated devices using PDMS. By using the device which is newly designed by us, we found that the microfabricated aperture such as microslit can produce cell fusion between suspended and adhered cells using a Sendai virus envelope (HVJ-E)-based cell fusion method [145]. However, the mixed fusion with nucleus like conventional cell fusion method still has been occurred in the microslit design, and detailed observations of cytoplasmic transfer between ES cell and fusion partner cell (e.g. embryonic fibroblast) were not performed in the previous studies.

Therefore, we introduced the newly designed-microfluidic device with microtunnel for further study. In terms of pluripotent-like cellular resources, application of ES cell is ultimately pursed to make a promising tool due to its tremendous potential. Although we demonstrated that the cytoplasmic fusion between live somatic cells such as fibroblast can be achieved by our microfluidic device, it is still difficult to apply ES cell to the

current device owing to its limitations such as small size of the cell. More importantly, we expected that the enlarged ES cells which contain a large amount of cytoplasm including organelles may effectively induce the prominent production of cellular resources for regenerative medicine. Because the cytoplasm and protein in the cells is highly associated with cellular modification.

In this chapter 3, we therefore introduced the enlarged ES cell by treatment of bioreagents such as demecolcine (DC) with HVJ-E method as shown in **Figure 3.2**. Furthermore, we focused on the feasibility and potential property of cytoplasmic fusion to contribute the novel technique to regenerative medicine.

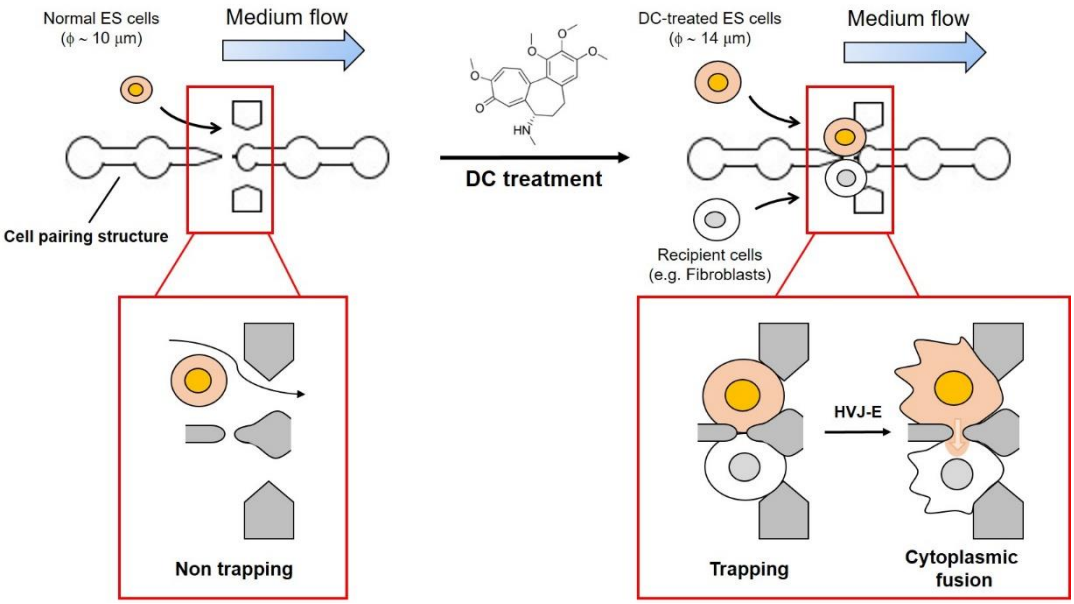

Figure 3.2. Application of ES cell through a bioreagent and a microfluidic device.

3.2.2. Single cell research

Understanding cellular behaviors and the mechanism for arising of cells is ultimately important for fundamental study as well as advanced study in regenerative medicine.

To reveal unknown mechanisms, the research should be started from single cell level with understanding of organelles. Because initiation of tissue and organ is generally originated from the single cell and organelles in the initiation and development of cells have greatly associated with controlling cellular behaviors. In this study, we aimed to investigate how single cell is manipulated by the micro structure, and to control various cells such as ES cells for regenerative medicine through microfabricated device and bioreagents. As summarized in schematic illustration (**Figure 3.3**), we presented that new approach towards cellular modification, and monitoring the cytoplasmic exchange in live cells by using newly designed-microfluidic device and also revealing the potential and feasibility of organelles to elicit cellular reprogramming through use of enlarged ES cell.

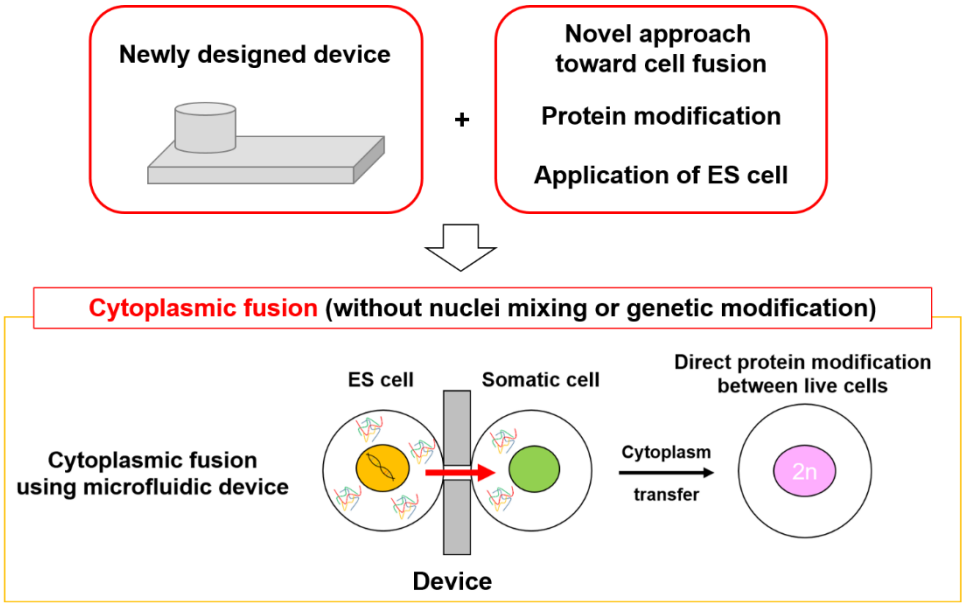

Figure 3.3. Schematic illustration of aim and methodology of this study.

3.3. Materials and Methods

3.3.1. Preparation for cell fusion

Cell fusion experiment can be performed in accordance with different strategies as shown in **Figure 3.4**. In terms of cell fusion using a microfluidic device, we focused on the strategy (b) and cell lines such as ES cell and fibroblast cell were accordingly prepared to study cytoplasmic fusion. In particular, those cells were transfected by fluorescence plasmid DNA such as EGFP and mCherry so that the phenomenon of cytoplasmic transport could be monitored in a microfluidic device.

3.3.2. Sendai virus (HVJ) induced cell fusion

Sendai virus (also known as hemagglutinating virus of Japan; HVJ) was used as a main method for cell fusion as described in **Figure. 3.4** (**Figure 3.5**). HVJ Envelope Cell Fusion Kit (GenomONE-CF) was obtained from Cosmo Bio Co., LTD., Japan. The cell fusion experiment was performed according to the manufactures' protocol. Briefly, HVJ (Sendai virus) was inactivated and purified as a HVJ envelope (HVJ-E). The purified HVJ-E product was dissolved in HVJ-E suspending buffer and/or cell growth medium. The prepared reagent was immediately used or stocked in -80 °C. Cell A and cell B are suspended in the medium containing HVJ-E suspension (2.5 μL of HVJ-E suspension / 100 μL of growth medium), and they were mixed by gentle pipetting. The mixed cells were then transferred to the microfluidic device for further incubation.

(a)

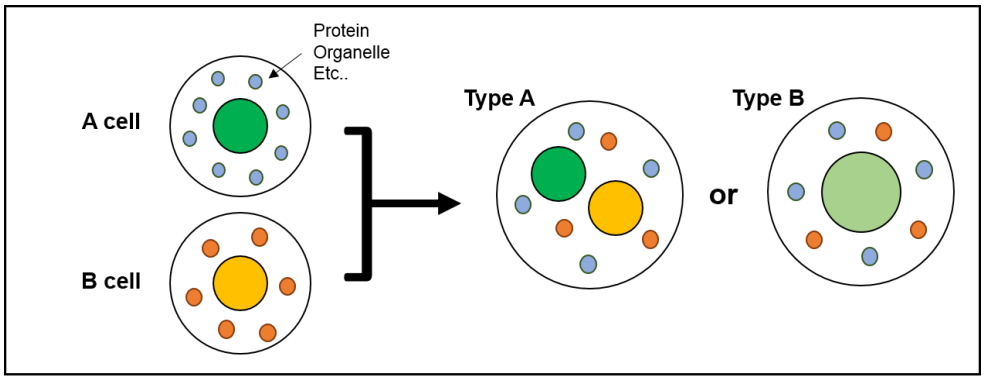

(b)

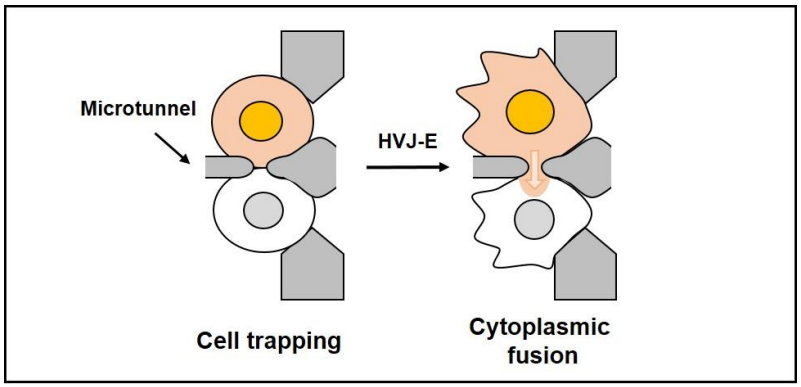

Figure 3.4. Schematic illustration of cell fusion by different strategies.

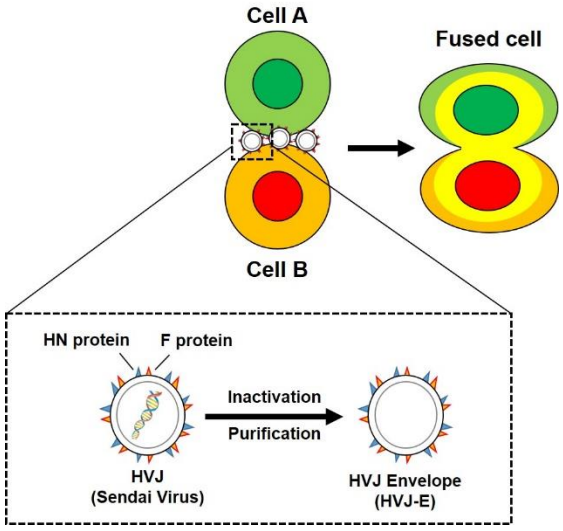

Figure 3.5. Principles of cell fusion by HVJ-E method.

3.3.3. Cytoplasmic fusion using microfluidics devices

A newly designed microfluidic device was used for cytoplasmic fusion without nuclei mixing. A poly (dimethylsiloxane) (PDMS)-based chip was fabricated as described previous reports [137,138]. This device has a cell pairing structure (CPS) that can make cell pairs through microtunnels with several μm width. A silicon tube with a 3 mm inner diameter was glued to the top of the chip as an inlet reservoir. The microfluidic device was attached onto the bottom of a 35 mm culture dish. To perform cell fusion experiment, the microchannel in the chip was degas-driven flow and was then filled with a culture medium [146]. Cell suspension (10–30 μL) was prepared with approximately 1×10^6 cells/mL and applied to the inlet reservoir. After cells are subjected by hydrodynamic forces through centrifugation at 500 rpm for 1 min, the cells were subsequently trapped and fused in the CPS by the HVJ-E method.

3.3.4. Cell culture

Mouse embryonic stem (ES) cell line, feeder-free EB3 cells (129/Ola-derived EB3 ES cells), was supplied by Dr. Niwa group (CBD, RIKEN, Japan) and was cultured in Glasgow minimum essential medium (GMEM; Nacalai Tesque, INC., Japan) supplemented with 15% fetal bovine serum (FBS; Biowest, USA), 1mM sodium pyruvate (Thermo Fisher Scientific, USA), 0.1 mM 2-mercaptoethanol (Sigma-Aldrich, USA), 1x nonessential amino acids (NEAA; Thermo Fisher Scientific, USA), and 1000 U/mL of leukemia inhibitory factor (LIF; FUJIFILM Wako Pure Chemical Corporation, Japan). Primary mouse embryonic fibroblast (MEF) cells (Chemicon, USA) were cultured in Dulbecco's modified Eagle's medium (DMEM; FUJIFILM Wako Pure Chemical

Corporation, Japan) supplemented with 10% FBS. They were cultured on gelatin-coated dishes in an incubator at 37 °C with 5% CO_2, and were maintained under experimental conditions or passed when they present about 70–80% confluence.

3.3.5. Transfection

EB3 cell was transfected with pcDNA3-Mito-EGFP-IP and pcDNA3-mCherry-IH2 using Lipofectamine^{TM} 3000 (Thermo Fisher Scientific, USA). The cells were cultured in GMEM medium supplemented with 15% FBS, 1mM sodium pyruvate, 0.1 mM 2-mercaptoethanol, 1x NEAA, and 1000 U/mL of LIF. The stable cell lines labeled with green (EGFP) and red (mCherry) at mitochondria and cytoplasmic areas, were obtained by cultivation in the presence of puromycin (Pur) or hygromycin B (Hyg), respectively.

3.3.6. Application of cell cycle inhibitor protein

Before applying EB3 cells to the microfluidic device, the cells were cultured in the presence of demecolcine (DC; FUJIFILM Wako Pure Chemical Corporation, Japan). The DC-treated cells were washed by PBS (–) (x 3) and then introduced to the microfluidic device with a fusion partner cell (e.g. MEF) for cytoplasmic fusion experiments.

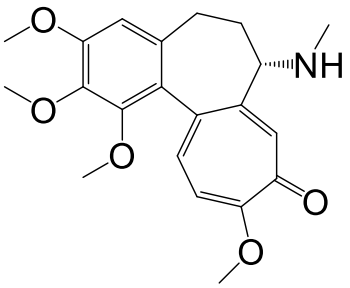

Figure 3.6. Chemical structure of demecolcine.

3.3.7. Real-time PCR (RT-PCR) measurement

To compare the pluripotency of ES cells before and after DC treatment, the gene expression regarding pluripotency was measured by a real-time polymerase chain reaction (RT-PCR). Total RNA was extracted from the cells using an RNeasy Mini kit (QIAGEN, Germany). Complementary DNA (cDNA) was synthesized using the extracted total RNA by reverse transcription reaction. The resulting cDNA was mixed with SYBR® Green Master Mix (Toyobo, Japan) and the following primer pairs (*Nanog*, *Oct4*, *Sox2*, and *Gapdh*) and then used for quantification of gene expression.

Quantification cycle values were determined by regression analysis of the amplification traces. The RT-PCR measurement was performed using the following primer pairs: *Nanog* (forward: CAG GTG TTT GAG GGT AGC, reverse: CGG TTC ATC ATG GTA CAG), *Oct4* (forward: TCT TTC CAC CAG GCC CCC, reverse: TGC GGG CGG ACA TGG GGA), *Sox2* (forward: TAG AGC TAG ACT CCG GGC, reverse: TTG CCT TAA ACA AGA CCA), *Gapdh* (forward: GGA GAA ACC TGC CAA GTA, reverse: AGC CGT ATT CAT TGT CAT).

3.3.8. Cytometric analysis

Using the transfected-EB3 cell lines labeled with green (EGFP) and red (mCherry), the cell size and intensity of each fluorescence color were simultaneously measured using cytometer (Thermo Fisher Scientific, USA). Two colors (green and red) indicate mitochondria and cytoplasm, respectively. For statistical analysis, the total number of cells counted per sample for each condition using 500 cells from three different images.

3.3.9. Statistical analysis

At least three representative samples were used from each case. The data were presented as the mean value ± standard deviation (S.D.). Statistical comparisons were performed by a Student's t test and a one-way ANOVA followed by the post–hoc Tukey test. $P < 0.01$ and $P < 0.05$ was considered as statistically significant**.**

3.4. Results

3.4.1. Structure of microfluidic device

A microfluidic device was firstly designed to perform cell fusion research (**Figure 3.7**). The microtunnel in cell pairing structures (CPSs) was designed by changing the height from bottom side were applied to the structure.

The microfluidic device was achieved by using the master mold as shown in **Figure 3.8**. After preparation of master mold designed with the microstructures, PDMS is pouring and replicated on the master mold. The PDMS chip is released from the master mold after replication and inlet reservoir is glued on the chip. As shown in **Figure 3.9**, the device is mainly categorized in four areas such as inlet, separation, CPS, and out areas. Intensity and height including roughness shows the different topology of the master mold in the four areas. The microfludic device is subsequently used for further *in vitro* cellular experiments.

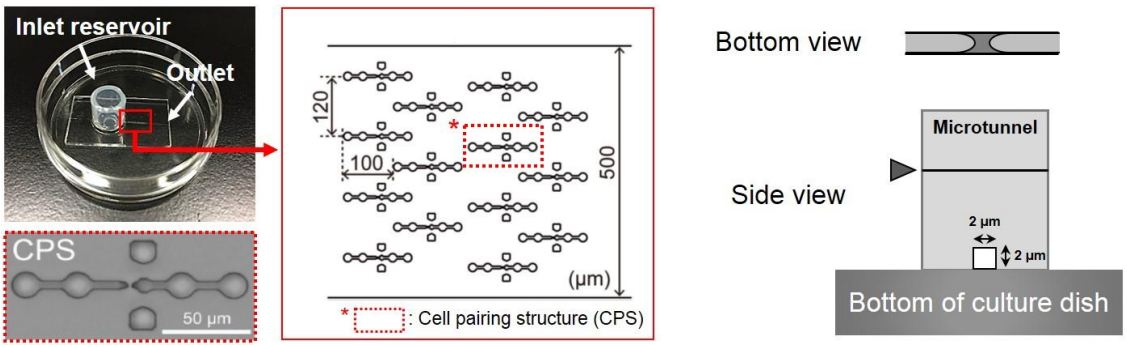

Figure 3.7. Design of the microfluidic device with cell pairing structures (CPSs) and bottom and side views of microtunnel in the device.

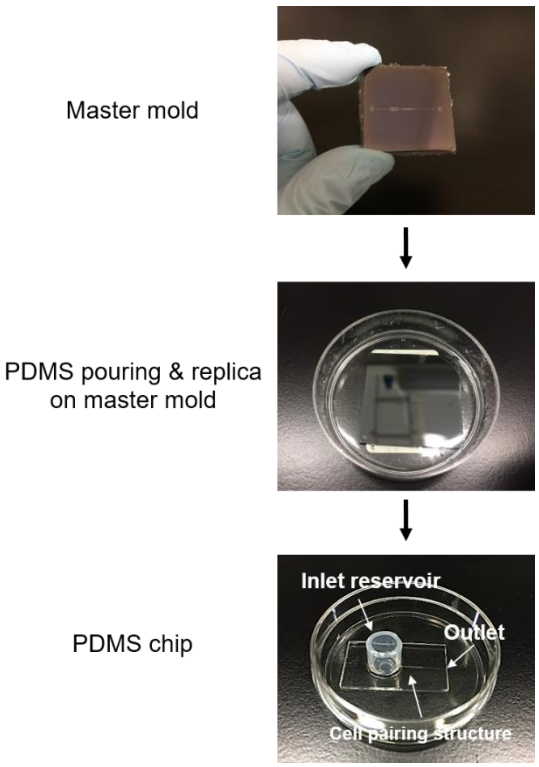

Figure 3.8. Procedures of preparation for the microfluidic device. After preparation of master mold designed with microstructures, PDMS is pouring and replicated on the master mold. The PDMS chips is separated after replication and inlet reservoir glued on the chip.

(a)

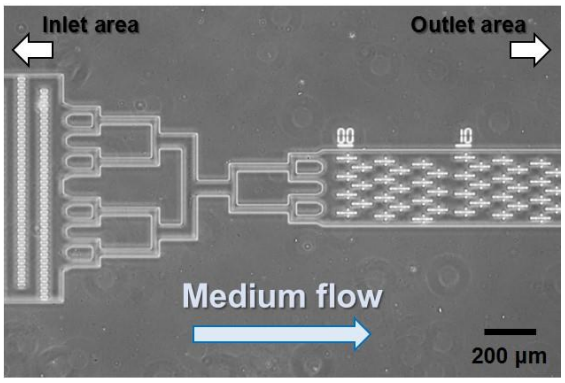

(b)

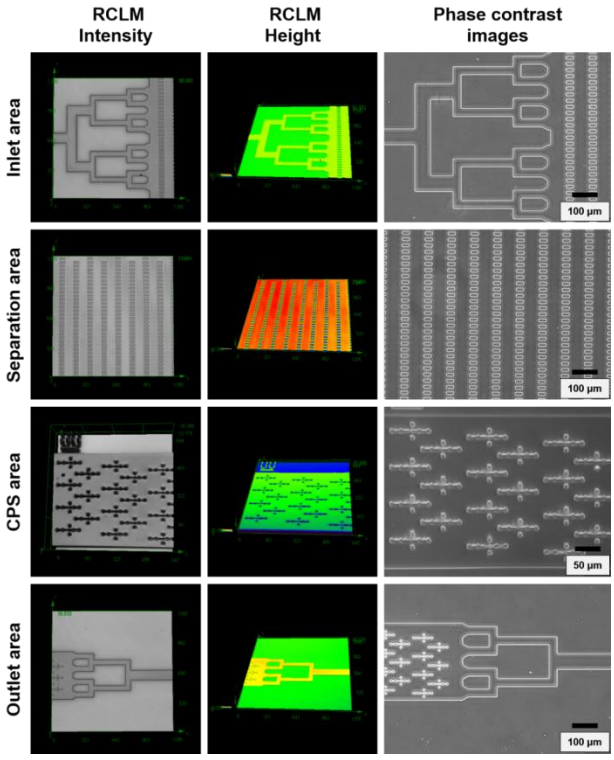

Figure 3.9. Identification of structures of the microfluidic device. (a) A phase contrast image of whole structures of the prepared device and (b) the structures of master mold and the device made on the mold was measured using RCLM and phase contrast microscopy, respectively.

3.4.2. Cell fusion in the microfluidic device

Moreover, the cell fusion experiment was performed with the device. Cells are introduced from the reservoir and the cells were then flowed to inlet area and separated in separation area as a single cell. The separated cells are randomly trapped in the CPS area by hydrodynamic flow of medium. Otherwise, cells go out from outlet area. The medium is flowed from inlet area to outlet area. When the cells are introduced to the device, several types can be occurred as shown in **Figure 3.10**. Before and after fusion (Pre-fusion and Post-fusion), 1:1 pairing (Homogeneous fusion or Heterogeneous fusion) and direct contacting which results in mixed fusion was mainly found. Unmixed fusion (or cytoplasmic fusion) and mixed fusion (or entirely fusion) were found in post-fusion. Otherwise, no fusion was occurred. After 1 hour, the cells are fused with each other or migrated somewhere in the device. Based on the fluorescence, we can identify each cell and also trace the cells in pre-fusion and post-fusion. Based on previous report [147], Y-27632 inhibitor (also known as ROCK; Rho-associated coiled-coil forming kinase) was introduced to compare the frequency of fused types such as mixed and unmixed fusion (**Figure 3.11**). Although the mixed fusion which is fusion of cytoplasm with nuclei was still occurred, the mixed fusion was significantly decreased so that cytoplasmic fusion without nuclei fusion would be occurred.

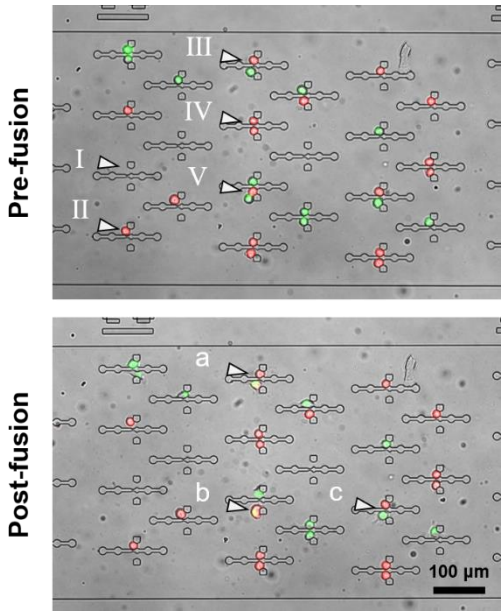

Figure 3.10. Identification of fusion types in the microfluidic device during cell fusion. When cells are introduced to the device, the cells are identified as the following definition. In pre-fusion, I: No capture, II: Single cell capture, III: 1:1 pairing (Heterogeneous fusion), IV: 1:1 pairing (Homogeneous fusion), V: Direct contacting. In post-fusion, a: unmixed fusion (or cytoplasmic fusion), b: Mixed fusion (or entirely fusion), c: No fusion.

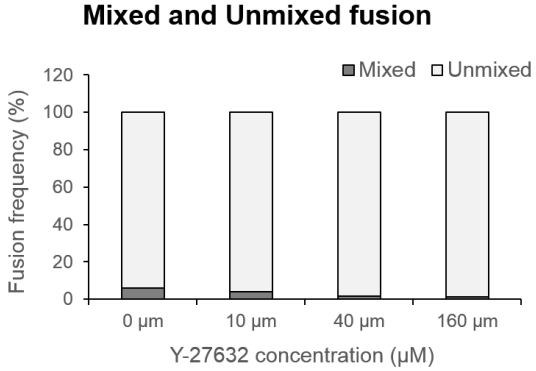

Figure 3.11. Frequency of cell fusion in the microfluidic device. According to different design and amount of Y-27632, the frequency of cell fusion was compared. The mixed fusion and unmixed fusion are defined as entirely fusion and cytoplasmic fusion, respectively. Each data were made from three samples per condition.

3.4.3. Transfection of fluorescence protein

In order to monitor the transferring cytoplasm in the device, the fluorescence plasmid vectors were transfected to the ES cell. After transfection using each plasmid vector (mCherry or EGFP) as shown in **Figure 3.12**, the cells were cultured in the presence of antibiotic reagents such as Hygromycin and Puromycin so that the transfected cells (mCherry-Hyg^R and EGFP-Pur^R) were stably obtained with fluorescence expressions, respectively. As shown in **Figure 3.13**, the unstable or non-transfected cells are gradually dead after 3 days, but the stable transfected cells can be surviving in the presence of each antibiotic reagent due to resistance gene towards the antibiotics. After 9 days, the mCherry-expressed ES cell in cytoplasmic area and the EGFP-expressed ES cell in mitochondria are achieved, respectively. The cells are maintained and passaged until getting the stable expressed cell lines. After that, they were introduced to further experiments.

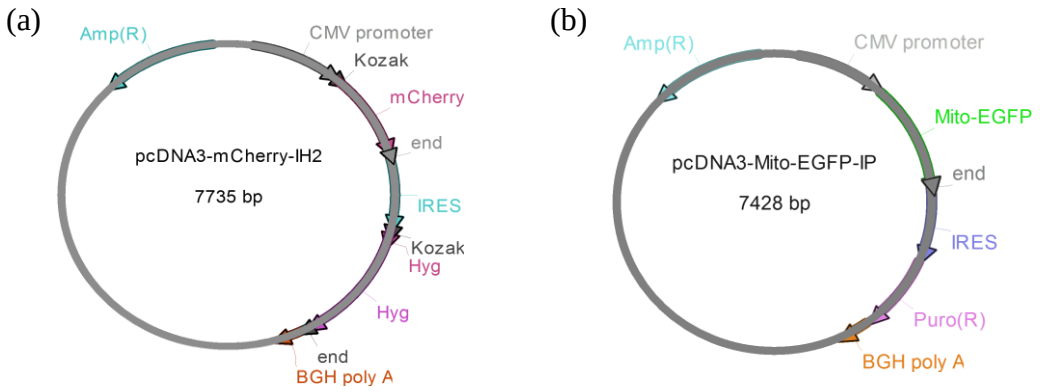

Figure 3.12. Information of vectors expressing fluorescence. (a) pcDNA3-mCherry-IH. This plasmid vector is against Hygromycin (Hyg^R). The red fluorescence is expressed in cytoplasmic area of cell. (b) pcDNA3-Mito-EGFP-IP. This plasmid vector is against Puromycin (Pur^R). The green fluorescence is expressed in mitochondria area of cell.

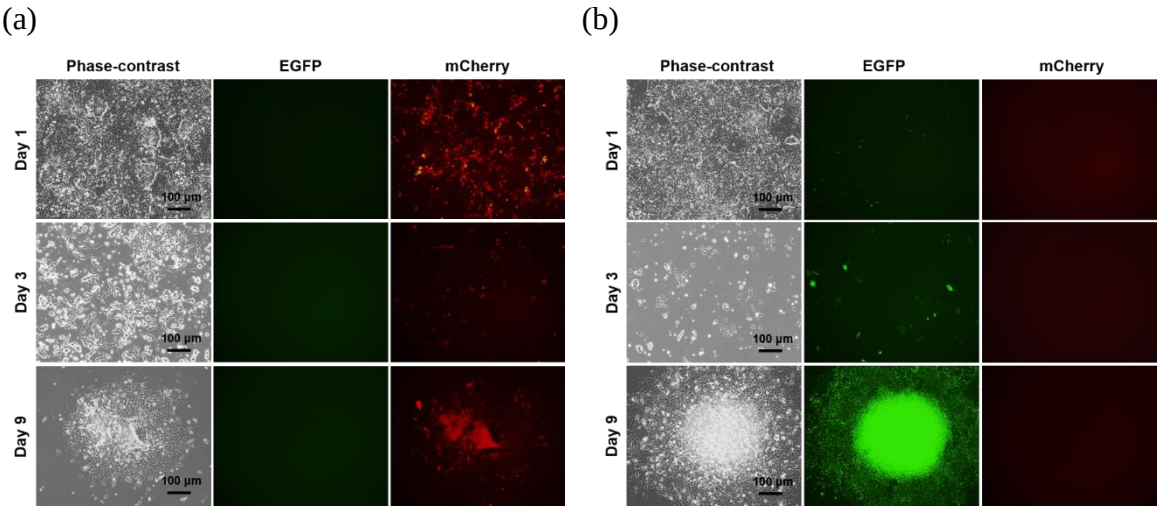

Figure 3.13. Expressing fluorescence in ES cell. (a) The red fluorescence (pcDNA3-mCherry-IH) is expressed in cytoplasmic area of cell. The cells were cultured in the presence of Hyg. (b) The green fluorescence (pcDNA3-Mito-EGFP-IP) is expressed in mitochondria area of cell. The cells were cultured in the presence of Pur.

3.4.4. Characterization of DC-treated ES cell

Although we demonstrated that somatic cells such as myogenic cell and fibroblast can be applied to the current microfluidic device, ES cells still present limitations to be adapted to the device due to morphological property. In addition, the sufficient cytoplasm and mitochondria is required to successfully be resulting in protein modification.

Therefore, we considered the enlargement of ES cells by cell cycle regulatory protein such as demecolcine (DC). The morphological characteristic was compared before and after DC treatment (**Figure 3. 14**). DC limits microtubule formation and inactivates spindle fibre formation of cells, the DC-treated cells are accordingly arrested in metaphase (M phase) during cell cycle. After DC treatment, the cells show the morphological characteristic such as inhibiting spindle formation.

In order to determine the enlarged cell size, the cell were treated with varying concentrations of DC (10, 30, 100, and 300 ng/mL). None treated cells are considered as negative control. The cell sizes are increased dependently to the concentration, and the sizes present 9.0 ± 0.7 μm (10 ng/mL), 11.0 ± 0.7 μm (30 ng/mL), 13.3 ± 1.2 μm (100 ng/mL), and 15.0 ± 1.2 μm (300 ng/mL), respectively. In case of 300 ng/mL, the size are increased about 1.5-2.0 times larger than compared with negative control (8.0 ± 0.9 μm).

In particular, the ES cell was transfected by vectors expressing fluorescence such as mCherry and EGFP (**Figure 3. 15**). By utilizing flow cytometry, we can analyze the fluorescence intensity associated protein quantitation. The colors are presented in relative fluorescence units (RFU). The RFU of red color indicating cytoplasm was increased from 374.7 ± 83.2 (10 ng/mL) to 667.4 ± 38.1 (300 ng/mL) in accordance with increased DC concentration. Despite no significant difference when compared in 10 ng/mL with the

untreated group (309.7 ± 77.8), the RFU apparently shows high intensity when the DC concentration is higher than 30 ng/mL (607.8 ± 57.6).

In addition, the RFU of green color indicating mitochondria also shoes similar tendency to RFU of red color. The intensity was increased from 1517.4 ± 297.4 (10 ng/mL) to 3198.1 ± 216.3 (300 ng/mL). The RFU of green in 30 ng/mL and 100 ng/mL shows similar intensity (2705.4 ± 272.3 and 2800.6 ± 317.7, respectively), but the intensity in 30 ng/mL-300ng/mL, was increased approximately 2.0-3.0 times higher than that in the untreated group (1171.4 ± 170.3).

The results show that the fluorescence associated protein quantitation show increased intensity both red (Cytoplasm) and green (Mitochondria) dependently to DC concentration.

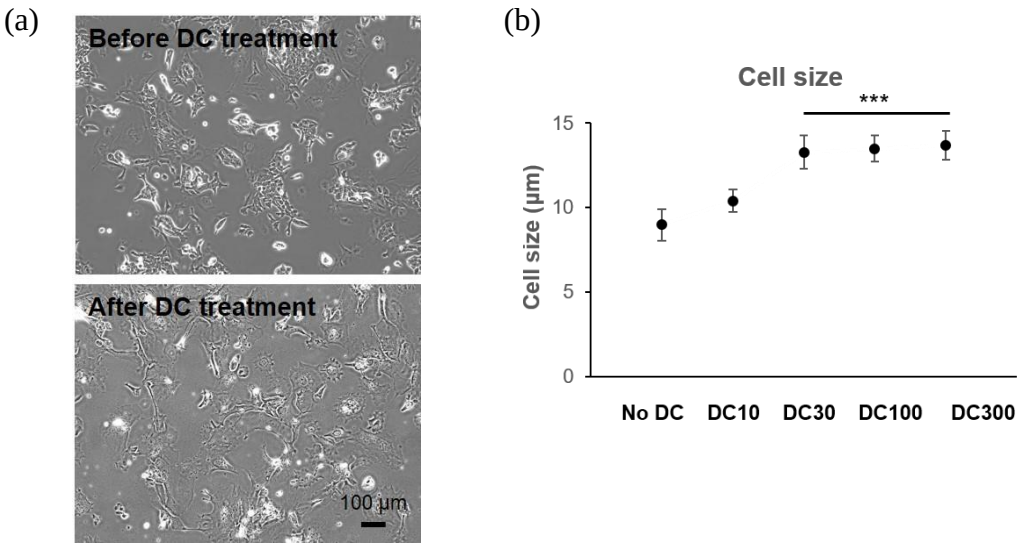

Figure 3.14. Comparison of cellular characteristics after DC treatment. (a) Phase contrast images of ES cell before and after DC treatment. (b) Comparison graph of cell size of DC-treated cells. No DC: Negative control, DC10-300; 10 ng/mL-300 ng/mL. Data are presented as the mean ± SD, $n = 3$. $P < 0.001$;***, significant difference.

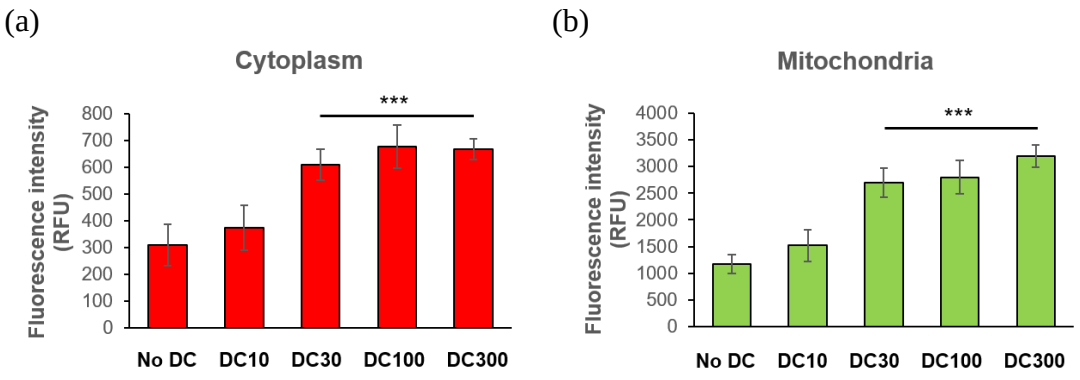

Figure 3. 15. Comparison of fluorescence intensity after DC treatment. (a) Red fluorescence indicating cytoplasm of DC-treated cells. (b) Green fluorescence indicating mitochondria of DC-treated cells. No DC: Negative control, DC10-300; 10 ng/mL-300 ng/mL. Data are presented as the mean ± SD, $n = 3$. $P < 0.001$;***, significant difference.

3.4.5. Estimation of pluripotency

In case of ES cell, one of the crucial properties is pluripotency which enable the cell to differentiate into different cell types. The ES cells were cultured in either the presence of DC or absence of DC. To determine the pluripotency of ES cell, the cell was estimated by immunostaining method using pluripotency markers such as *Oct4* and *SSEA4* (**Figure 3.16**). The both untreated and DC-treated ES cells showed the expression of *Oct4* and *SSEA4*. It indicates that the ES cell can maintain its pluripotency regardless of treatment of DC.

Moreover, specific genes associated with pluripotency such as *Nanog*, *Oct4*, and *Sox2* were selected to measure its pluripotency using q-PCR. Before and after DC treatment, each gene expression was relatively compared for quantification. *Gapdh* is used as a reference gene. As shown in **Figure 3.17**, the relative level shows about 0.1%, 0.05%, and 0.16% of *Nanog*, *Oct4*, and *Sox2*, respectively, in both non- and DC-treated ES cells. Although ES cells were treated with DC, the cell still presents its pluripotency based on immunostaining and q-PCR results.

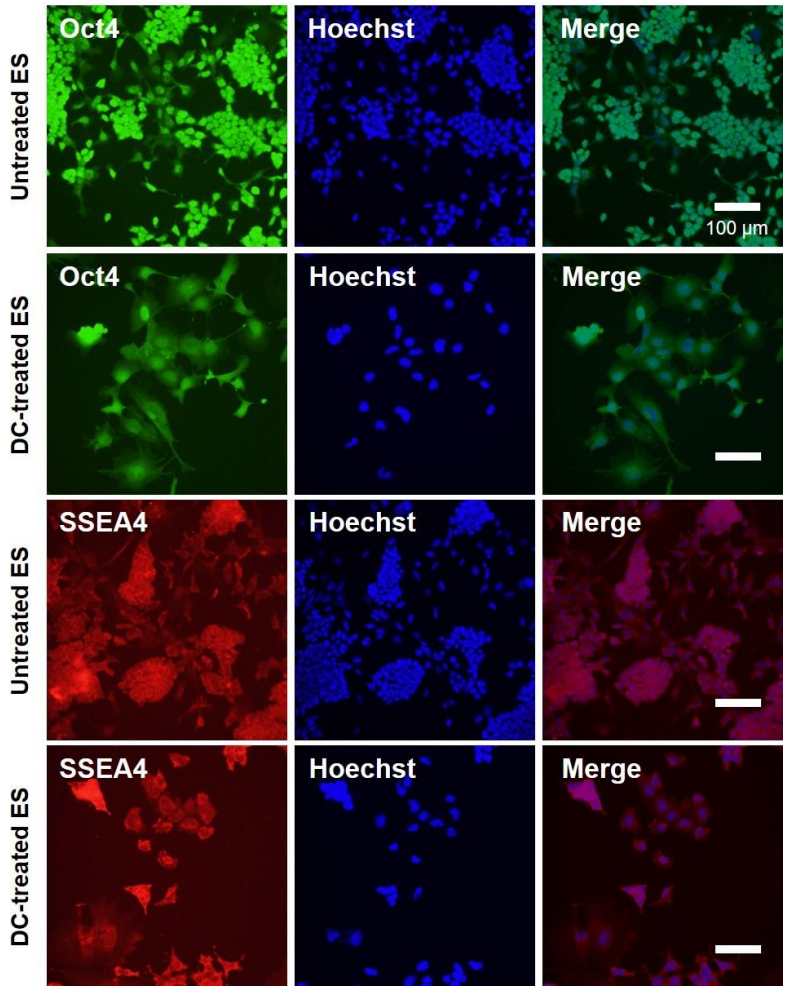

Figure 3.16. Fluorescence images of immunostaining of *Oct4* and *SSEA4*. Images of *Oct4*, *SSEA4*, and *Hoechst* staining, and merged images of *Hoechst* (blue) with *Oct4* (green) and *SSEA4* (Red). ES cells before and after DC treatment were stained.

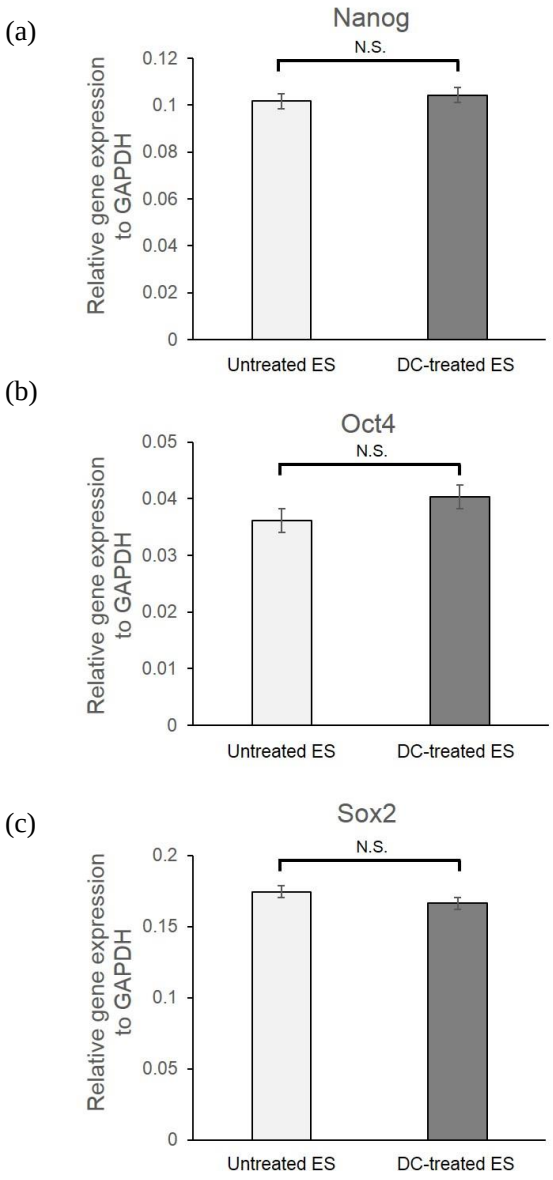

Figure 3.17. Analysis of gene expression regarding pluripotency. Three representative genes (a: *Nanog*, b: *Oct4*, c: *Sox2*) associated with pluripotency were selected to analyze gene expressions. *GAPDH* is used as a reference gene. Untreated ES cells are defined as a negative control. Data are presented as the mean ± SD, n = 3. N.S., no significant difference.

3.4.6. Efficiency of trapping and pairing in the microfluidic device

To carry out the cell fusion experiment using the microfluidic device and ES cell, the cell trapping and pairing in CPS should be considered for further steps such as cytoplasmic fusion. The trapping and pairing ratio were respectively compared before and after DC treatment (**Figure 3.18**). To compare the ratio, if cells are trapped or paired in the CPS, the cells were selected in the five sections in one microfluidic device. In case of trapping rate of ES cell, the rate was significantly increased after DC treatment (71.4 ± 3.9%) compared with that of before DC treatment (11.4 ± 7.2%). After cell trapping in the CPS, the cell pairs present in 1:1 cell pairing (Donor: Recipient), single cell, or no cell. In particular, the 1:1 cell pairing rate which result in cytoplasmic fusion was estimated. Although 1:1 cell pairing was rarely occurred in the untreated ES cells (8.4 ± 3.2%), the pairing ratio of DC-treated ES cells apparently showed the significant increase (41.7 ± 6.0%). These results show that the increased efficiency of trapping and pairing rate in the microfluidic device.

(a)

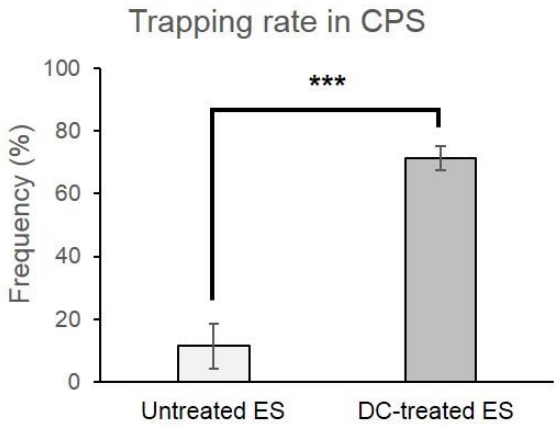

(b)

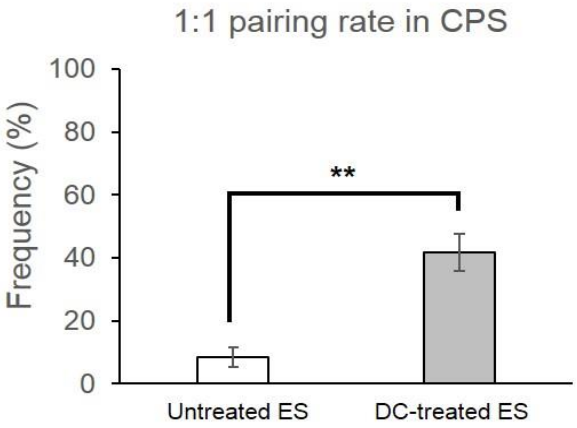

Figure 3.18. Frequency of cell trapping and 1:1 pairing in CPS. The ES cell was introduced before and after DC treatment and the cell trapping (a) and 1:1 cell pairing rate (b) were compared respectively. Data are presented as the mean ± SD, $n = 3$. $P < 0.01$;**, significant difference, $P < 0.001$;***, significant difference.

3.4.7. Visualization and characterization of cytoplasmic fusion

In order to monitor the cytoplasm transfer, mCherry vector was transfected to the nucleus and cytoplasm area of ES cell according to the protocol mentioned in the method section. And the cell was treated with DC and then applied to microfluidic device with a fusion partner cell (In this case, MEF cell). After trapping to CPS, DC-treated ES cell shows its mCherry fluorescence protein at cytoplasm and nucleus but MEF cell does not show any fluorescence signal (**Figure 3.19a**). However, 1 hour after trapping, the MEF cell also show the mCherry signal. It indicates that the cytoplasm was transferred to the recipient cell (MEF cell) from donor cell (DC-treated ES cell).

In addition to the live cell imaging, the fusion maintenance (**Figure 3.19b**) and the quantification of the transferred cytoplasm (**Figure 3.19c**) were measured based on fluorescence intensity. The result showed that increased transferring amount of cytoplasm after 1 hour. By tracing the fluorescence signal and cell position in the microfluidic device, we also observed that the fusion can be maintained at least for 4 hours though the maintenance rate decreased by time flow.

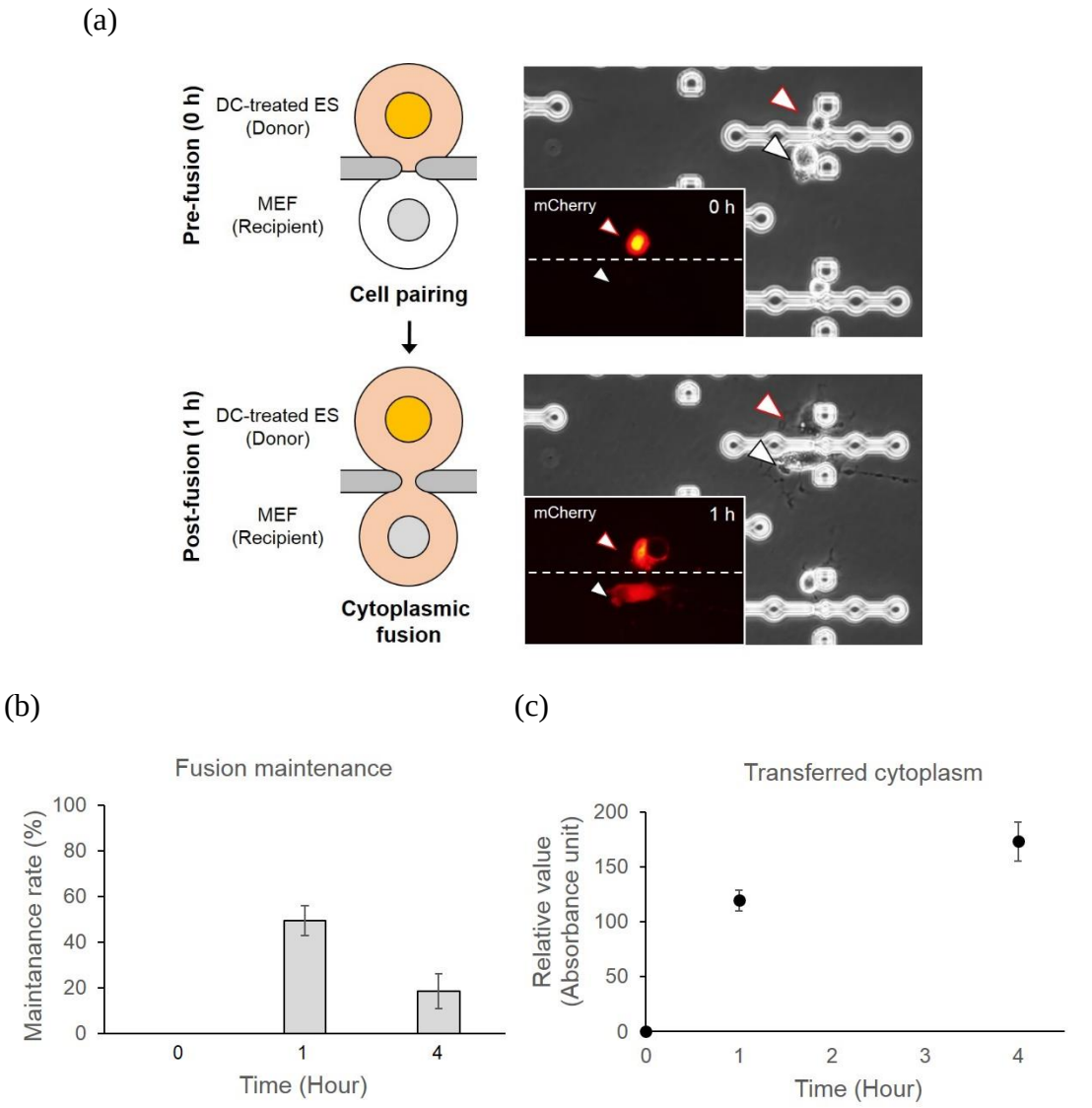

Figure 3.19. Visualization and characterization of cytoplasmic fusion. (a) Observation of cytoplasmic transfer. The schematic illustration of the experiment was described (Left). Cell fusion was induced between DC-treated ES (Donor) and MEF (Recipient) cells in the microfluidic device and the fusion was observed by phase contrast and fluorescence microscopy. (b) Maintenance of cell fusion. The observation based on fluorescence signal and cell position was performed by live cell imaging. (c) Measurement of transferred cytoplasm. Fluorescence intensity was measured to evaluate the transferred cytoplasm. Data are presented as the mean ± SD, n = 3.

3.5. Discussion

Characterization and methodology of a microfluidic device and cell fusion

In this chapter, we first presented microfluidic devices with a cell pairing structure (CPS) and a microtunnel, and showed the cytoplasmic fusion phenomenon between live single cells by cell fusion through the microtunnel. Based on the device and HVJ-E method, we introduced several cell lines such as ES cell and fibroblasts in accordance with specific objectives and performed cell fusion research. This method has specific features and advantages such as wide usability, safety, and easy manipulation to transfect varying molecules (plasmid DNAs, SiRNAs, oligonucleotides, proteins, antibodies, and etc.) as a highly flexible tool. The procedure for cell fusion using same or different types of cells can be performed regardless of either suspending or plating cells.

Many researches related with cell fusion and cellular resource have been studied with different concepts and combinations of cells and genetic factors such as ES-like cell and iPS cell [38,148]. Despite the importance of genetic transduction, protein-based transduction and modification have gradually been becoming promising issue due to its potential and advantages in regenerative medicine field.

Classic cell fusion methods such as enucleated oocytes and embryonic germ cells with somatic cells [37] have provided important evidence for epigenetic reprogramming and shown the possibility of cellular resources. In addition to this biological approach, various technical (e.g. microfludic device) [44,136], chemical (e.g. polyethylene glycol; PEG) [126,127], physical (electric pulse) [128,129], or biological (e.g. viruses or receptors) [130–132] techniques have also demonstrated the ability to properly manipulate cells for cell fusion. Using a new geometry and design, PDMS-based microfludic devices among

the previous techniques have prominently shown its feasibility mimicking cellular environment. However, the current methods still produce nuclear mixing that might results in abnormal karyotypes, and thus the resulting fused cells cannot be used for the aforementioned purposes [149,150].

Efficiency of the microfluidic-based device on cytoplasmic fusion

Meanwhile, in order to focus on protein transduction using living cells, the direct cytoplasmic transfer between donor cell and fusion partner cell should be considered. Accordingly, several parameters such as design of microfluidic device (e.g. microstructure) and materials (e.g. cell types, bioreagents, and etc.) have been improved and produced by our purpose and technology.

For these reasons, we have sought the novel method which can make cytoplasmic fusion without nucleus mixing. Especially, cytoplasmic fusion (or unmixed fusion) is important to identify the further cellular study. Using the bioreagent (e.g. Y-27632), we demonstrated that the frequency of mixed fusion was decreased lower than 10%. In other words, the frequency of cytoplasmic fusion was increased higher than 90% as previously reported [147]. Besides, the fusion rate was increased by the design of the microfluidic device such as a microtunnel type compared with that of a microslit type [137].

Considering the efficiency of producing fused cells with our protocol with that using conventional methods, our biological fusion-based protocol with the microtunnel-based microfludic chip showed higher fusion efficiencies (> 20%) than previous report (< 10%) [136] because the membrane contact between cells trapped in CPS probably resulted in the tight contact when the cells were fused by pairing. These results suggest that biological, chemical, and topographical properties play important roles in the cytoplasmic fusion. When we applied cells such as ES cell to the microfluidic device, two cells with

very different sizes may be difficult to induce cytoplasmic fusion due to non-trapping or passing by hydrodynamic force.

Characterization and application of DC-treated ES cell

In order to properly perform cytoplasmic fusion using ES cell, therefore, the ES cell was first enlarged by a cell cycle inhibitory reagent like demecolcine (DC) because ES cell presents small size which is not available to be applied to the microfluidic device [151]. Also, ES cell containing much amount of cytoplasm and mitochondria is pursued to be transferring their properties to a fusion partner such as fibroblast cell, probably resulting in successful protein transduction.

While DC treatment to ES cells shows its ability as an applicable bioreagent to obtain enlarged ES cells [152], we should confirm several factors such as pluripotency before applying the DC-treated ES cell. Basically, this bioreagent inhibits spindle fiber formation in M phase and polyploidizes cells relying on the cell type. The enlarged ES cells, tetraploid ES cells, can be subsequently established from diploid ES cells through polyploidization using DC [153]. Based on the observation using phase contrast microscope and the measurement of flow cytometry, we found that the ES cells showed enlarged size after varying concentration of DC treatment. The size of ES cells was increased dependently to the concentration of DC (10, 30, 100, and 300 ng/mL), but the size seemed not to continuously increase when the concentration is over 100 ng/mL. Considering the fusion efficiency depends on both cell pairing and cell size, our result prominently showed the increased yield of cell pairs in the microfluidic device (> 35%). It indicates that the morphological characteristic (e.g. size) of cells represent the important components for high yield induction and efficiency of successfully fused cells.

Through immunostaining method and RT-PCR analysis, the pluripotency of ES cells was examined after DC treatment. The DC-treated ES cells showed expression of *Oct4* and *SSEA4* similarly to untreated ES cells. *Oct4* is necessary for the maintenance of pluripotent potential and *SSEA4* is representative marker expressed on the surface of ES cells. While the result shows the maintaining pluripotency, moreover, the pluripotency was measured by RT-PCR. The RT-PCR can enable us to monitor the amplification of a targeted DNA molecule during the PCR. The method was used to quantitatively detect levels of gene expression. The expression levels of pluripotent genes such as *Nanog*, *Oct4*, and *Sox2* showed similar levels before and after DC treatment. These results demonstrated that the ES cell can maintain its pluripotency even after DC treatment. Other report also demonstrated the pluripotency by the positive activity of alkaline phosphatase and its ability to form teratocarcinomas [154].

Visualization and characterization of cytoplasmic fusion

We therefore performed the cytoplasmic fusion experiment using enlarged ES cells with DC treatment. To trace the cytoplasmic transfer, the visualization is fundamentally pursued in this research. Also, the visualization can offer better understanding for the cellular behavior or unknown mechanism during cell fusion. To visualize the phenomenon such as exchange of cytoplasm and organelles, the ES cell was transfected by using fluorescent proteins such as mCherry. Accordingly, the transferring cytoplasm between live cells could be monitored using a fluorescence microscope. Although the fusion and membrane reorganization was not initiated with the same time, the close inspection revealed that the cytoplasm of donor cell can be transferred to the fusion partner cell and the fused cells can reorganize the cell membrane to probably initiate

further step. The visualization of cytoplasmic exchange enabled us to promptly understand the fusion events and observe the membrane reorganization in cells.

Based on the results, we demonstrated the high expressed-fluorescence intensity indicating increased amount of proteins (cytoplasm and mitochondria) in the cells in accordance with the concentration of DC, and our method is suitable for observing and tracing the step of cytoplasmic fusion. Importantly, the increased amount of cytoplasm may result in proper protein transduction which can elicit a specific lineage such as reprogramming. Therefore, the application using live cells (e.g. ES cell) will provide a novel type of cellular resource associated with directing protein modification through our microfluidic device-based method.

3.6. Conclusion

Novel concepts towards cell fusion were presented in terms of cellular reprogramming and resources. By using newly designed microfluidic device, we have successfully performed cell fusion experiments (In our case, cytoplasmic fusion) and we demonstrated that the cytoplasmic fraction was transferred through the microtunnel without nuclear mixing. In addition, the fusion rate depends on the design of the microfluidic device such as a tunnel type and/or bioreagents such as Y-inhibitor. The results suggest that chemical and topographical properties play important roles in the cytoplasmic fusion.

In case of application of ES cell, we considered that the enlarged ES cells containing large amount of cytoplasm and mitochondria would be useful cellular resources to support reprogramming or other purposes such as protein modification. By utilizing demecolcine, we improved the current limitations in application of ES cell as well as showed the feasibility of enlarged ES cells containing much amount of cytoplasm and mitochondria for further protein modification while we found that the maintenance of pluripotency even after DC treatment.

Overall, we have successfully applied microfabricated system and bioreagents to our fusion protocol for each purpose and the data suggest that our cell fusion system provides a promising approach to modulate cytoplasm and/or mitochondria transfer to a fusion partner cell.

Thus, the cell fusion methods using microfluidics and/or bioreagents will be promising protocols as a new type through the modification with powerful proteins and nutrients.

Chapter 4.
Summary and future perspective

4.1. Summary

In chapter 1, general introduction was described to explain microfabricated device and technology such as bio-MEMS, microfluidic system, and etc. The technologies are categorized in photolithography, photo-immobilization, and microfluidic device. In terms of regenerative medicine, cell fusion method was introduced, and the manipulation of cells was also described with various examples and methods for specific objectives in regenerative medicine. In addition, critical issues and approaches have been suggested to bring the current limitations and problems in regenerative medicine up. Composition and objective of this thesis was described in detail with our novel technology and approach.

In chapter 2, we introduced NGF-immobilized system for neuronal regeneration. Controlling neuronal cell organization via micropatterns-immobilized NGF and the biochemical and topographical cues of immobilized NGF were presented in understanding neurite formation and neuronal network. In methods section, preparation of photoreactive gelatin, surface immobilization of growth factor, determination of NGF amount and NGF-immobilized surface, morphological characteristic of micropatterned-immobilized substrate, and estimation of neurite formation were described with the results according to the each content. In particular, the NGF-immobilized substrate with micropatterns was characterized, and the formation and behaviors of neuronal cells were investigated on the immobilization system. To sum up the results, the micropatterning of NGF was achieved using photoreactive gelatin and the immobilized NGF enhanced the neurite extension of PC12 cell. Based on the immunostaining, we found that the PC12 cell respond differently to the soluble and immobilized NGF. Orientation of outgrowing neurites was regulated by narrower micropatterning of NGF. The neurite formation can be controlled by the immobilized height and pattern widths.

Overall, we proposed the combined biocomposite materials (P-gelatin) with a neurotrophin (NGF) on a biological substrate by using various micropatterns to properly modulate neuronal network and understand the desirable environment for nerve regeneration. The proposed micropatterned-immobilization platform showed remarkable effects on neuronal regeneration with simultaneous biochemical and topographical cues.

In chapter 3, we first presented that a microfluidic device with cell pairing structures and a microtunnel, and showed the cytoplasmic fusion phenomenon between live single cells by cell fusion through the newly designed-microfluidic device. Based on this device, we introduced several cell lines such as ES cell and fibroblasts in accordance with specific objectives and performed cell fusion research. In methods section, cell fusion using HVJ-E method, principles of cell fusion, cytoplasmic fusion using microfluidic chip, transfection by fluorescence plasmid DNA, application of cell cycle regulatory protein such as demecolcine (DC), introduction of enlarged ES cells, measurement of pluripotency using immunocytochemistry and RT-PCR methods, and visualization of cytoplasmic transfer were described with the results according to the each content. To sum up the results, cytoplasmic fusion was successfully completed without nuclei mixing through the newly designed microfluidic device with microtunnel structure. Enlargement of ES cell was achieved using DC and the DC-treated ES cell showed the maintenance of its pluripotency and increased protein amount. Therefore, the enlarged-ES cells containing much cytoplasm and mitochondria could be applied to our system for further research as a promising source. Cytoplasmic transfer between live ES and somatic cells was visualized based on expressing florescence signals in the cells. The feasibility of direct protein transfer between live cells was demonstrated via our newly designed microfluidic device and concept.

Overall, the data indicate that our cell fusion system provides a promising approach to modulate cytoplasm transfer to a fusion partner cell. Also, the cell fusion method with a microfluidic device and bioreagents will hold a new type of cell fusion protocol introducing powerful protein modification as a cellular resource. Therefore, we can consider further steps to study cellular behaviors or property for reprogramming without genetic modification.

Taken together, the sophisticated-microfluidic platform can be designed to precisely control various cells (e.g. nerve cell, ES cell, and etc.) considering the microenvironment. In another aspect, specific cells (e.g. potential pluripotent-like cell) can be obtained after protein modification using the microfluidic device. Then, the resulting cells can be deeply studied for its practical application in regenerative medicine and for revealing cellular mechanism. Our system contributed to the development of useful platforms for directing cellular behaviors and protein transduction through well organized-microfabricated technology and device. By combining the proposed method and technology, we can consider the further study on neuronal regeneration and cell manipulation. Generation of nerve system and network will be deeply studied under multi-functional tools with aforementioned as well as novel properties, and that micro-manipulation of cells will be continuously studied by microfabricated devices with multi-function for various purposes.

In terms of remaining challenges and problems, major clinical challenges still remain particularly for patients who suffer from multiple nerve injuries while the current researches show promising results. For example, the combined therapies should focus on how each parameter can be functionally and modulated properly in response to the type and speed of regeneration. During the regeneration process, the localized concentration of the growth factor with topographical structures may need in the proximal and distal

nerve at an initial step of the process, and then other parameters such as electrical cue can assist the axonal growth and nerve regeneration at the particular location. Therefore, in future new methods, multiple cues will be integrated for long-term regeneration and function. Investigating and understanding the complicated and unknown cellular networks should be undertaken through simultaneously extending our knowledges of wide disciplines and developing new tools. The microfluidic device-based platform promisingly offers a new paradigm for directing the form and function of integrated cellular environments and systems. For example, we can focus on the extensive investigation of various cell culture models such as disease models, 3D organ developing, cancer research, and etc. Through the application of microfluidic platform, transferring proteins or desirable materials and modulating tissues and organs are still subject to the remaining challenges in human therapy. The microfluidic platform will support many kinds of researches in bioengineering and regenerative medicine and will enable us to extend multiple research models in building functionalized system.

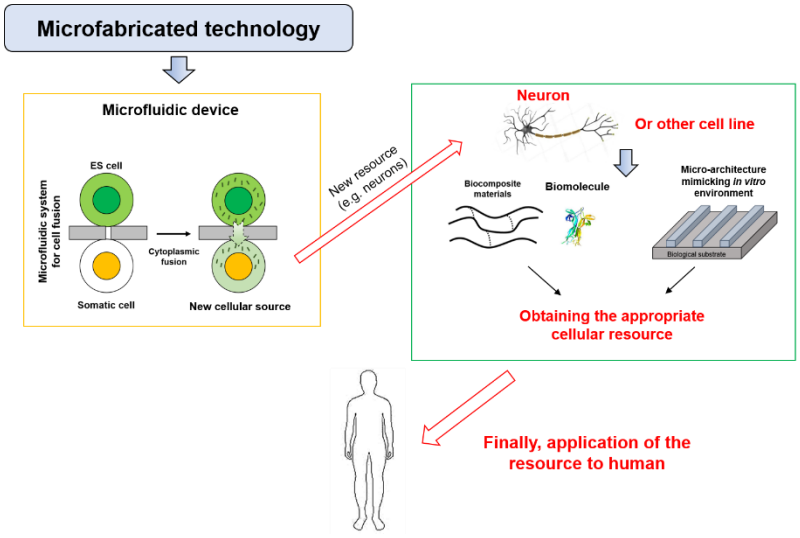

Figure 4.1. New approach through the integrated microfabricated technology for regenerative medicine.

4.2. Future perspective

We introduced microfabricated technology to properly manipulate various cells for multi-purposes in regenerative medicine.

In case of neuronal network, the environment is basically a dense and complex involving 3D interconnected network of neurons. By introducing biochemical and topographical components at once, we revealed enhanced and controllable system for neuronal formation, resulting in neuroregeneration. Considering our approach (e.g. biocomposite materials, biochemical and topographical property) and previous research (e.g. nanofiber, conducting materials, biological substrates), in essence, neuronal network is very complicate and multi-cues are simultaneously required to create well organized-environment. Consequently, we moreover need to seek how to properly integrate all parameters such as biochemical, topographical, electrical cues with advanced technologies to develop useful platforms for nerve regeneration.

In the meantime, we should focus on the improvement of the current methods and suggest further strategies in regenerative medicine in terms of cellular material while conventional and advanced research such as cell fusion showed promising results to generate different cell types. Therefore, we presented the novel approaches using microfluidic system and bioreagents for cellular modification. The result showed that the cytoplasmic transfer can be achieved by our system. It is close to direct protein transduction using living cell. The proposed concept by our system represents the potential and feasibility as a new cellular resource for further application. Considering the present study and future study, the modification of proteins is a crucial tool for investigating natural systems and creating therapeutic conjugates. Although there are

various methods to achieve protein transduction or modification, stable and efficient tools are still pursued to develop the promising method for a practical application of superior cellular resource in regenerative medicine. This kind of direct protein modification using live cells will be one of strong and promising tools to create an effective and functional diversity without genetic modification.

In future perspective, we therefore summarize and suggest our several views.

1. The multi-functional platform will be developed for tissue engineering and nerve regeneration.
2. The application of protein like cytoplasm via living cells will be promising tool in bioengineering fields involving cellular modification and modeling.
3. Micromanipulation of cells will be continuously studied and pursued through advanced tools with multi-functions for various purposes.

We finally predict that precise manipulation of various cells for obtaining appropriate cellular resource and directing therapy will be realized on well integrated-microarchitecture mimicking *in vitro* environment through deep understanding in both microfabricated technology and cellular mechanism.

References

References

[1] MEMS materials and processes handbook, Choice Rev. Online. (2013). doi:10.5860/choice.49-0882.

[2] Theoretical microfluidics, Choice Rev. Online. (2013). doi:10.5860/choice.45-5602.

[3] V. Casquillas, T. Houssin, PDMS: A Review, Elveflow. (2015).

[4] J.A. Rogers, R.G. Nuzzo, Recent progress in soft lithography, Mater. Today. (2005). doi:10.1016/S1369-7021(05)00702-9.

[5] B. Zhang, Q. Dong, C.E. Korman, Z. Li, M.E. Zaghloul, Flexible packaging of solid-state integrated circuit chips with elastomeric microfluidics, Sci. Rep. (2013). doi:10.1038/srep01098.

[6] P. Watts, S.J. Haswell, Microengineering in Biotechnology, 2010. doi:10.1007/978-1-60327-106-6.

[7] D.L. Polla, A.G. Erdman, W.P. Robbins, D.T. Markus, J. Diaz-Diaz, R. Rizq, Y. Nam, H.T. Brickner, A. Wang, P. Krulevitch, Microdevices in Medicine, Annu. Rev. Biomed. Eng. (2000). doi:10.1146/annurev.bioeng.2.1.551.

[8] A. Khademhosseini, R. Langer, J. Borenstein, J.P. Vacanti, Microscale technologies for tissue engineering and biology, Proc. Natl. Acad. Sci. (2006). doi:10.1073/pnas.0507681102.

[9] M. Madou, C. Wang, Photolithography, in: Encycl. Nanotechnol., 2015. doi:10.1007/978-94-007-6178-0_342-2.

[10] M.D. Shelley, R. Zaouk, B.Y. Park, M.J. Madou, Introduction to Microfabrication Techniques, in: Microfluid. Tech., 2006. doi:10.1385/1-59259-997-4:3.

[11] T. Betancourt, L. Brannon-Peppas, Micro-and nanofabrication methods in nanotechnological medical and pharmaceutical devices, Int. J. Nanomedicine. (2006). doi:10.2147/nano.2006.1.4.483.

[12] A.A. Tseng, Recent developments in micromilling using focused ion beam technology, J. Micromechanics Microengineering. 14 (2004). doi:10.1088/0960-1317/14/4/R01.

[13] L. Liu, W. Cao, J. Wu, W. Wen, D.C. Chang, P. Sheng, Design and integration of an all-in-one biomicrofluidic chip, Biomicrofluidics. (2008). doi:10.1063/1.2966453.

[14] J. Friend, L. Yeo, Fabrication of microfluidic devices using polydimethylsiloxane, Biomicrofluidics. (2010). doi:10.1063/1.3259624.

[15] Y.C. Toh, T.C. Lim, D. Tai, G. Xiao, D. Van Noort, H. Yu, A microfluidic 3D hepatocyte chip for drug toxicity testing, Lab Chip. (2009). doi:10.1039/b900912d.

[16] P.S. Dittrich, A. Manz, Lab-on-a-chip: Microfluidics in drug discovery, Nat. Rev. Drug Discov. (2006). doi:10.1038/nrd1985.

[17] L.Y. Yeo, H.C. Chang, P.P.Y. Chan, J.R. Friend, Microfluidic devices for bioapplications, Small. (2011). doi:10.1002/smll.201000946.

[18] J. Lee, S.H. Lee, Lab on a chip for in situ diagnosis: From blood to point of care, Biomed. Eng. Lett. (2013). doi:10.1007/s13534-013-0094-y.

[19] F. Cui, M. Rhee, A. Singh, A. Tripathi, Microfluidic Sample Preparation for Medical Diagnostics, Annu. Rev. Biomed. Eng. (2015). doi:10.1146/annurev-bioeng-071114-040538.

[20] K. Perez-toralla, G. Mottet, E. Tulukcuoglu-guneri, J. Champ, C. Bidard, J. Pierga, J. Klijanienko, I. Draskovic, L. Malaquin, J. Viovy, Microchip Diagnostics, in: Microchip Diagnostics, 2017. doi:10.1007/978-1-4939-6734-6.

[21] K.J. Regehr, M. Domenech, J.T. Koepsel, K.C. Carver, S.J. Ellison-Zelski, W.L. Murphy, L.A. Schuler, E.T. Alarid, D.J. Beebe, Biological implications of polydimethylsiloxane-based microfluidic cell culture, Lab Chip. (2009). doi:10.1039/b903043c.

[22] H. Shintaku, T. Kuwabara, S. Kawano, T. Suzuki, I. Kanno, H. Kotera, Micro cell encapsulation and its hydrogel-beads production using microfluidic device, in: Microsyst. Technol., 2007. doi:10.1007/s00542-006-0291-z.

[23] S. Kaneda, T. Fujii, Integrated microfluidic systems, Adv. Biochem. Eng. Biotechnol. (2010). doi:10.1007/10_2010_68.

[24] C.D. Paul, W.-C. Hung, D. Wirtz, K. Konstantopoulos, Engineered Models of Confined Cell Migration, Annu. Rev. Biomed. Eng. (2016). doi:10.1146/annurev-bioeng-071114-040654.

[25] N.K. Inamdar, J.T. Borenstein, Microfluidic cell culture models for tissue engineering, Curr. Opin. Biotechnol. (2011). doi:10.1016/j.copbio.2011.05.512.

[26] D. Huh, H.J. Kim, J.P. Fraser, D.E. Shea, M. Khan, A. Bahinski, G.A. Hamilton, D.E. Ingber, Microfabrication of human organs-on-chips, Nat. Protoc. (2013). doi:10.1038/nprot.2013.137.

[27] S.N. Bhatia, D.E. Ingber, Microfluidic organs-on-chips, Nat. Biotechnol. (2014). doi:10.1038/nbt.2989.

[28] S. Takayama, E. Ostuni, X. Qian, J.C. McDonald, X. Jiang, P. LeDuc, M.H. Wu, D.E. Ingber, G.M. Whitesides, Topographical micropatterning of

poly(dimethylsiloxane) using laminar flows of liquids in capillaries, Adv. Mater. (2001). doi:10.1002/1521-4095(200104)13:8<570::AID-ADMA570>3.0.CO;2-B.

[29] H. Yun, K. Kim, W.G. Lee, Cell manipulation in microfluidics, Biofabrication. (2013). doi:10.1088/1758-5082/5/2/022001.

[30] J. Xie, M.R. MacEwan, X. Li, S.E. Sakiyama-Elbert, Y. Xia, Neurite outgrowth on nanofiber scaffolds with different orders, structures, and surface properties, ACS Nano. (2009). doi:10.1021/nn900070z.

[31] L. Ghasemi-Mobarakeh, M.P. Prabhakaran, M. Morshed, M.H. Nasr-Esfahani, S. Ramakrishna, Electrospun poly(ε-caprolactone)/gelatin nanofibrous scaffolds for nerve tissue engineering, Biomaterials. (2008). doi:10.1016/j.biomaterials.2008.08.007.

[32] Y. Zou, J. Qin, Z. Huang, G. Yin, X. Pu, D. He, Fabrication of Aligned Conducting PPy-PLLA Fiber Films and Their Electrically Controlled Guidance and Orientation for Neurites, ACS Appl. Mater. Interfaces. (2016). doi:10.1021/acsami.6b00957.

[33] J.Y. Lee, C.A. Bashur, C.A. Milroy, L. Forciniti, A.S. Goldstein, C.E. Schmidt, Nerve growth factor-immobilized electrically conducting fibrous scaffolds for potential use in neural engineering applications, IEEE Trans. Nanobioscience. (2012). doi:10.1109/TNB.2011.2159621.

[34] S.H. Bhang, T.J. Lee, J.M. Lim, J.S. Lim, A.M. Han, C.Y. Choi, Y.H. Kim Kwon, B.S. Kim, The effect of the controlled release of nerve growth factor from collagen gel on the efficiency of neural cell culture, Biomaterials. 30 (2009) 126–132. doi:10.1016/j.biomaterials.2008.09.021.

[35] T. Honegger, M.I. Thielen, S. Feizi, N.E. Sanjana, J. Voldman, Microfluidic neurite guidance to study structure-function relationships in topologically-complex population-based neural networks, Sci. Rep. 6 (2016). doi:10.1038/srep28384.

[36] C.D. Spicer, B.G. Davis, Selective chemical protein modification, Nat. Commun. (2014). doi:10.1038/ncomms5740.

[37] M. Tada, Y. Takahama, K. Abe, N. Nakatsuji, T. Tada, Nuclear reprogramming of somatic cells by in vitro hybridization with ES cells, Curr. Biol. (2001). doi:10.1016/S0960-9822(01)00459-6.

[38] K. Takahashi, S. Yamanaka, Induction of Pluripotent Stem Cells from Mouse Embryonic and Adult Fibroblast Cultures by Defined Factors, Cell. (2006). doi:10.1016/j.cell.2006.07.024.

[39] S. Yamanaka, K. Takahashi, K. Okita, M. Nakagawa, Induction of pluripotent stem cells from fibroblast cultures, Nat. Protoc. (2007). doi:10.1038/nprot.2007.418.

[40] H. Zhou, S. Wu, J.Y. Joo, S. Zhu, D. Wook Han, T. Lin, S. Trauger, G. Bien, Y. Susan, Y. Zhu, S. Gary, R.S. Hans, L. Duan, S. Ding, Generation of Induced Pluripotent Stem Cells Using Recombinant Proteins, Cell Stem Cell. (2009). doi:10.1016/j.stem.2009.04.005.

[41] D. Kim, C.-H. Kim, J.-I. Moon, Y.-G. Chung, M.-Y. Chang, B.-S. Han, S. Ko, E. Yang, K.Y. Cha, R. Lanza, K.-S. Kim, Generation of Human Induced Pluripotent Stem Cells by Direct Delivery of Reprogramming Proteins, Cell Stem Cell. (2009). doi:10.1016/j.stem.2009.05.005.

[42] R.M. Schoeman, I. Vermes, D.A. Weitz, E.W.M. Kemna, F. Wolbers, A. van den Berg, High-yield cell ordering and deterministic cell-in-droplet encapsulation using Dean flow in a curved microchannel, Lab Chip. (2012). doi:10.1039/c2lc00013j.

[43] N. Hu, J. Yang, S. Qian, S.W. Joo, X. Zheng, A cell electrofusion microfluidic device integrated with 3D thin-film microelectrode arrays, Biomicrofluidics. (2011). doi:10.1063/1.3630125.

[44] A.M. Skelley, O. Kirak, H. Suh, R. Jaenisch, J. Voldman, Microfluidic control of cell pairing and fusion, Nat. Methods. (2009). doi:10.1038/nmeth.1290.

[45] C.E. Schmidt, J.B. Leach, Neural Tissue Engineering: Strategies for Repair and Regeneration, Annu. Rev. Biomed. Eng. 5 (2003) 293–347. doi:10.1146/annurev.bioeng.5.011303.120731.

[46] K.S. Houschyar, A. Momeni, M.N. Pyles, J.Y. Cha, Z.N. Maan, D. Duscher, O.S. Jew, F. Siemers, J. van Schoonhoven, The Role of Current Techniques and Concepts in Peripheral Nerve Repair, Plast. Surg. Int. (2016). doi:10.1155/2016/4175293.

[47] C. Simitzi, A. Ranella, E. Stratakis, Controlling the morphology and outgrowth of nerve and neuroglial cells: The effect of surface topography, Acta Biomater. (2017). doi:10.1016/j.actbio.2017.01.023.

[48] A.C. Pinho, A.C. Fonseca, A.C. Serra, J.D. Santos, J.F.J. Coelho, Peripheral Nerve Regeneration: Current Status and New Strategies Using Polymeric Materials, Adv. Healthc. Mater. 5 (2016) 2732–2744. doi:10.1002/adhm.201600236.

[49] P. Prang, R. Müller, A. Eljaouhari, K. Heckmann, W. Kunz, T. Weber, C. Faber, M. Vroemen, U. Bogdahn, N. Weidner, The promotion of oriented axonal regrowth in the injured spinal cord by alginate-based anisotropic capillary hydrogels, Biomaterials. 27 (2006) 3560–3569. doi:10.1016/j.biomaterials.2006.01.053.

[50] S.E. Stabenfeldt, A.J. Garcia, M.C. LaPlaca, Thermoreversible laminin-functionalized hydrogel for neural tissue engineering, J. Biomed. Mater. Res. - Part A. 77 (2006) 718–725. doi:10.1002/jbm.a.30638.

[51] A.C. Mitchell, P.S. Briquez, J.A. Hubbell, J.R. Cochran, Engineering growth factors for regenerative medicine applications, Acta Biomater. 30 (2016) 1–12. doi:10.1016/j.actbio.2015.11.007.

[52] a Wiedłocha, V. Sørensen, Signaling, internalization, and intracellular activity of fibroblast growth factor., Curr. Top. Microbiol. Immunol. 286 (2004) 45–79.

[53] D. Marchetti, R.W. Stach, R. Saneto, J. de Vellis, J.R. Perez-Polo, Binding constants of soluble NGF-receptors in rat oligodendrocytes and astrocytes in culture, Biochem. Biophys. Res. Commun. 147 (1987) 422–427. doi:10.1016/S0006-291X(87)80138-9.

[54] C.G. Shi, L.M. Wang, Y. Wu, P. Wang, Z.J. Gan, K. Lin, L.X. Jiang, Z.Q. Xu, M. Fan, Intranasal administration of nerve growth factor produces antidepressant-like effects in animals, Neurochem. Res. 35 (2010) 1302–1314. doi:10.1007/s11064-010-0183-6.

[55] Y. Ito, Covalently immobilized biosignal molecule materials for tissue engineering, Soft Matter. 4 (2008) 46–56. doi:10.1039/B708359A.

[56] M. Hajimiri, S. Shahverdi, G. Kamalinia, R. Dinarvand, Growth factor conjugation: Strategies and applications, J. Biomed. Mater. Res. - Part A. 103 (2015) 819–838. doi:10.1002/jbm.a.35193.

[57] Y. Ito, Regulation of cellular gene expression by artificial materials immobilized with biosignalmolecules., J. Artif. Organs. (1998).

[58] T.A. Kapur, M.S. Shoichet, Chemically-bound nerve growth factor for neural tissue engineering applications, J. Biomater. Sci. Polym. Ed. 14 (2003) 383–394. doi:10.1163/156856203321478883.

[59] L.M.Y. Yu, J.H. Wosnick, M.S. Shoichet, Miniaturized system of neurotrophin patterning for guided regeneration, J. Neurosci. Methods. 171 (2008) 253–263. doi:10.1016/j.jneumeth.2008.03.023.

[60] S.H. Bhang, T.J. Lee, H.S. Yang, W.G. La, A.M. Han, Y.H.K. Kwon, B.S. Kim, Enhanced nerve growth factor efficiency in neural cell culture by immobilization on the culture substrate, Biochem. Biophys. Res. Commun. 382 (2009) 315–320. doi:10.1016/j.bbrc.2009.03.016.

[61] J. Zeng, Z. Huang, G. Yin, J. Qin, X. Chen, J. Gu, Fabrication of conductive NGF-conjugated polypyrrole-poly(l-lactic acid) fibers and their effect on neurite

outgrowth, Colloids Surfaces B Biointerfaces. (2013). doi:10.1016/j.colsurfb.2013.05.012.

[62] N. Gomez, C.E. Schmidt, Nerve growth factor-immobilized polypyrrole: Bioactive electrically conducting polymer for enhanced neurite extension, J. Biomed. Mater. Res. - Part A. (2007). doi:10.1002/jbm.a.31047.

[63] M. Anderson, N.B. Shelke, O.S. Manoukian, X. Yu, L.D. McCullough, S.G. Kumbar, Peripheral Nerve Regeneration Strategies: Electrically Stimulating Polymer Based Nerve Growth Conduits, Crit. Rev. Biomed. Eng. (2015). doi:10.1615/CritRevBiomedEng.2015014015.

[64] L.Y. Chan, W.R. Birch, E.K.F. Yim, A.B.H. Choo, Temporal application of topography to increase the rate of neural differentiation from human pluripotent stem cells, Biomaterials. (2013). doi:10.1016/j.biomaterials.2012.09.033.

[65] A.D. Sharma, S. Zbarska, E.M. Petersen, M.E. Marti, S.K. Mallapragada, D.S. Sakaguchi, Oriented growth and transdifferentiation of mesenchymal stem cells towards a Schwann cell fate on micropatterned substrates, J. Biosci. Bioeng. (2016). doi:10.1016/j.jbiosc.2015.07.006.

[66] K.J. Jang, M.S. Kim, D. Feltrin, N.L. Jeon, K.Y. Suh, O. Pertz, Two distinct filopodia populations at the growth cone allow to sense nanotopographical extracellular matrix cues to guide neurite outgrowth, PLoS One. 5 (2010). doi:10.1371/journal.pone.0015966.

[67] T. Houchin-Ray, A. Huang, E.R. West, M. Zelivyanskaya, L.D. Shea, Spatially patterned gene expression for guided neurite extension, J. Neurosci. Res. 87 (2009) 844–856. doi:10.1002/jnr.21908.

[68] D. Bring, C. Reno, P. Renstrom, P. Salo, D. Hart, P. Ackermann, Prolonged immobilization compromises up-regulation of repair genes after tendon rupture in a rat model, Scand. J. Med. Sci. Sport. 20 (2010) 411–417. doi:10.1111/j.1600-0838.2009.00954.x.

[69] Y. Ito, Tissue engineering by immobilized growth factors, Mater. Sci. Eng. C. 6 (1998) 267–274. doi:10.1016/S0928-4931(98)00061-7.

[70] Y. Ito, Growth Factor Engineering for Biomaterials, ACS Biomater. Sci. Eng. (2019). doi:10.1021/acsbiomaterials.8b01649.

[71] H. Mao, S.M. Kim, M. Ueki, Y. Ito, Serum-free culturing of human mesenchymal stem cells with immobilized growth factors, J. Mater. Chem. B. 5 (2017) 928–934. doi:10.1039/C6TB02867E.

[72] X. Cao, M.S. Shoichet, Defining the concentration gradient of nerve growth factor for guided neurite outgrowth, Neuroscience. 103 (2001) 831–840. doi:10.1016/S0306-4522(01)00029-X.

[73] T.A. Kapur, M.S. Shoichet, Immobilized concentration gradients of nerve growth factor guide neurite outgrowth, J. Biomed. Mater. Res. 68A (2004) 235–243. doi:10.1002/jbm.a.10168.

[74] T. Houchin-Ray, L.A. Swift, J.H. Jang, L.D. Shea, Patterned PLG substrates for localized DNA delivery and directed neurite extension, Biomaterials. 28 (2007) 2603–2611. doi:10.1016/j.biomaterials.2007.01.042.

[75] Better technology for neuronal manipulation, Nat. Biomed. Eng. (2018). doi:10.1038/s41551-018-0274-2.

[76] Y. Ito, M. Nogawa, Preparation of a protein micro-array using a photo-reactive polymer for a cell-adhesion assay, Biomaterials. (2003). doi:10.1016/S0142-9612(03)00134-0.

[77] T. Konno, H. Hasuda, K. Ishihara, Y. Ito, Photo-immobilization of a phospholipid polymer for surface modification, Biomaterials. (2005). doi:10.1016/j.biomaterials.2004.04.047.

[78] Y. Ito, Micropattern immobilization of polysaccharide, J. Inorg. Biochem. (2000). doi:10.1016/S0162-0134(99)00159-2.

[79] H. Mao, S.M. Kim, M. Ueki, Y. Ito, Serum-free culturing of human mesenchymal stem cells with immobilized growth factors, J. Mater. Chem. B. (2017). doi:10.1039/c6tb02867e.

[80] S. Van Vlierberghe, E. Vanderleyden, V. Boterberg, P. Dubruel, Gelatin functionalization of biomaterial surfaces: Strategies for immobilization and visualization, Polymers (Basel). (2011). doi:10.3390/polym3010114.

[81] Y. Ito, H. Hasuda, T. Yamauchi, N. Komatsu, K. Ikebuchi, Immobilization of erythropoietin to culture erythropoietin-dependent human leukemia cell line, Biomaterials. 25 (2004) 2293–2298. doi:10.1016/j.biomaterials.2003.09.002.

[82] T. Kitajima, S. Obuse, T. Adachi, M. Tomita, Y. Ito, Recombinant human gelatin substitute with photoreactive properties for cell culture and tissue engineering, Biotechnol. Bioeng. 108 (2011) 2468–2476. doi:10.1002/bit.23192.

[83] S.H. Park, S.Y. Seo, J.H. Kang, Y. Ito, T. Il Son, Preparation of photocured azidophenyl-fish gelatin and its capturing of human epidermal growth factor on titanium plate, J. Appl. Polym. Sci. 127 (2013) 154–160. doi:10.1002/app.37854.

[84] M. Pool, J. Thiemann, A. Bar-Or, A.E. Fournier, NeuriteTracer: A novel ImageJ plugin for automated quantification of neurite outgrowth, J. Neurosci. Methods. 168 (2008) 134–139. doi:10.1016/j.jneumeth.2007.08.029.

[85] W. Yu, H.K. Lee, S. Hariharan, W. Bu, S. Ahmed, Quantitative Neurite Outgrowth Measurement Based on Image Segmentation with Topological Dependence, Cytom. Part A. 75 (2009) 289–297. doi:10.1002/cyto.a.20664.

[86] A.J. Haas, S. Prigent, S. Dutertre, Y. Le Dréan, Y. Le Page, Neurite analyzer: An original Fiji plugin for quantification of neuritogenesis in two-dimensional images, J. Neurosci. Methods. (2016). doi:10.1016/j.jneumeth.2016.07.011.

[87] D. Press, Superparamagnetic iron oxide nanoparticles combined with NGF and quercetin promote neuronal branching morphogenesis of PC12 cells, (2019) 2157–2169.

[88] J.S. Chua, C.P. Chng, A.A.K. Moe, J.Y. Tann, E.L.K. Goh, K.H. Chiam, E.K.F. Yim, Extending neurites sense the depth of the underlying topography during neuronal differentiation and contact guidance, Biomaterials. (2014). doi:10.1016/j.biomaterials.2014.06.008.

[89] A. Béduer, C. Vieu, F. Arnauduc, J.C. Sol, I. Loubinoux, L. Vaysse, Engineering of adult human neural stem cells differentiation through surface micropatterning, Biomaterials. (2012). doi:10.1016/j.biomaterials.2011.09.073.

[90] M. Heydari, H. Hasuda, M. Sakuragi, Y. Yoshida, K. Suzuki, Y. Ito, Modification of the titan surface with photoreactive gelatin to regulate cell attachment, J. Biomed. Mater. Res. - Part A. (2007). doi:10.1002/jbm.a.31368.

[91] J.J. Medina Benavente, H. Mogami, T. Sakurai, K. Sawada, Evaluation of silicon nitride as a substrate for culture of PC12 cells: An interfacial model for functional studies in neurons, PLoS One. (2014). doi:10.1371/journal.pone.0090189.

[92] K.P. Das, T.M. Freudenrich, W.R. Mundy, Assessment of PC12 cell differentiation and neurite growth: A comparison of morphological and neurochemical measures, Neurotoxicol. Teratol. (2004). doi:10.1016/j.ntt.2004.02.006.

[93] K. Kalil, E.W. Dent, Branch management: Mechanisms of axon branching in the developing vertebrate CNS, Nat. Rev. Neurosci. 15 (2014) 7–18. doi:10.1038/nrn3650.

[94] R.D. Deegan, O. Bakajin, T.F. Dupont, G. Huber, S.R. Nagel, T.A. Witten, Contact line deposits in an evaporating drop, Phys. Rev. E - Stat. Physics, Plasmas, Fluids, Relat. Interdiscip. Top. 62 (2000) 756–765. doi:10.1103/PhysRevE.62.756.

[95] X. Du, R.D. Deegan, Ring formation on an inclined surface, J. Fluid Mech. 775 (2015). doi:10.1017/jfm.2015.312.

[96] D.R. Lide, CRC Handbook of Chemistry and Physics, 84th Edition, 2003-2004, Handb. Chem. Phys. (2003). doi:10.1136/oem.53.7.504.

[97] Y.S. Park, Y. Ito, Micropattern-immobilization of heparin to regulate cell growth with fibroblast growth factor., Cytotechnology. (2000). doi:10.1023/A:1008154326954.

[98] Y. Ito, Regulation of cell functions by micropattern-immobilized biosignal molecules, Nanotechnology. (1998). doi:10.1088/0957-4484/9/3/009.

[99] S. Tsuzuki, A. Wada, Y. Ito, Photo-immobilization of biological components on gold-coated chips for measurements using surface plasmon resonance (SPR) and a quartz crystal microbalance (QCM), Biotechnol. Bioeng. 102 (2009) 700–707. doi:10.1002/bit.22102.

[100] G. Chen, N. Kawazoe, Y. Ito, Photo-crosslinkable hydrogels for tissue engineering applications, in: Photochem. Biomed. Appl. From Device Fabr. to Diagnosis Ther., 2018: pp. 277–300. doi:10.1007/978-981-13-0152-0_10.

[101] M.C. Marlin, G. Li, Biogenesis and Function of the NGF/TrkA Signaling Endosome, Int. Rev. Cell Mol. Biol. 314 (2015) 239–257. doi:10.1016/bs.ircmb.2014.10.002.

[102] M. Hirose, Y. Kuroda, E. Murata, NGF/TrkA Signaling as a Therapeutic Target for Pain, Pain Pract. 16 (2016) 175–182. doi:10.1111/papr.12342.

[103] Y. Ito, Surface micropatterning to regulate cell functions, Biomaterials. (1999). doi:10.1016/S0142-9612(99)00162-3.

[104] Y. Ito, G. Chen, Y. Imanishi, T. Morooka, E. Nishida, Y. Okabayashi, M. Kasuga, Differential control of cellular gene expression by diffusible and non-diffusible EGF., J. Biochem. 129 (2001) 733–737. doi:10.1093/oxfordjournals.jbchem.a002913.

[105] D. Vaudry, P.J.S. Stork, P. Lazarovici, L.E. Eiden, Signaling pathways for PC12 cell differentiation: Making the right connections, Science (80-.). (2002). doi:10.1126/science.1071552.

[106] P. Sun, H. Watanabe, K. Takano, T. Yokoyama, J.I. Fujisawa, T. Endo, Sustained activation of M-Ras induced by nerve growth factor is essential for neuronal differentiation of PC12 cells, Genes to Cells. (2006). doi:10.1111/j.1365-2443.2006.01002.x.

[107] G.L. Ming, S.T. Wong, J. Henley, X.B. Yuan, H.J. Song, N.C. Spitzer, M.M. Poo, Adaptation in the chemotactic guidance of nerve growth cones, Nature. (2002). doi:10.1038/nature745.

[108] M. Piper, S. Salih, C. Weinl, C.E. Holt, W.A. Harris, Endocytosis-dependent desensitization and protein synthesis-dependent resensitization in retinal growth cone adaptation, Nat. Neurosci. (2005). doi:10.1038/nn1380.

[109] R.J. Andrews, Neuroprotection and nanoneurosurgery: Techniques and potential applications, Int. J. Neuroprot. Neuroregener. 3 (2007).

[110] A. Fabbro, M. Prato, L. Ballerini, Carbon nanotubes in neuroregeneration and repair, Adv. Drug Deliv. Rev. 65 (2013) 2034–2044. doi:10.1016/j.addr.2013.07.002.

[111] A.M. Siddiqui, M. Khazaei, M.G. Fehlings, Translating mechanisms of neuroprotection, regeneration, and repair to treatment of spinal cord injury, in: Prog. Brain Res., 2015: pp. 15–54. doi:10.1016/bs.pbr.2014.12.007.

[112] A. Ferrari, M. Cecchini, A. Dhawan, S. Micera, I. Tonazzini, R. Stabile, D. Pisignano, F. Beltram, Nanotopographic control of neuronal polarity, Nano Lett. (2011). doi:10.1021/nl103349s.

[113] R.W. Gundersen, J.N. Barrett, Neuronal chemotaxis: Chick dorsal-root axons turn toward high concentrations of nerve growth factor, Science (80-.). (1979). doi:10.1126/science.493992.

[114] M. Oren-Suissa, B. Podbilewicz, Cell fusion during development, Trends Cell Biol. 17 (2007) 537–546. doi:10.1016/j.tcb.2007.09.004.

[115] R.H. Kennett, Cell Fusion, Methods Enzymol. 58 (1979) 345–359. doi:10.1016/S0076-6879(79)58149-X.

[116] E.H. Chen, E. Grote, W. Mohler, A. Vignery, Cell-cell fusion, FEBS Lett. 581 (2007) 2181–2193. doi:10.1016/j.febslet.2007.03.033.

[117] E.H. Chen, E.N. Olson, Unveiling the mechanisms of cell-cell fusion, Science (80-.). (2005). doi:10.1126/science.1104799.

[118] A. Sapir, O. Avinoam, B. Podbilewicz, L. V. Chernomordik, Viral and Developmental Cell Fusion Mechanisms: Conservation and Divergence, Dev. Cell. (2008). doi:10.1016/j.devcel.2007.12.008.

[119] J.H. Shinn-Thomas, W.A. Mohler, New insights into the mechanisms and roles of cell-cell fusion, in: Int. Rev. Cell Mol. Biol., 2011. doi:10.1016/B978-0-12-386039-2.00005-5.

[120] I. Wilmut, A.E. Schnieke, J. McWhir, A.J. Kind, K.H.S. Campbell, Viable offspring derived from fetal and adult mammalian cells, Nature. (1997). doi:10.1038/385810a0.

[121] J. Rajasingh, E. Lambers, H. Hamada, E. Bord, T. Thorne, I. Goukassian, P. Krishnamurthy, K.M. Rosen, D. Ahluwalia, Y. Zhu, G. Qin, D.W. Losordo, R.

Kishore, Cell-free embryonic stem cell extract-mediated derivation of multipotent stem cells from NIH3T3 fibroblasts for functional and anatomical ischemic tissue repair, Circ. Res. (2008). doi:10.1161/CIRCRESAHA.108.176115.

[122] N. Bhutani, J.J. Brady, M. Damian, A. Sacco, S.Y. Corbel, H.M. Blau, Reprogramming towards pluripotency requires AID-dependent DNA demethylation, Nature. (2010). doi:10.1038/nature08752.

[123] M. Álvarez-Dolado, M. Martínez-Losa, Cell fusion and tissue regeneration, Adv. Exp. Med. Biol. 713 (2011) 161–175. doi:10.1007/978-94-007-0763-4_10.

[124] F. Lluis, M.P. Cosma, Cell-fusion-mediated somatic-cell reprogramming: A mechanism for tissue regeneration, J. Cell. Physiol. 223 (2010) 6–13. doi:10.1002/jcp.22003.

[125] S. Sullivan, K. Eggan, The potential of cell fusion for human therapy, Stem Cell Rev. 2 (2006) 341–349. doi:10.1007/BF02698061.

[126] G. Pontecorvo, Production of mammalian somatic cell hybrids by means of polyethylene glycol treatment, Somatic Cell Genet. (1975). doi:10.1007/BF01538671.

[127] R.L. Davidson, P.S. Gerald, Improved techniques for the induction of mammalian cell hybridization by polyethylene glycol, Somatic Cell Genet. (1976). doi:10.1007/BF01542629.

[128] U. Zimmermann, J. Vienken, Electric field-induced cell-to-cell fusion, J. Membr. Biol. (1982). doi:10.1007/bf01868659.

[129] M. Tada, T. Tada, Electrofusion: Nuclear reprogramming of somatic cells by cell hybridization with pluripotential stem cells, in: Cell Biol. Four-Volume Set, 2006. doi:10.1016/B978-012164730-8/50026-5.

[130] G. Köhler, C. Milstein, Continuous cultures of fused cells secreting antibody of predefined specificity, Nature. (1975). doi:10.1038/256495a0.

[131] R.K. Plemper, G.B. Melikyan, Membrane fusion, in: Encycl. Biol. Chem. Second Ed., 2013. doi:10.1016/B978-0-12-378630-2.00639-3.

[132] S.C. Harrison, Viral membrane fusion, Virology. (2015). doi:10.1016/j.virol.2015.03.043.

[133] F.W.Y. Chiu, H. Bagci, A.G. Fisher, A.J. deMello, K.S. Elvira, A microfluidic toolbox for cell fusion, J. Chem. Technol. Biotechnol. (2016). doi:10.1002/jctb.4803.

[134] L. Kim, Y.C. Toh, J. Voldman, H. Yu, A practical guide to microfluidic perfusion culture of adherent mammalian cells, Lab Chip. (2007). doi:10.1039/b704602b.

[135] W. Wu, Y. Qu, N. Hu, Y. Zeng, J. Yang, H. Xu, Z.Q. Yin, A cell electrofusion chip for somatic cells reprogramming, PLoS One. (2015). doi:10.1371/journal.pone.0131966.

[136] K.I. Wada, K. Hosokawa, E. Kondo, Y. Ito, M. Maeda, Cell fusion through a microslit between adhered cells and observation of their nuclear behavior, Biotechnol. Bioeng. (2014). doi:10.1002/bit.25190.

[137] K.-I. Wada, K. Hosokawa, Y. Ito, M. Maeda, A Novel Cell Fusion Method for Direct Cytoplasmic Transfer Using a Microfluidic Device, in: 2017: pp. 227–236. doi:10.1021/bk-2017-1253.ch011.

[138] K.-I. Wada, K. Hosokawa, Y. Ito, M. Maeda, Quantitative control of mitochondria transfer between live single cells using a microfluidic device, Biol. Open. 6 (2017) 1960–1965. doi:10.1242/bio.024869.

[139] J.M. Lee, J.E. Kim, J. Borana, B.H. Chung, B.G. Chung, Dual-micropillar-based microfluidic platform for single embryonic stem cell-derived neuronal differentiation, Electrophoresis. 34 (2013) 1931–1938. doi:10.1002/elps.201200578.

[140] W.T. Fung, A. Beyzavi, P. Abgrall, N.T. Nguyen, H.Y. Li, Microfluidic platform for controlling the differentiation of embryoid bodies, Lab Chip. 9 (2009) 2591–2595. doi:10.1039/b903753e.

[141] K. Fujikawa-Yamamoto, S. Wang, H. Yamagishi, C. Ohdoi, H. Murano, T. Ikeda, Establishment of a tetraploid Meth-A cell line through polyploidization by demecolcine but not by staurosporine, K-252A and paclitaxel, Cell Prolif. 34 (2001) 211–222. doi:10.1046/j.1365-2184.2001.00204.x.

[142] S. Ohshima, A. Seyama, Formation of bipolar spindles with two centrosomes in tetraploid cells established from normal human fibroblasts, Hum. Cell. 25 (2012) 78–85. doi:10.1007/s13577-012-0046-3.

[143] J.B. Gurdon, D.A. Melton, Nuclear reprogramming in cells, Science (80-.). (2008). doi:10.1126/science.1160810.

[144] Y. Kimura, M. Gel, B. Techaumnat, H. Oana, H. Kotera, M. Washizu, Dielectrophoresis-assisted massively parallel cell pairing and fusion based on field constriction created by a micro-orifice array sheet, Electrophoresis. (2011). doi:10.1002/elps.201100129.

[145] N. Sasaki, J. Gong, M. Sakuragi, K. Hosokawa, M. Maeda, Y. Ito, Hydrodynamic cell pairing and cell fusion through a microslit on a microfluidic device, Jpn. J. Appl. Phys. (2012). doi:10.1143/JJAP.51.030206.

[146] D.Y. Liang, A.M. Tentori, I.K. Dimov, L.P. Lee, Systematic characterization of degas-driven flow for poly(dimethylsiloxane) microfluidic devices, Biomicrofluidics. 5 (2011). doi:10.1063/1.3584003.

[147] K.I. Wada, K. Hosokawa, Y. Ito, M. Maeda, Effects of ROCK inhibitor Y-27632 on cell fusion through a microslit, Biotechnol. Bioeng. 112 (2015) 2334–2342. doi:10.1002/bit.25641.

[148] K. Okita, S. Yamanaka, Induction of pluripotency by defined factors, Exp. Cell Res. (2010). doi:10.1016/j.yexcr.2010.04.023.

[149] D. Bastida-Ruiz, K. Van Hoesen, M. Cohen, The dark side of cell fusion, Int. J. Mol. Sci. 17 (2016). doi:10.3390/ijms17050638.

[150] Z. Storchova, C. Kuffer, The consequences of tetraploidy and aneuploidy, J. Cell Sci. 121 (2008) 3859–3866. doi:10.1242/jcs.039537.

[151] T. Takahashi, K.O. Okeyo, J. Ueda, K. Yamagata, M. Washizu, H. Oana, A microfluidic device for isolating intact chromosomes from single mammalian cells and probing their folding stability by controlling solution conditions, Sci. Rep. 8 (2018). doi:10.1038/s41598-018-31975-5.

[152] K. Fujikawa-Yamamoto, X. Luo, M. Miyagoshi, H. Yamagishi, DNA stable pentaploid H1 (ES) cells obtained from an octaploid cell induced from tetraploid cells polyploidized using demecolcine, J. Cell. Physiol. (2010). doi:10.1002/jcp.22042.

[153] K. Fujikawa-Yamamoto, M. Miyagoshi, H. Yamagishi, Establishment of a tetraploid cell line from mouse H-1 (ES) cells highly polyploidized with demecolcine, Cell Prolif. (2007). doi:10.1111/j.1365-2184.2007.00442.x.

[154] K. Fujikawa-Yamamoto, M. Miyagoshi, H. Yamagishi, Cell cycle, morphology and pluripotency of octaploid embryonic stem cells in comparison with those of tetraploid and diploid cells, Hum. Cell. (2009). doi:10.1111/j.1749-0774.2009.00070.x.

List of publications

Journal papers

1. Seong Min Kim, Ken-ichi Wada, Masashi Ueki, Kazuo Hosokawa, Mizuo Maeda, Yasuyuki Sakai, and Yoshihiro Ito, Cytoplasmic fusion between an enlarged embryonic stem cell and a somatic cell by a microtunnel device, Biochem. Biophys. Res. Commun., 2019, *Submitted*.
2. Seong Min Kim, Masashi Ueki, Xueli Ren, Jun Akimoto, Yasuyuki Sakai, and Yoshihiro Ito, Micropatterned nanolayers immobilized with nerve growth factor for neurite formation of PC12 cells, *Int. J. Nanomed.*, 2019, *Accepted*.

Presentations

International conference

1. Seong Min Kim, Masashi Ueki, Yasuyuki Sakai, and Yoshihiro Ito, Study on cell fusion-mediated transdifferentiation via a novel approach, *TERMIS 2018*, Kyoto, Japan.
2. Seong Min Kim, Masashi Ueki, Yasuyuki Sakai, and Yoshihiro Ito, Cell fusion-mediated transdifferentiation and reprogramming through microfluidics and biomaterials, *ISSCR 2018*, Melbourne, Australia.

Domestic conference

1. Seong Min Kim, Masashi Ueki, Yasuyuki Sakai, and Yoshihiro Ito, Study on cell fusion system mediated by biomaterials and microfluidics for regenerative medicine, *2018 RIKEN*, Tskuba, Japan.
2. Seong Min Kim, Masashi Ueki, Yasuyuki Sakai, and Yoshihiro Ito, Study of cell fusion-mediated transdifferentiation and reprogramming via a novel approach, *CEMSupra 2018*, Tokyo, Japan.
3. Seong Min Kim, Yasuyuki Sakai, and Yoshihiro Ito, Fabrication and characteristics of dual functionalized vascular stent by spatio-temporal coating, *2016 RIKEN*, Tskuba, Japan.

Acknowledgement

Acknowledgement

First of all, this thesis is built on a lot of supports from my supervisors and colleagues. I would like to express my heartfelt gratitude to all people for helping me.

Firstly, I would like to thank Prof. Yoshihiro Ito for giving me the great opportunity to work at RIKEN and the good environments to study a lot of things. I am thankful to him for his valuable ideas and suggestions for my research during a PhD course. And I would deeply like to thank him that he has always accepted and understood me with big heart when I show difficulty and shortage. Especially, it was my great honors to give a bouquet to him and his wife as a student representative when he had 60^{th} birthday.

I also would like to thank Prof. Yasuyuki Sakai for giving me the great chance to do my PhD course at The University of Tokyo. He has always been friendly to me and also helped me out whenever I need his help. I was able to experience many things in our lab and society thanks to his consideration, and I would really like to thank him for his warmth and valuable comments.

I also would like to extend my gratitude to Dr. Masashi Ueki who is my leader at RIKEN and Mrs. Yamanaka and Mrs. Shimizu who helped me to solve various issues at RIKEN and the University. Thanks to their kind support, I was able to stay Japan without any problem.

I was financially supported by the Junior Research Associate (JRA) scholarship program for a PhD course from RIKEN. I am thankful to all staffs at the student support team. I have worked with many nice lab mates, and I could learn and experience various things from them. Especially, I would like to thank all leaders, technical staffs, and friends who helped me a lot. I have spent good time in Japan with them as a lab mate as well as a friend, and the good memory what we have made will be being part of my life.

Last but not least, I would like to thank my family. First and foremost, I am very thankful to my parents. Thanks to their devoted support and love, I was able to pursue my life and study up to this day. Moreover, I am really thankful to my elder brother, his wife, and my cute nephew and niece. They have played a huge role in my life, and I am very fortunate to be part of their family. I also would like to thank my girlfriend who will be my wife in the near future and her family, and all of my loved ones who helped me in my life.

Lastly, I cannot express my deep gratitude to them enough but I am convinced that I cannot be being without them up to this day. I would like to thank my family and all of them again for believing in me and sending me their tremendous love and encouragement.